Magnetic anisotropy and orbital magnetic moment in Co films and Co/X bilayers (X = Pd and Pt)

M. Cinal [*]

Institute of Physical Chemistry, Polish Academy of Sciences, 01-224 Warsaw, Poland

Magnetocrystalline anisotropy (MCA) energy and the anisotropy of the orbital magnetic moment (AOM), relations between them, and methods of their calculation are investigated for the (001) fcc Co film and Co/X bilayers (X = Pd and Pt), using a realistic tight-binding model. The relations derived by Bruno [Phys. Rev. B **39**, 865 (1989)] and van der Laan [J. Phys.: Condens. Matter **10**, 3239 (1998)], including the AOM of Co only, are found to give largely incorrect mean values of the MCA energy but reproduce its oscillatory variation versus the Co thickness, with scaling factors needed for the bilayers. The presently proposed extension of the Bruno relation, with the AOM of both Co and Pd or Pt included, predicts the correct sign of the MCA energy for both bilayers and reproduces its magnitude and oscillation pattern very well, without extra scaling, for the Co/Pd bilayer, though this relation is not satisfied locally, by the MCA and AOM layer terms. A similarly extended van der Laan relation fails to reproduce the MCA energy, its sign, and the oscillation pattern, and largely overestimates its magnitude. For all investigated systems, the Co orbital moment oscillates versus the Co thickness with the 2 monolayer (ML) period for the out-of-plane direction of magnetization and the 5 ML period for the in-plane direction while the oscillations of the Pd and Pt orbital moments are more complex and similar for both magnetization directions. The exact and approximate MCA energies obtained with the force theorem and the perturbation theory (PT), respectively, are close to each other for the Co film and the Co/Pd bilayer. For the Co/Pt bilayer, only the mean value of the MCA energy is well approximated by the PT while its oscillation amplitude is overestimated a few times due to the large SOC in Pt. It is also shown that the MCA energy includes the intraband term, usually neglected, but, in fact, finite and vital for systems without the inversion symmetry as its magnitude is comparable to that of the interband term for the Co/Pd bilayer.

DOI: 10.1103/PhysRevB.105.104403

I. INTRODUCTION

The spin-orbit coupling (SOC) has a pronounced effect on properties of magnetic systems. In particular, alongside the magnetic dipole-dipole interaction, it determines the magnetic anisotropy of such systems, and, thus, the easy and hard directions of their magnetization. The SOC contribution to the difference between the system energies for the two directions is known as the magnetocrystalline anisotropy (MCA) energy and it strongly depends of the electronic structure. In ferromagnet/nonmagnet (FM/NM) systems, especially FM/heavy metal bilayers, the SOC also plays a crucial role in several other physical phenomena, like the Rashba, spin Hall, and inverse spin galvanic effects which can be used to manipulate electron spins with electric fields or electric currents in spintronic applications. The spin-orbit interaction also results in finite orbital magnetic moments which emerge as a small but sizable addition to the spin moments forming spontaneous magnetization in ferromagnetic metals [1]. In the absence of the SOC, such orbital moments are fully quenched in extended systems due to the time reversal symmetry [2]. Experimentally, the spin and orbital magnetic moments can be determined separately for specific elements present in the

system using the results of the x-ray magnetic circular dichroism (XMCD) spectroscopy. Each of these two components of the total magnetic moment is expressed with the relevant sum rule in terms of the integrated line intensities of the absorption spectra at the L_2 and L_3 edges measured with left and right circularly polarized light in finite magnetic field [3–7].

The orbital moments in ferromagnetic materials depend on the magnetization direction as does the energy of such systems. A simple relation between the MCA energy and the anisotropy of the orbital moment (AOM), represented by the difference of the orbital moments for the easy and hard directions of the magnetization, was originally proposed by Bruno [8] and later elaborated by van der Laan [9]. The relations have been invoked in the theoretical investigations of the magnetic anisotropy not only for layered systems (see, e.g., Refs. [10,11]) but also for nanoclusters [12–14]. In particular, these approximate relations are found to be satisfied to a moderate degree for thin Fe films on a GaAs substrate in the density functional calculations [15]. It is also shown theoretically that the oscillatory patterns of the MCA energy and AOM variations with increasing the film thickness are well correlated with each other for unsupported Fe films [16]. However, the Bruno relation has not been explicitly investigated to explain this correlation in Ref. [16], and, in particular, the scaling factor between the MCA energy and AOM oscillations has not been examined. This theoretical finding is line with an earlier experimental report where the correlation

*mcinal@ichf.edu.pl

between the MCA energy and the AOM is found for the Fe film on a vicinal Ag substrate [17].

Despite their limited accuracy, the Bruno and van der Laan relations are often used to discuss the experimental results for ferromagnetic films, specifically those obtained with the XMCD measurements [17–22]. However, in experimental setups, such films are in contact with a nonmagnetic substrate and, optionally, an overlayer which may both have a strong SOC. Therefore the direct use of the Bruno or van der Laan relations should be done with even more caution since these relations have been derived for homogeneous ferromagnetic systems, characterized with a single SOC constant. For heterogenous systems, like magnetic multilayers, the relation between the MCA energy and the AOM, even given its approximate nature, may need suitable modifications. A modified form of the van der Laan relation proposed by Gimbert and Calmels [23] for the Co/Ni bilayer represents the MCA energy with the SOC constants and the orbital moments of both parts of the bilayer. Such a particular form stems from the expression for the MCA energy obtained within the perturbation theory (PT) approach, though the actual derivation is not given in Ref. [23].

In this paper, the validity of the original Bruno and van der Laan relations and their possible extensions are investigated for multilayer systems and specifically elaborated for magnetic bilayers. In particular, the derivation of the extended van der Laan relation, previously proposed for the Co/Ni bilayer [23], is presented in detail. The present paper provides a more general form of this relation, applicable to any multilayer system, and specifically addresses the case of the Co/NM bilayer where one of the layers is nonmagnetic but can strongly affect the MCA and the AOM due to its large SOC. It also investigated whether it is possible to establish a Bruno-like relation that expresses the MCA energy with the full AOMs of both ferromagnetic and nonmagnetic parts of the bilayer, instead of the differences of the AOM spin components which appear in the extended van der Laan relation. The MCA energy, its spin-pair terms and the terms due to different pairs of the SOCs of the constituent elements are calculated for the Co/Pd and Co/Pt bilayers, alongside the Co film, and the results are compared with the obtained orbital moments of Co, Pd, and Pt in the respective systems. In particular, the oscillation patterns in variations of the investigated quantities with increasing the Co thickness are carefully examined and the identified oscillation periods are related to specific quantum-well (QW) states. In addition, the contributions to the MCA energy from individual atomic layers, the layer orbital moments, and the layer terms of the AOM are examined, in particular, to investigate if they satisfy a local Bruno-like relation. The calculations of the MCA energy are performed with two methods, one using the force theorem (FT) [24] based on the exact solutions of the full Hamiltonian including the SOC, and the approximate approach provided by the perturbation theory (PT). The form of the commonly used PT expression for the MCA energy [8,25,26] is re-examined for systems without the inversion symmetry and its validity in relation to the strength of the SOC is tested for the investigated systems.

The oscillations of the MCA energy with increasing the thicknesses of both ferromagnetic and nonmagnetic layers have previously been found for the Co and Fe films as well as

the Co/Cu and Co/Pd bilayers, experimentally [27–29] and theoretically [16,28–33]. Such oscillations have been shown to come from QW d states in Co and Pd [31–33] as well as QW sp states in Cu hybridized with d states in Co [29]. The oscillation periods of the MCA energy are related to the extremal dimensions of the three-dimensional Fermi surface of the ferromagnetic or nonmagnetic element whose layer thickness varies, in a similar way as it was originally found for the oscillations of the interlayer exchange coupling with increasing the thickness of a nonmagnetic spacer in magnetic FM/NM/FM trilayers [34]. More recently, the MCA oscillations versus the thickness of the Ta and Hf caps have been predicted by the *ab initio* calculations for the Co_2FeAl/Ta [35] as well as Cu/FeCo/Hf and Cu/FeCo/Ta [36] heterostructures. Also, a recent paper reports the oscillations of in-plane magnetic anisotropy with increasing the Au thickness which have been observed for the Au/Fe(110) and Co/Au/Fe(110) films with the magneto-optic Kerr effect [37].

II. THEORY

A. Spin-orbit coupling and magnetocystalline anisotropy in layered systems

The spin **S** of an electron with the momentum **p** interacts in an electric field $\mathbf{E} = -\nabla V(\mathbf{r})$ at position **r** via the SOC H_{so} proportional to $(\mathbf{p} \times \mathbf{E}) \cdot \mathbf{S}$ [38]. For an atomically layered system with the effective potential $V(\mathbf{r})$ approximated by the sum of the layer-specific atomic-like potentials $V_l(r' = |\mathbf{r} - \mathbf{R}_{lj}|)$, spherically symmetric around each atomic site (nucleus) $\mathbf{R}_{lj}$, the SOC takes the form (e.g., Refs. [2,11])

$$H_{so} = \sum_{lj} \xi_{at}^{(l)}(|\mathbf{r} - \mathbf{R}_{lj}|) \mathbf{L}(\mathbf{r} - \mathbf{R}_{lj}) \cdot \mathbf{S}, \qquad (1)$$

where the operator of orbital angular momentum $\mathbf{L}(\mathbf{r} - \mathbf{R}_{lj})$ is calculated with respect to the consecutive atomic positions $\mathbf{R}_{lj}$. The radial function

$$\xi_{at}^{(l)}(r') = \frac{\hbar^2}{2m_e^2 c^2} \frac{1}{r'} \frac{dV_l}{dr'}, \qquad (2)$$

(where $\hbar$, m_e and c are the reduced Planck constant, the electron mass and the light velocity, respectively) defines the strength of the SOC at each site in layer l and its expectation value for the valence p and d orbitals yields the corresponding SOC constants (the SOC vanishes for s orbitals due to its angular part). In transition metals, where magnetic properties are mainly affected by d orbitals, the SOC can be further approximated by its common form

$$H_{so} = \sum_{lj} \xi_l \mathbf{L}(\mathbf{r} - \mathbf{R}_{lj}) \cdot \mathbf{S}, \qquad (3)$$

which includes the layer-specific SOC constant ξ_l corresponding to these orbitals. Note that the spin and orbital angular momentum are assumed to be in units of $\hbar$.

The energy E of a thin film of a ferromagnetic material or a film comprising a ferromagnetic layer depends on the direction of its magnetization **M**. One factor that leads to this magnetic anisotropy is the magnetic dipole-dipole interaction which gives rise to the dependence of the system energy on the sample geometry (shape anisotropy) and, for films, promotes

in-plane magnetization direction, parallel to the film surface. The other contribution to the magnetic anisotropy comes from the SOC and is called the MCA. For cubic films with (001) and (111) surfaces, the MCA energy is defined, at zero temperature, as the difference

$$E_{\text{MCA}} = E(\hat{\mathbf{M}}_\perp) - E(\hat{\mathbf{M}}_{||}) \tag{4}$$

between the total energies $E(\hat{\mathbf{M}})$ for perpendicular and in-plane magnetization directions $\hat{\mathbf{M}}$, usually chosen as the z and x (or y) axes, respectively, in the fixed frame of reference $Oxyz$ associated with the film crystallographic structure. For the (001) fcc films and bilayers presently investigated, the x, y, and z axes are assumed to be oriented along the (001), (010), and (001) directions, respectively.

The MCA energy is determined by the electronic structure of the system perturbed by H_{so} and, at zero temperature, it is usually expressed by the difference $E_{\text{b}}(\hat{\mathbf{M}}_\perp) - E_{\text{b}}(\hat{\mathbf{M}}_{||})$ of the band energies $E_{\text{b}} = (1/N_{\text{2D}}) \sum_{m\mathbf{k}}^{\text{occ}} \epsilon_m(\mathbf{k})$ for two magnetization directions where $\mathbf{k}$ denotes the two-dimensional wave vector and m is the band index (replacing a pair of separate spin and band indices valid in the absence of the SOC). This approach, known as the force theorem (FT) [24], involves the energies $\epsilon_m(\mathbf{k})$ of the occupied electron states in the non-interacting Kohn-Sham system representing the interacting electron system within the density functional theory (DFT) and has proved to provide a very good approximation for the MCA energy found with the total energies $E(\hat{\mathbf{M}})$ of the interacting system; see, e.g., Refs. [11,35,39].

To improve the convergence of E_{MCA} with increasing the number N_{2D} of $\mathbf{k}$ points in the two-dimensional Brillouin zone (BZ) [2], the MCA energy is calculated at finite temperature T,

$$E_{\text{MCA}} = E_{\text{MCA}}^{\text{FT}} = F(\hat{\mathbf{M}}_\perp) - F(\hat{\mathbf{M}}_{||}), \tag{5}$$

using the FT for the free energy $F = E_{\text{b}} - TS$ where S is the entropy. The free energy

$$F(\hat{\mathbf{M}}) = \Omega + \epsilon_{\text{F}} N \tag{6}$$

can also be expressed in terms of the grand potential

$$\Omega(\hat{\mathbf{M}}) = \frac{1}{N_{\text{2D}}} \sum_{m\mathbf{k}} g[\epsilon_m(\mathbf{k})] \epsilon_m(\mathbf{k}) \tag{7}$$

and the number of the electrons

$$N = \frac{1}{N_{\text{2D}}} \sum_{m\mathbf{k}} f[\epsilon_m(\mathbf{k})] \tag{8}$$

defined, respectively, with the function $g(\epsilon) = -k_{\text{B}}T \ln\{1 + \exp[(\epsilon_{\text{F}} - \epsilon)/k_{\text{B}}T]\}$ [40] and the Fermi-Dirac function $f(\epsilon) = 1/(1 + \exp[(\epsilon - \epsilon_{\text{F}})/k_{\text{B}}T])$, where ϵ_{F} is the Fermi energy (or, more precisely, the chemical potential) and k_{B} denotes the Boltzmann constant. The number N_{2D} of $\mathbf{k}$ points in the two-dimensional BZ is equal to the number of atoms in each atomic plane (assuming one atom per primitive unit cell), with the periodic boundary conditions imposed for electron wave functions on its edges. Thus the above formulas with the scaling factor $1/N_{\text{2D}}$ define the MCA energy per one surface atom. The use of the free energy in the definition (5) of the MCA energy corresponds to describing the system in the canonical ensemble where the number of electrons N is

fixed while the Fermi energies ϵ_{F} are different for the two magnetization directions. The Fermi energy $\epsilon_{\text{F}} = \epsilon_{\text{F}}(\hat{\mathbf{M}})$ is then found from the condition (8) with the energies $\epsilon_m(\mathbf{k})$ of the occupied eigenstates $|m\mathbf{k}\rangle$ of the perturbed Hamiltonian $H + H_{\text{so}}$ (where H is the Hamiltonian of the unperturbed system).

The temperature is introduced here mainly to facilitate the MCA calculations and its effect on the saturation magnetization M_{s}, due to spin waves, is not considered. The actual effect of temperature in this formulation is limited to reducing the amplitude of the MCA oscillations [2] due to smearing of the Fermi level; a strong reduction of the magnetic anisotropy oscillations with temperature is confirmed experimentally for Fe and Co films on vicinal substrates [27,28]. Such a smearing is also used in the MCA calculations based on the DFT approach (e.g., Refs. [21,39,41,42]) where the band energy is found as the free energy, in fact (though the actual smearing method can be different), like it is done, e.g., in the Vienna *ab initio* simulation package (VASP) (see Refs. [43], [44], and, in particular, [45]). For the presently assumed temperature of $T = 300$ K, the parameter $k_{\text{B}}T$, which determines the smearing width, is 0.026eV while the MCA oscillations for the (001) Co films are reported [2] to almost disappear at $T = 1000$ K, or $k_{\text{B}}T = 0.086$ eV. Thus the actual value of such a smearing parameter can strongly affect the amplitude of the MCA oscillations or even prevent their occurrence if it is large enough, which is presumably the case for its default value 0.2 eV assumed in VASP.

The free energy F can be also calculated with the perturbation theory (PT) by using, in Eq. (7), the expansion of the state energies $\epsilon_m = \epsilon_{n\sigma}^{\text{per}} = \epsilon_{n\sigma} + \epsilon_{n\sigma}^{(1)} + \epsilon_{n\sigma}^{(2)}$ up to the second order in H_{so} where $\epsilon_{n\sigma} = \epsilon_{n\sigma}(\mathbf{k})$ is the energy of the unperturbed state $|n\sigma\mathbf{k}\rangle$ with spin σ ($\uparrow$ or $\downarrow$), band index n and the wave vector $\mathbf{k}$. As shown in Appendix, the first-order correction $F^{(1)}$ to the free energy vanishes due to cancellation of the $\mathbf{k}$ and $-\mathbf{k}$ contributions to this term, while its second-order term $F^{(2)}$ is equal to the second-order correction $\Omega^{(2)}$ to the grand potential calculated with the Fermi energy $\epsilon_{\text{F}} = \epsilon_{\text{F0}}$ of the unperturbed system. This corresponds to an alternative description of the system, within the grand canonical ensemble with the fixed Fermi energy and using the grand potential Ω instead of the free energy to define the MCA energy with the FT (cf. Ref. [2]),

$$E_{\text{MCA}} = \widetilde{E}_{\text{MCA}}^{\text{FT}} = \Omega(\hat{\mathbf{M}}_\perp) - \Omega(\hat{\mathbf{M}}_{||}), \tag{9}$$

and later find its approximate form $E_{\text{MCA}}^{\text{PT}}$ with the PT. Since the first-order correction $\Omega^{(1)}$ (equal to $F^{(1)}$) in the perturbed grand potential $\Omega = \Omega_0 + \Omega^{(1)} + \Omega^{(2)}$ vanishes the dominant term in the PT expansion of the MCA energy

$$E_{\text{MCA}} = E_{\text{MCA}}^{\text{PT}} = \Omega^{(2)}(\hat{\mathbf{M}}_\perp) - \Omega^{(2)}(\hat{\mathbf{M}}_{||}) \tag{10}$$

for thin films comes from the second-order correction [2,46]

$$\Omega^{(2)}(\hat{\mathbf{M}}) = \frac{1}{2} \frac{1}{N_{\text{2D}}} \sum_{\mathbf{k}\in\text{BZ}} \sum_{\sigma,\sigma'} \sum_{n,n'} \frac{f_0(\epsilon_{n\sigma}(\mathbf{k})) - f_0(\epsilon_{n'\sigma'}(\mathbf{k}))}{\epsilon_{n\sigma}(\mathbf{k}) - \epsilon_{n'\sigma'}(\mathbf{k})}$$
$$\times |\langle n'\mathbf{k}\sigma'|H_{\text{so}}|n\mathbf{k}\sigma\rangle|^2, \tag{11}$$

where the occupation factor $f_0(\epsilon) = f(\epsilon; \epsilon_{\text{F}} = \epsilon_{\text{F0}})$ corresponds to the unperturbed system with the Fermi energy ϵ_{F0}.

The detailed derivation of the expression for $\Omega^{(2)}$, with suitable consideration of degenerate states, given in Appendix, shows that the second-order term $\Omega^{(2)}$ includes not only the contributions from the second-order corrections $\epsilon_{n\sigma}^{(2)}$ to state energies, but also contributions from the first-order corrections $\epsilon_{n\sigma}^{(1)}$. In particular, it is shown that while the diagonal (intraband) terms, $n\sigma = n'\sigma'$, are absent in the second-order correction $E^{(2)}$ to the band energy in the usual PT approach to the MCA energy at zero temperature [8,25,26], such terms are present in the MCA calculations with Eq. (11) at finite T since the second-order correction $\Omega^{(2)}$ includes terms proportional to $f_0'(\epsilon_{n\sigma})(\epsilon_{n\sigma}^{(1)})^2$. The ratio $[f_0(\epsilon_{n\sigma}) - f_0(\epsilon_{n'\sigma})]/(\epsilon_{n\sigma} - \epsilon_{n'\sigma})$ is also replaced with the derivative $f_0'(\epsilon_{n\sigma})$ for nondiagonal terms with equal energies $\epsilon_{n\sigma} = \epsilon_{n'\sigma'}$. With such a replacement, the PT formula (11) is valid even for degenerate states, present at the high-symmetry points and lines in the BZ. In particular, diagonalization of the perturbation H_{so} in each degenerate subspace of states, required by the usual recipe of the PT, is not needed prior to application of this formula provided that all terms $n\sigma$ and $n'\sigma$ are included in the summation. The same expression for $\Omega^{(2)}$, with the diagonal terms and degenerate states included, is obtained by expanding $\Omega = \Omega_0 + \Omega^{(1)} + \Omega^{(2)}$ in orders of H_{so} using the Dyson expansion for the perturbed Green function [2], and noting that the linear term $\Omega^{(1)}$ vanishes.

Thus the expression (11) with all terms included gives the second-order term $\Omega^{(2)}$ of the grand potential $\Omega(\hat{\mathbf{M}}) = \Omega_0 + \Omega^{(2)}(\hat{\mathbf{M}})$ and consequently defines the PT formula (10) for the MCA energy at finite temperature. The inclusion of diagonal terms in Eq. (11) is necessary for the Co/NM bilayers since for systems without the inversion symmetry the elements $\langle n\mathbf{k}\sigma|H_{so}|n\mathbf{k}\sigma\rangle$ can be finite, as confirmed by the results shown in Sec. III B. In the absence of the inversion symmetry, the summation over the wave vectors $\mathbf{k}$ in Eq. (11), as well as in Eqs. (7) and (8) used in the MCA calculations with the FT, must be done over the whole BZ since respective terms with $-\mathbf{k}$ and $\mathbf{k}$ are not equal. For homogenous ferromagnetic films and symmetric magnetic trilayers, like Co and Pd/Co/Pd slabs investigated in the author's previous studies [2,31–33], the diagonal elements of H_{so} vanish due to the inversion symmetry so that inclusion of the diagonal terms in the PT formula for the MCA energy is irrelevant in such cases. The formula without such terms, in an equivalent form valid for $T = 0$, was also used to analyze the results obtained with the FT in the *ab initio* calculations [21,39,41,42] for various FM/NM and FM1/FM2 superlattices, FM=Fe, Ni and Co, all with the inversion symmetry.

In the limit $T \to 0$, the MCA energy includes diagonal terms proportional to $|\langle n\mathbf{k}\sigma|H_{so}|n\mathbf{k}\sigma\rangle|^2$ and the Dirac delta function $f_0'(\epsilon_{n\sigma}) = \delta(\epsilon_{n\sigma}(\mathbf{k}) - \epsilon_{F0}))$ which defines sheets of the Fermi surface as lines in the two-dimensional BZ. Although the integral of such terms over $\mathbf{k}$ is finite for systems without the inversion symmetry, the diagonal terms are not included in the usual PT formula [8,25] for the MCA energy at $T = 0$, which implicitly assumes that only those perturbed states are occupied that originate from the occupied unperturbed states. While such an assumption helps to achieve convergence [47] it fails for some states with energies very close to the Fermi energy and it is not made in the present

derivation of $\Omega^{(2)}$ at finite T. Thus the PT expression for the MCA energy at $T = 0$ needs to be reconsidered if the inversion symmetry is absent so that it agrees with the $T \to 0$ limit of E_{MCA} found with Eqs. (10) and (11).

The dependence of $\Omega^{(2)}$ on the magnetization orientation $\hat{\mathbf{M}}$ arises due to the fact that the spin states $|\sigma\rangle$ and $|\sigma'\rangle$ refer to the spin quantization axis ζ along the vector $\mathbf{M}$. Indeed, the spin operator represented as $\mathbf{S} = (S_\xi, S_\eta, S_\zeta)$ in the rotated frame of reference $O\xi\eta\zeta$, is given by the Pauli matrices σ_1, σ_2, σ_3 while the corresponding components L_ξ, L_η, L_ζ of the orbital angular momentum $\mathbf{L}$ are expressed in terms of L_x, L_y, L_z and the angles θ_M and ϕ_M (polar and azimuthal) that define the direction of $\mathbf{M}$ with respect to the film surface in the fixed frame of reference $Oxyz$. Thus, although the SOC operator

$$\mathbf{L} \cdot \mathbf{S} = L_x S_x + L_y S_y + L_z S_z = L_\xi S_\xi + L_\eta S_\eta + L_\zeta S_\zeta$$
$$= L_\zeta S_\zeta + \tfrac{1}{2}(L_+' S_-' + L_-' S_+') \quad (12)$$

(where $L_\pm' = L_\xi \pm iL_\eta$ and $S_\pm' = S_\xi \pm iS_\eta$) is invariant under simultaneous rotation of orbital and spin momenta, its mixed representation in the two different frames of reference: $O\xi\eta\zeta$ for spin and $Oxyz$ for electron position $\mathbf{r}$ and other spatial operators like $\mathbf{L}$, includes the sine and cosine functions of θ_M and ϕ_M [48]. As a result, the matrix elements of $\mathbf{L} \cdot \mathbf{S}$ between atomic spin-orbitals $|\mu\sigma\rangle$ with spatial parts represented in the $Oxyz$ frame of reference depend on the angles θ_M and ϕ_M [49]; the same applies to the matrix elements of H_{so} between the wave functions $\psi_{n\mathbf{k}}^\sigma(\mathbf{r}) = \psi_{n\mathbf{k}}^\sigma(x, y, z)$ in Eq. (11). Then, the PT expression (11) leads, for films with cubic structure (fcc, bcc) and the (001) or (111) surfaces, to the simple dependence $K_1 \cos^2 \theta_M$ of the dominant term of the free energy (or Ω) on the magnetization orientation $\hat{\mathbf{M}}$, with the anisotropy constant K_1 equal to the MCA energy defined above. Further terms, of the fourth order in the SOC, are dependent also on the azimuthal angle ϕ_M and give rise to the bulklike contributions to the MCA anisotropy.

The MCA energy of a layered system, given by Eqs. (10) and (11), can be decomposed into contributions

$$E_{MCA}^{(ll')} = \xi_l \xi_{l'} \left[\omega_{ll'}^{(2)}(\hat{\mathbf{M}}_\perp) - \omega_{ll'}^{(2)}(\hat{\mathbf{M}}_{||}) \right] \quad (13)$$

coming from the SOC in pairs of layers l and l' so that each $E_{MCA}^{(ll')}$ is the part of the MCA energy that results from the SOC in layer l when the electron states are modified by the SOC in layer l'. The terms

$$\omega_{ll'}^{(2)}(\hat{\mathbf{M}}) = \frac{1}{2} \frac{1}{N_{2D}} \sum_{\mathbf{k} \in BZ} \sum_{\sigma,\sigma'} \sum_{n,n'} \frac{f_0(\epsilon_{n\sigma}(\mathbf{k})) - f_0(\epsilon_{n'\sigma'}(\mathbf{k}))}{\epsilon_{n\sigma}(\mathbf{k}) - \epsilon_{n'\sigma'}(\mathbf{k})}$$
$$\times \langle n'\mathbf{k}\sigma'|\mathcal{O}_l|n\mathbf{k}\sigma\rangle \langle n\mathbf{k}\sigma|\mathcal{O}_{l'}|n'\mathbf{k}\sigma'\rangle \quad (14)$$

are defined with the operators $\mathcal{O}_l = \sum_j \mathbf{L}(\mathbf{r} - \mathbf{R}_{lj}) \cdot \mathbf{S}$. The matrix element $\langle n'\mathbf{k}\sigma'|\mathcal{O}_l|n\mathbf{k}\sigma\rangle$ is equal to $N_{2D}\langle n'\mathbf{k}\sigma'|\mathbf{L}(\mathbf{r} - \mathbf{R}_{l0}) \cdot \mathbf{S}|n\mathbf{k}\sigma\rangle$ (calculated for any chosen atom $j = 0$ in the lth atomic plane) since each of its terms $\langle n'\mathbf{k}\sigma'|\mathbf{L}(\mathbf{r} - \mathbf{R}_{lj}) \cdot \mathbf{S}|n\mathbf{k}\sigma\rangle$ is the same due to the Bloch form of the electron wave functions with the same prefactor $\exp(i\mathbf{kr})$ multiplied by periodic functions of $\mathbf{r}$. The elements $\langle n'\mathbf{k}\sigma'|\mathcal{O}_l|n\mathbf{k}\sigma\rangle$ are independent of N_{2D} since the wave functions, defined over whole atomic planes, have the normalization factor $1/\sqrt{N_{2D}}$.

Let us note that $\omega_{ll'}^{(2)}$, and hence also the MCA layer-pair contribution $E_{\text{MCA}}^{(ll')}$, are symmetric in the layer indices l and l', since the expression for $\omega_{ll'}^{(2)}$ becomes equal to $\omega_{l'l}^{(2)}$ once the pairs of electron state indices $n\sigma$ are renamed as $n'\sigma'$ and vice versa.

The layer-pair terms $E_{\text{MCA}}^{(ll')}$ for a Co/Pd bilayer are presented in Sec. III D and compared with the results of the recent *ab initio* calculations where such contributions are also determined, for the 5 ML Co film with hcp-like stacking and a Co/Ni multilayer [50]. Note that the intersite MCA terms with $l < l'$ are only considered in Ref. [50] so that they are defined as $E_{\text{MCA}}^{(ll')} + E_{\text{MCA}}^{(l'l)} = 2E_{\text{MCA}}^{(ll')}$. The layer-pair contributions $E_{\text{MCA}}^{(ll')}$ could be formally mapped onto a spin Hamiltonian including the on-site ($l = l'$) and two-site ($l \neq l'$) anisotropy terms [51] with respective magnetic anisotropy constants $K_{ll'}$ proportional to $E_{\text{MCA}}^{(ll')}$. However, it requires a further investigation whether such a rather arbitrary association is valid for metallic layered systems, e.g., by simulating of the temperature dependence of the effective anisotropy constant like it is done in Ref. [52].

For the Co/NM bilayers, the MCA energy expressed as the sum of the layer-pair contributions $E_{\text{MCA}}^{(ll')}$ can be represented as the sum of four terms

$$E_{\text{MCA}} = E_{\text{MCA}}^{\text{CoCo}} + E_{\text{MCA}}^{\text{CoNM}} + E_{\text{MCA}}^{\text{NMCo}} + E_{\text{MCA}}^{\text{NM NM}}, \tag{15}$$

where the XY pair term

$$\begin{aligned} E_{\text{MCA}}^{XY} &= \sum_{l \in \text{X}} \sum_{l' \in \text{Y}} E_{\text{MCA}}^{(ll')} \\ &= \xi_X \xi_Y \sum_{l \in \text{X}} \sum_{l' \in \text{Y}} \left[\omega_{ll'}^{(2)}(\hat{\mathbf{M}}_\perp) - \omega_{ll'}^{(2)}(\hat{\mathbf{M}}_{||}) \right] \end{aligned} \tag{16}$$

is the combined contribution of the SOC in the X and Y parts of the bilayer. The mixed terms are equal, $E_{\text{MCA}}^{\text{CoNM}} = E_{\text{MCA}}^{\text{NMCo}}$, since $E_{\text{MCA}}^{(ll')}$ is symmetric in l, l'. Furthermore, the total MCA energy and each of its XY components can be decomposed into the spin-pair contributions

$$E_{\text{MCA}} = E_{\text{MCA}}^{\downarrow\downarrow} + E_{\text{MCA}}^{\downarrow\uparrow} + E_{\text{MCA}}^{\uparrow\downarrow} + E_{\text{MCA}}^{\uparrow\uparrow}, \tag{17}$$

$$E_{\text{MCA}}^{XY} = E_{\text{MCA}}^{XY,\downarrow\downarrow} + E_{\text{MCA}}^{XY,\downarrow\uparrow} + E_{\text{MCA}}^{XY,\uparrow\downarrow} + E_{\text{MCA}}^{XY,\uparrow\uparrow}. \tag{18}$$

The decomposition of the MCA energy into contributions from individual layers is also possible and two different methods to achieve this goal are presented in Sec. III D, alongside exemplary results for the Co/Pd bilayer.

B. Orbital moments

In the absence of the SOC, the orbital angular momentum of an extended system is fully quenched since for each occupied eigenstate $|n\mathbf{k}\sigma\rangle$ with the wave function $\psi_{n\mathbf{k}}^\sigma(\mathbf{r})$ there is another state $|n, -\mathbf{k}, \sigma\rangle$ with the wave function $\psi_{n,-\mathbf{k}}^\sigma(\mathbf{r}) = [\psi_{n\mathbf{k}}^\sigma(\mathbf{r})]^*$ which is also occupied but has the opposite expectation value of $\mathbf{L}$ (this value can be nonvanishing in systems without the inversion symmetry) see, e.g., Ref. [2]. Once the electronic states are perturbed by H_{so} their overall contribution to the orbital angular momentum becomes finite. For the sake of simplicity, we refer to the orbital angular momentum also

as the orbital moment which, when multiplied by the gyromagnetic ratio $g = -\mu_B/\hbar$ (where μ_B is the Bohr magneton), gives the orbital magnetic moment.

The orbital moment at atomic site j in layer l

$$\langle \mathbf{L} \rangle_{lj} = \sum_{\mathbf{k} \in \text{BZ}} \sum_m f(\epsilon_m(\mathbf{k})) \langle m\mathbf{k} | \mathbf{L}(\mathbf{r} - \mathbf{R}_{lj}) | m\mathbf{k} \rangle_{\text{MT}} \tag{19}$$

is defined as the sum of the expectation values of $\mathbf{L}(\mathbf{r} - \mathbf{R}_{lj})$ in the occupied states $|m\mathbf{k}\rangle$ of the perturbed Hamiltonian $H + H_{\text{so}}$. The calculations of the orbital moments with Eq. (19) will be referred to as the FT approach, in a similar way as for the MCA energy found with Eq. (5) which is also based on the direct diagonalization of $H + H_{\text{so}}$.

Using the PT expansions for the perturbed eigenstates

$$\begin{aligned} |m\mathbf{k}\rangle = |n\mathbf{k}\sigma\rangle^{\text{per}} &= |n\mathbf{k}\sigma\rangle \\ &+ \sum_{\mathbf{k} \in \text{BZ}} \sum_{\substack{n'\sigma' \\ (n'\sigma') \neq (n\sigma)}} \frac{\langle n'\mathbf{k}\sigma' | H_{\text{so}} | n\mathbf{k}\sigma \rangle}{\epsilon_{n\sigma}(\mathbf{k}) - \epsilon_{n'\sigma'}(\mathbf{k})} |n'\mathbf{k}\sigma'\rangle, \end{aligned} \tag{20}$$

and their energies $\epsilon_m = \epsilon_{n\sigma}^{\text{per}} = \epsilon_{n\sigma} + \epsilon_{n\sigma}^{(1)}$, both including the first-order corrections, the orbital angular momentum at an atomic site (lj) can be expressed as follows:

$$\begin{aligned} \langle \mathbf{L} \rangle_{lj} &= \sum_{\mathbf{k} \in \text{BZ}} \sum_{n\sigma} f(\epsilon_{n\sigma}(\mathbf{k}))\, ^{\text{per}}\langle n\mathbf{k}\sigma | \mathbf{L}(\mathbf{r} - \mathbf{R}_{lj}) | n\mathbf{k}\sigma \rangle_{\text{MT}}^{\text{per}} \\ &= \frac{1}{2} \sum_{\mathbf{k} \in \text{BZ}} \sum_\sigma \sum_{nn'} \frac{f_0(\epsilon_{n\sigma}(\mathbf{k})) - f_0(\epsilon_{n'\sigma}(\mathbf{k}))}{\epsilon_{n\sigma}(\mathbf{k}) - \epsilon_{n'\sigma}(\mathbf{k})} \\ &\quad \times [\langle n'\mathbf{k}\sigma | H_{\text{so}} | n\mathbf{k}\sigma \rangle \langle n\mathbf{k}\sigma | \mathbf{L}(\mathbf{r} - \mathbf{R}_{lj}) | n'\mathbf{k}\sigma \rangle_{\text{MT}} + \text{c.c.}], \end{aligned} \tag{21}$$

where the terms $n = n'$ are included since they come from the expansion

$$\begin{aligned} f(\epsilon_m) &= f\left(\epsilon_{n\sigma} + \epsilon_{n\sigma}^{(1)}\right) = f_0\left(\epsilon_{n\sigma} + \epsilon_{n\sigma}^{(1)} - \delta\epsilon_{\text{F}}\right) \\ &= f_0(\epsilon_{n\sigma}) + f_0'(\epsilon_{n\sigma})\left(\epsilon_{n\sigma}^{(1)} - \delta\epsilon_{\text{F}}\right) \\ &= f_0(\epsilon_{n\sigma}) + f_0'(\epsilon_{n\sigma})\epsilon_{n\sigma}^{(1)}, \end{aligned} \tag{22}$$

where $\epsilon_{n\sigma}^{(1)} = \langle n\mathbf{k}\sigma | H_{\text{so}} | n\mathbf{k}\sigma \rangle$ and the shift $\delta\epsilon_{\text{F}} = \epsilon_{\text{F}} - \epsilon_{\text{F0}}$ of the Fermi energy is neglected as it is of the second-order in the SOC; see Appendix. Thus the orbital moment is of the first-order in H_{so} since the zero-order term (i.e., the moment at zero SOC) vanishes, as explained above. Note that the spin moment $\langle S_\zeta \rangle = \sum_{m\mathbf{k}} f(\epsilon_m(\mathbf{k})) \langle m\mathbf{k} | S_\zeta | m\mathbf{k} \rangle$ along the magnetization direction is not changed by the SOC in the first-order of H_{so} since we find $\langle m\mathbf{k} | S_\zeta | m\mathbf{k} \rangle = \langle n\sigma\mathbf{k} | S_\zeta | n\sigma\mathbf{k} \rangle = 1/2$ from Eq. (20) (note that S_ζ is diagonal in the $|n\sigma\mathbf{k}\rangle$ basis) and the second term in $\langle S_\zeta \rangle = (1/2) \sum_{n\mathbf{k}\sigma} f_0(\epsilon_{n\sigma}) + (1/2) \sum_{n\mathbf{k}\sigma} f_0'(\epsilon_{n\sigma})\epsilon_{n\sigma}^{(1)} = (1/2) \sum_{n\mathbf{k}\sigma} f_0(\epsilon_{n\sigma})$ vanishes as the contributions from $\mathbf{k}$ and $-\mathbf{k}$ cancel out in this term.

In the above expressions (19) and (21) for the orbital moment at atomic site (lj), the spatial integration in the matrix elements of $\mathbf{L}(\mathbf{r} - \mathbf{R}_{lj})$ is limited to the MT sphere centered on site (lj) and, accordingly, the integrals involve different angular components of the Bloch wave functions inside this sphere. In fact, the integration can also be limited to the MT spheres for the matrix elements of H_{so} in Eqs. (11) and (21) since the SOC is strongly localized around each nucleus (as $|\mathbf{r} - \mathbf{R}_{lj}|^{-3}$) and its approximated form given by Eq. (1) is

not valid in the interstitial region where the potential seizes to be spherically symmetric. Limiting the integration region to the MT sphere of the radius r_{lj}^{MT} around each site $\mathbf{R}_{lj}$ can be introduced formally by incorporating the step function $\theta(r_{lj}^{\mathrm{MT}} - r')$ (where $r' = |\mathbf{r} - \mathbf{R}_{lj}|$) into the operators of the orbital angular momentum $\mathbf{L}(\mathbf{r} - \mathbf{R}_{lj})$ at this site and the site contribution to the SOC in Eqs. (1) and (3), like it is recently done in Ref. [53]. While this approach is strictly applicable in the DFT calculations, its goal can be also achieved by keeping only on-site elements of $\mathbf{L}(\mathbf{r} - \mathbf{R}_{lj})$ for each site (lj) if the electron states are represented in a local orbital basis as it is done in the tight-binding (TB) model used in this work (see Sec. II D).

The so-defined atomic orbital moments well approximate the local orbital magnetic moment determined for each atom with the Wannier functions within the exact approach of the modern theory of orbital magnetization [54–56]. This theory also recognizes the second, itinerant, term of the orbital moment which comes from the interstitial region but it is usually significantly smaller than its local term [55,56]. However, in fact, it is the local (atomic-like) orbital moment, alongside the spin moment, that is determined experimentally since these moments are obtained from the XMCD spectra with the sum rules which are derived by considering light absorption of isolated atoms [3,4].

In layered systems, the atomic orbital moments depend only on the layer index, $\langle\mathbf{L}\rangle_{lj} = \langle\mathbf{L}\rangle_{l0} = \langle\mathbf{L}\rangle_l$. The sum of local moments $\langle\mathbf{L}\rangle_l$ from all atomic layers l yields the total orbital moment (its local part) of the film. In the case of a Co/NM bilayer including N_{Co} monolayers (ML) of Co and N_{NM} ML of NM, its total moment

$$
\begin{aligned}
\langle\mathbf{L}\rangle_{\mathrm{tot}} &= \sum_l \langle\mathbf{L}\rangle_l = \sum_{l\in\mathrm{Co}} \langle\mathbf{L}\rangle_l + \sum_{l\in\mathrm{NM}} \langle\mathbf{L}\rangle_l \\
&= \langle\mathbf{L}\rangle_{\mathrm{tot,Co}} + \langle\mathbf{L}\rangle_{\mathrm{tot,NM}} = N_{\mathrm{Co}}\mathbf{L}_{\mathrm{Co}} + N_{\mathrm{NM}}\mathbf{L}_{\mathrm{NM}}
\end{aligned}
\tag{23}
$$

is the sum of the total orbital moments $\langle\mathbf{L}\rangle_{\mathrm{tot,Co}}$ and $\langle\mathbf{L}\rangle_{\mathrm{tot,NM}}$ of the Co and NM layers and can be further expressed with the average atomic moments $\langle\mathbf{L}\rangle_{\mathrm{Co}} = \langle\mathbf{L}\rangle_{\mathrm{tot,Co}}/N_{\mathrm{Co}}$ and $\langle\mathbf{L}\rangle_{\mathrm{NM}} = \langle\mathbf{L}\rangle_{\mathrm{tot,NM}}/N_{\mathrm{NM}}$ in the respective parts of the bilayer. Such average element-specific moments $\langle L_\zeta\rangle_X$ are detected in the XMCD experiments.

Since most of unperturbed electron states have extended wave functions with finite values in both Co and NM parts of the bilayer the SOC in NM modifies each of such wave functions not only in NM but also in Co, through the first-order corrections in Eq. (20) which span over the whole bilayer. Physically, if an electron is in a state which has finite probability amplitudes in both Co and NM, this state changes in the whole bilayer once the electron is subject to the spin-orbit interaction in the NM part. In a similar way, the electron wave functions change throughout the whole bilayer due to the SOC in Co. Thus a finite orbital moment in each layer l arises as a result of the changes of the wave function in this layer due to the SOC present in the same layer l as well as all other layers l', also in the nonmagnetic part of the Co/NM bilayer. Accordingly, the atomic orbital moment in layer l,

$$
\langle\mathbf{L}\rangle_l = \sum_{l'} \langle\mathbf{L}\rangle_l^{l'},
\tag{24}
$$

has contributions which are induced by the SOC in all layers l', in both Co and NM. These terms are given by

$$
\begin{aligned}
\langle\mathbf{L}\rangle_l^{l'} = {}&\frac{1}{2}N_{\mathrm{2D}}\xi_{l'} \sum_{\mathbf{k}\in\mathrm{BZ}} \sum_\sigma \sum_{nn'} \frac{f(\epsilon_{n\sigma}(\mathbf{k})) - f(\epsilon_{n'\sigma}(\mathbf{k}))}{\epsilon_{n\sigma}(\mathbf{k}) - \epsilon_{n'\sigma}(\mathbf{k})} \\
&\times [\langle n'\mathbf{k}\sigma|L_\zeta(\mathbf{r} - \mathbf{R}_{l'0})S_\zeta|n\mathbf{k}\sigma\rangle_{\mathrm{MT}} \\
&\times \langle n\mathbf{k}\sigma|\mathbf{L}(\mathbf{r} - \mathbf{R}_{l0})|n'\mathbf{k}\sigma\rangle_{\mathrm{MT}} + \text{c.c.}]
\end{aligned}
\tag{25}
$$

where each of the two matrix elements is proportional to $1/N_{\mathrm{2D}}$ so that effectively Eq. (25) includes the factor $1/N_{\mathrm{2D}}$ which combined with the sum over N_{2D} wave vectors $\mathbf{k}$ leads to $\langle\mathbf{L}\rangle_l^{l'}$ independent of N_{2D} in the limit of large N_{2D}; see also Eq. (44) below. Note that the SOC operator $\mathbf{L} \cdot \mathbf{S}$, defined in Eq. (12), is replaced by $L_\zeta S_\zeta$ in Eq. (25) because the matrix element of this operator is calculated for pair of states with the same spin σ.

The total orbital moments $\langle\mathbf{L}\rangle_{\mathrm{tot},X}$ in the $X = \mathrm{Co}$ and $X = \mathrm{NM}$ parts of the bilayer can then be decomposed into the terms $\langle\mathbf{L}\rangle_{\mathrm{tot},X}^Y$ coming from the SOC in $Y = \mathrm{Co}$ and $Y = \mathrm{NM}$,

$$
\langle\mathbf{L}\rangle_{\mathrm{tot, Co}} = \langle\mathbf{L}\rangle_{\mathrm{tot,Co}}^{\mathrm{Co}} + \langle\mathbf{L}\rangle_{\mathrm{tot,Co}}^{\mathrm{NM}},
\tag{26}
$$

$$
\langle\mathbf{L}\rangle_{\mathrm{tot,NM}} = \langle\mathbf{L}\rangle_{\mathrm{tot,NM}}^{\mathrm{Co}} + \langle\mathbf{L}\rangle_{\mathrm{tot,NM}}^{\mathrm{NM}},
\tag{27}
$$

where $\langle\mathbf{L}\rangle_{\mathrm{tot},X}^Y = \sum_{l\in X} \sum_{l'\in Y} \langle\mathbf{L}\rangle_l^{l'}$. Accordingly, the average atomic moment $\langle\mathbf{L}\rangle_X = \langle\mathbf{L}\rangle_{\mathrm{tot},X}/N_X$ in the X part can be expressed as the sum of the two terms $\langle\mathbf{L}\rangle_X^Y = \langle\mathbf{L}\rangle_{\mathrm{tot},X}^Y/N_X$, with $Y = \mathrm{Co}$ and $Y = \mathrm{NM}$.

The layer orbital moments $\langle\mathbf{L}\rangle_l$, the total orbital moments in Co and NM, as well as their different parts $\langle\mathbf{L}\rangle_{\mathrm{tot},X}^Y$ are parallel to the magnetization $\mathbf{M}$, if it is oriented in-plane ($\zeta = x$ and y) or out-of-plane ($\zeta = z$), for the considered layered systems with the cubic structure and the (001) surface. This can be shown if one applies the system symmetries, $x \to -x$ or $y \to -y$, in Eq. (25). Such a symmetry operation Q transforms each eigenstate $|n\mathbf{k}\sigma\rangle$ to another eigenstate $|n\mathbf{k}'\sigma\rangle$ with the $\mathbf{k}' = Q^{-1}\mathbf{k} = Q\mathbf{k}$ point which is also present in the summation over the BZ. The components L_α ($\alpha = x, y, z$) of the operator $\mathbf{L}$ are either unchanged by the symmetries $x \to -x$ and $y \to -y$ or changed to $-L_\alpha$. In particular, if $\alpha \neq \zeta$ at least one these symmetries gives $QL_\alpha = -L_\alpha$ and $QL_\zeta = L_\zeta$ or $QL_\alpha = L_\alpha$ and $QL_\zeta = -L_\zeta$. Thus each term in Eq. (25) is equal to the opposite of the respective term for $\mathbf{k}'$ so that the two terms cancel out and, as a result, the α components of the orbital moment perpendicular to the magnetization direction ζ vanish. The terms in Eq. (25) do not change sign for $\alpha = \zeta$ upon these symmetry operations so that the component of the orbital moment along the magnetization direction is finite. Note that for an oblique magnetization, with the orientation ζ neither parallel nor perpendicular to the film surface, the orbital moment is no longer collinear with $\mathbf{M}$ [9].

C. Relations between magnetocrystalline anisotropy energy and orbital moments

In each layer, the atomic orbital moment has two terms, $\langle\mathbf{L}\rangle_l^\uparrow$ and $\langle\mathbf{L}\rangle_l^\downarrow$, which come from the majority (spin-up) and minority (spin-down) energy bands, respectively. The second-order correction $\Omega^{(2)}$ and the resulting MCA energy E_{MCA} are expressed as sums of the spin-pair contributions: $\Omega_{\sigma\sigma'}^{(2)}$

and $E_{\text{MCA}}^{\sigma\sigma'}$, respectively. From Eqs. (11), (12), and (21), it follows that the spin-diagonal part of $\Omega^{(2)}$ can be expressed with the contributions of the spin-up and spin-down bands to the orbital moment component $\langle L_\zeta \rangle_l$ along the magnetization direction, namely,

$$\Omega_{\uparrow\uparrow}^{(2)} + \Omega_{\downarrow\downarrow}^{(2)} = -\frac{1}{4} \sum_l \xi_l [\langle L_\zeta \rangle_l^\downarrow - \langle L_\zeta \rangle_l^\uparrow]. \quad (28)$$

Accordingly, the relation between the sum of the spin-diagonal terms $E_{\text{MCA}}^{\sigma\sigma'}$ in the MCA energy and the difference of the respective contributions to the AOM $\Delta \langle L_\zeta \rangle_l = \Delta \langle L_\zeta \rangle_l^\uparrow + \Delta \langle L_\zeta \rangle_l^\downarrow$ is obtained

$$E_{\text{MCA}}^{\uparrow\uparrow} + E_{\text{MCA}}^{\downarrow\downarrow} = -\frac{1}{4} \sum_l \xi_l [\Delta \langle L_\zeta \rangle_l^\downarrow - \Delta \langle L_\zeta \rangle_l^\uparrow], \quad (29)$$

where $\Delta \langle L_\zeta \rangle_l^\sigma = \langle L_z \rangle_l^\sigma |_{\mathbf{M}||z} - \langle L_x \rangle_l^\sigma |_{\mathbf{M}||x}$ Let us note that the Δ symbol is placed outside the brackets to mark that it refers not only to two different components of the orbital moment but also to the system's two states of different total spin directions, i.e., magnetization orientations.

For the Co/NM bilayers, the relations (28) and (29) take the following form:

$$\Omega_{\uparrow\uparrow}^{(2)} + \Omega_{\downarrow\downarrow}^{(2)} = -\frac{1}{4}\xi_{\text{Co}}(\langle L_\zeta \rangle_{\text{tot,Co}}^\downarrow - \langle L_\zeta \rangle_{\text{tot,Co}}^\uparrow)$$
$$- \frac{1}{4}\xi_{\text{NM}}(\langle L_\zeta \rangle_{\text{tot,NM}}^\downarrow - \langle L_\zeta \rangle_{\text{tot,NM}}^\uparrow), \quad (30)$$

$$E_{\text{MCA}}^{\uparrow\uparrow} + E_{\text{MCA}}^{\downarrow\downarrow} = -\frac{1}{4}\xi_{\text{Co}}(\Delta \langle L_\zeta \rangle_{\text{tot,Co}}^\downarrow - \Delta \langle L_\zeta \rangle_{\text{tot,Co}}^\uparrow)$$
$$- \frac{1}{4}\xi_{\text{NM}}(\Delta \langle L_\zeta \rangle_{\text{tot,NM}}^\downarrow - \Delta \langle L_\zeta \rangle_{\text{tot,NM}}^\uparrow), \quad (31)$$

where

$$\Delta \langle L_\zeta \rangle_{\text{tot},X}^\sigma = \langle L_z \rangle_{\text{tot},X}^\sigma \big|_{\mathbf{M}||z} - \langle L_x \rangle_{\text{tot},X}^\sigma \big|_{\mathbf{M}||x} \quad (32)$$

is the anisotropy of the total orbital moment (the spin-σ term of its ζ component) $\langle L_\zeta \rangle_{\text{tot},X}^\sigma = \sum_{l \in X} \langle L_\zeta \rangle_l^\sigma$ in the X part of the bilayer. Thus the spin-diagonal terms of $\Omega^{(2)}$ and the MCA energy are decomposed into the contributions from the spin-up and spin-down subbands to the total orbital moments (their ζ components along $\mathbf{M}$) in Co and NM,

$$\langle L_\zeta \rangle_{\text{tot,Co}} = \langle L_\zeta \rangle_{\text{tot,Co}}^\uparrow + \langle L_\zeta \rangle_{\text{tot,Co}}^\downarrow, \quad (33)$$

$$\langle L_\zeta \rangle_{\text{tot,NM}} = \langle L_\zeta \rangle_{\text{tot,NM}}^\uparrow + \langle L_\zeta \rangle_{\text{tot,NM}}^\downarrow. \quad (34)$$

The terms $-\frac{1}{4}\xi_X \Delta \langle L_\zeta \rangle_{\text{tot},X}^\downarrow$ and $\frac{1}{4}\xi_X \Delta \langle L_\zeta \rangle_{\text{tot},X}^\uparrow$ ($X =$ Co, NM) in Eq. (31) are equal, respectively, to the $\downarrow\downarrow$ and $\uparrow\uparrow$ contributions to $E_{\text{MCA}}^{XX} + E_{\text{MCA}}^{XY}$ [Eq. (18)] which thus define the spin components of the AOM in the X layer. Accordingly, the spin-components of the total orbital moment $\langle L_\zeta \rangle_{\text{tot},X}$ in the X part of the bilayer can be expressed with the diagonal spin-pair contributions to the XX and XY components of $\Omega^{(2)} = \Omega^{(2)}(\hat{\mathbf{M}})$, namely,

$$\langle L_\zeta \rangle_{\text{tot},X}^\downarrow = -\frac{4}{\xi_X}\left[\Omega_{XX,\downarrow\downarrow}^{(2)} + \Omega_{XY,\downarrow\downarrow}^{(2)}\right] \quad (35)$$

$$\langle L_\zeta \rangle_{\text{tot},X}^\uparrow = \frac{4}{\xi_X}\left[\Omega_{XX,\uparrow\uparrow}^{(2)} + \Omega_{XY,\uparrow\uparrow}^{(2)}\right]. \quad (36)$$

where $X =$ Co, $Y =$ NM, or vice versa and the magnetization $\mathbf{M}$ is along the ζ axis.

Equations (28), (29), and their bilayer versions, Eqs. (30) and (31), are exact relations between the spin-diagonal terms of the MCA and the spin terms of the AOM, found with the PT. They are an extension of the exact relation given by van der Laan [9] which includes only one SOC constant and is strictly valid for homogenous ferromagnetic films. The presence of layer- or element-specific SOC constants makes the extended relations (28) and (29) valid for magnetic multilayers, comprising layers of two or more different elements.

If the spin-flip ($\downarrow\uparrow$ and $\uparrow\downarrow$) terms of the MCA energy are neglected, as originally done by Bruno and van der Laan [8,9],

$$E_{\text{MCA}} \approx E_{\text{MCA}}^{\downarrow\downarrow} + E_{\text{MCA}}^{\uparrow\uparrow}, \quad (37)$$

the relation (31) can be used to approximate the MCA energy as follows:

$$E_{\text{MCA}} \approx -\frac{1}{4}\xi_{\text{Co}}(\Delta \langle L_\zeta \rangle_{\text{tot,Co}}^\downarrow - \Delta \langle L_\zeta \rangle_{\text{tot,Co}}^\uparrow)$$
$$- \frac{1}{4}\xi_{\text{NM}}(\Delta \langle L_\zeta \rangle_{\text{tot,NM}}^\downarrow - \Delta \langle L_\zeta \rangle_{\text{tot,NM}}^\uparrow). \quad (38)$$

This extended approximate van der Laan relation reduces to its original form [9]

$$E_{\text{MCA}} \approx -\frac{1}{4}\xi_{\text{Co}}(\Delta \langle L_\zeta \rangle_{\text{tot,Co}}^\downarrow - \Delta \langle L_\zeta \rangle_{\text{tot,Co}}^\uparrow) \quad (39)$$

once the contributions from the SOC of NM are completely neglected. It is further simplified to the original Bruno formula [8]

$$E_{\text{MCA}} \approx -\frac{1}{4}\xi_{\text{Co}}\Delta \langle L_\zeta \rangle_{\text{tot,Co}} \quad (40)$$

when the difference of the AOM spin terms is replaced with the full AOM of Co by assuming that its spin-up term is negligible. Alternatively, the Bruno approach could be literally followed for both parts of the bilayer, by replacing, in Eq. (38), the differences $\Delta \langle L_\zeta \rangle_{\text{tot},X}^\downarrow - \Delta \langle L_\zeta \rangle_{\text{tot},X}^\uparrow$ with the full AOM $\Delta \langle L_\zeta \rangle_{\text{tot},X}$ for both $X =$ Co and $X =$ NM. As a result, the extended, partly phenomenological, Bruno relation

$$E_{\text{MCA}} \approx -\frac{1}{4}\xi_{\text{Co}}\Delta \langle L_\zeta \rangle_{\text{tot,Co}} - \frac{1}{4}\xi_{\text{NM}}\Delta \langle L_\zeta \rangle_{\text{tot,NM}} \quad (41)$$

is obtained. However, this approach is rather arbitrary since, while the minority-spin term $\Delta \langle L_\zeta \rangle_{\text{tot,Co}}^\downarrow$ is expected to be the main term in the AOM $\Delta \langle L_\zeta \rangle_{\text{tot,Co}}$ for a hard FM like Co, it is not clear whether one of the spin components $\Delta \langle L_\zeta \rangle_{\text{tot,NM}}^\sigma$ dominates in the orbital moment of NM so that one could replace such a leading term with the full AOM $\Delta \langle L_\zeta \rangle_{\text{tot,NM}}$ and neglect the term from the other spin subband.

The original Bruno relation, given by Eq. (40) for Co, has been found to be rather inaccurate for Fe films [15], however it has been shown [16] that the oscillations of the AOM $\Delta \langle L_\zeta \rangle_{\text{tot},X}$ with increasing the thickness N of a homogenous ferromagnetic Fe film well match the suitably scaled oscillatory term of the MCA energy $E_{\text{MCA}}(N)$. The extended van der Laan relation (38) has been found to give a plausible approximation for the MCA energy of the Co/Ni bilayer [23] though this may be partly due to the similar SOC of Co and Ni. For films of ferromagnetic $3d$ metals (here Co), the minority-spin band is expected to give the dominating contribution to the orbital moment, like it does for the Fe film [16]. However, the MCA energy of the Co film also includes large spin-flip terms [33] while for Co/NM layered systems including a nonmagnetic part with a strong SOC, like

the Pd/Co/Pd trilayer [31,32], there are large contributions $E_{\mathrm{MCA}}^{\sigma\sigma'}$ from all four spin pairs $(\sigma, \sigma') = \downarrow\downarrow, \downarrow\uparrow, \uparrow\downarrow, \uparrow\uparrow$. Thus the neglect of the spin-flip MCA terms can lead to largely incorrect values of the MCA energy so that the validity of the above approximate relations between the MCA and AOM is questionable for multilayer systems. These specific points and different forms of the approximate relation between the MCA and AOM are investigated for the Co/NM bilayers in Sec. III where the results of the calculations are presented and discussed. In particular, it is investigated how well the considered relations reproduce the oscillations of the MCA energy in terms of the oscillations of the AOM.

In Ref. [9], van der Laan has proposed a more accurate expression for the MCA energy of a homogenous ferromagnetic system by approximating the spin-flip contributions. This has been done by assuming a constant exchange splitting between the spin-down and spin-up energy bands and expressing the matrix element of $\mathbf{L} \cdot \mathbf{S}$ between the states of opposite spins with the matrix element of the so-called magnetic dipole term, which, for small SOC, can be represented with the quadrupole moment of the charge distribution. However, such a assumption of the rigid exchange splitting though being roughly valid for d states in the ferromagnetic 3d metals of Fe, Co, and Ni, is rather poor approximation for the Co/NM bilayers where the exchange splitting of particular states largely depends on whether they are localized mainly in Co or NM parts of the bilayer or span across the whole film. Therefore the spin-flip terms of MCA energy cannot be accounted for, even in an approximate manner, along similar lines in the investigated relation between the MCA and the AOM, though they are obviously included in the numerical calculations of the MCA energy with Eqs. (10) and (11).

D. Tight-binding model of electronic structure

In the present work, the local orbital moments and the MCA energy are determined within in the tight-binding (TB) framework. For a layered system built of transition metals, the wave functions of the electron states $|n\mathbf{k}\sigma\rangle$ with the wave vector $\mathbf{k}$ and spin σ are expressed as combinations of the Bloch basis functions $\varphi_{\mathbf{k}l\mu}^{\sigma}(\mathbf{r})$ built of atomic orbitals $\varphi_{l\mu}^{\sigma}$, proportional to the cubic harmonics $Y_{\mu}^{c}(\theta, \phi)$ with s, p and d symmetry and localized on all N_{2D} atoms j in each atomic plane l,

$$\psi_{n\mathbf{k}}^{\sigma}(\mathbf{r}) = \sum_{l\mu} a_{nl\mu}^{\sigma}(\mathbf{k}) \varphi_{\mathbf{k}l\mu}^{\sigma}(\mathbf{r})$$

$$= \sum_{l\mu} a_{nl\mu}^{\sigma}(\mathbf{k}) \left[\frac{1}{\sqrt{N_{\mathrm{2D}}}} \sum_{j} e^{i\mathbf{k}\cdot\mathbf{R}_{lj}} \varphi_{l\mu}^{\sigma}(\mathbf{r} - \mathbf{R}_{lj}) \right]. \quad (42)$$

The matrix elements of the SOC operator H_{so} between such states (with spatial integration limited to the MT spheres) are then well approximated with the site-diagonal terms found with the orbitals centered on each atom lj. Thus we obtain

$$\langle n'\mathbf{k}\sigma' | H_{\mathrm{so}} | n\mathbf{k}\sigma \rangle_{\mathrm{MT}}$$

$$= \sum_{l} \sum_{\mu\nu} \xi_{l} \left[a_{n'l\nu}^{\sigma'}(\mathbf{k}) \right]^{*} a_{nl\mu}^{\sigma}(\mathbf{k}) \langle \nu\sigma' | \mathbf{L} \cdot \mathbf{S} | \mu\sigma \rangle, \quad (43)$$

where the state $|\mu\sigma\rangle = |\mu\rangle \otimes |\sigma\rangle$ denotes the angular part of the atomic orbital, with spatial subpart $|\mu\rangle$ given by a cubic harmonic Y_{μ}^{c} in the $Oxyz$ frame of reference and the spin subpart $|\sigma\rangle$ defined in the rotated frame of reference $O\xi\eta\zeta$. A similar expression holds for the elements of the orbital moment at site (lj)

$$\langle n'\mathbf{k}\sigma | \mathbf{L}(\mathbf{r} - \mathbf{R}_{lj}) | n\mathbf{k}\sigma \rangle_{\mathrm{MT}}$$

$$= \frac{1}{N_{\mathrm{2D}}} \sum_{\mu\nu} \left[a_{n'l\nu}^{\sigma'}(\mathbf{k}) \right]^{*} a_{nl\mu}^{\sigma}(\mathbf{k}) \langle \nu | \mathbf{L} | \mu \rangle. \quad (44)$$

The expressions for the matrix elements $\langle \nu\sigma' | \mathbf{L} \cdot \mathbf{S} | \mu\sigma \rangle$ of the SOC for an arbitrary magnetization orientation defined with angles θ_M and ϕ_M are given in Ref. [49] while the matrix elements $\langle \nu | L_{\zeta} | \mu \rangle$ of the orbital angular momentum along the magnetization direction are equal to $2\langle \nu\sigma | \mathbf{L} \cdot \mathbf{S} | \mu\sigma \rangle$ with $\sigma = \uparrow$.

The amplitudes $a_{nl\mu}^{\sigma}(\mathbf{k})$ that determine the electron states in Eq. (42) and their energies $\epsilon_{n\sigma}(\mathbf{k})$ for a film with N atomic layers are found for each spin σ by diagonalizing the $9N \times 9N$ matrix $H_{l\mu,l'\nu}^{\sigma}(\mathbf{k}) = \langle \mathbf{k}l\mu\sigma | H | \mathbf{k}l'\nu\sigma \rangle$ of the unperturbed Hamiltonian H in the Bloch basis built of nine s, p, d orbitals on each site. The Hamiltonian does not include the SOC but depends on electron spin σ for a system including layers of a ferromagnetic metal. Its spin-dependence is accounted for by the exchange splitting between on-site energies $\epsilon_{l\mu}^{\downarrow}$ and $\epsilon_{l\mu}^{\uparrow}$ defined as $\epsilon_{l\mu}^{\sigma} = \epsilon_{lj\mu}^{\sigma} = \langle lj\mu\sigma | H | lj\mu\sigma \rangle$ (independent of j) for $\sigma = \downarrow, \uparrow$; these energies also determine the diagonal elements of the Hamiltonian matrix $H_{l\mu,l\mu}^{\sigma}(\mathbf{k}) = \epsilon_{l\mu}^{\sigma}$ in the Bloch representation. The off-diagonal part of the Hamiltonian matrix is found within the Slater-Koster approach using the two-center hopping integrals between the first and second nearest neighbors, which have been obtained by accurate fitting *ab initio* energy bands of bulk metals [57]. The two-center TB hopping parameters for a pair of atoms of different type at the Co/NM interface are found as the geometric mean of the corresponding hopping parameters of Co and NM, or their arithmetic mean if the two parameters are of the opposite signs [58]. Since the TB fit for ferromagnetic fcc Co is not available in Ref. [57] the two-center parameters found for paramagnetic fcc Co given therein are used instead.

The orbital energies ϵ_{μ} obtained from these fits for the paramagnetic Co and NM bulk metals are used in determining the on-site energies $\epsilon_{l\mu}^{\uparrow} = \epsilon_{\mu} + \delta\epsilon_{l\mu} - \Delta_{\mathrm{ex}}^{(l)}/2$ and $\epsilon_{l\mu}^{\downarrow} = \epsilon_{\mu} + \delta\epsilon_{l\mu} + \Delta_{\mathrm{ex}}^{(l)}/2$ [33] where the nonzero layer-dependent exchange splitting $\Delta_{\mathrm{ex}}^{(l)}$ is present in the Co atomic layers. This splitting is assumed to be proportional to the layer magnetic moment $M^{(l)}$ and set to 1.8 eV [59] with the moment of 1.57 μ_B [33] in bulk Co. The on-site energies are adjusted with layer-dependent shifts $\delta\epsilon_{l\mu}$ to provide charge neutrality in each atomic layer. These shifts also include an additional crystal splitting Δ_{cr} between d orbitals oriented out-of-plane ($yz, zx, 3z^2 - r^2$) and in-plane ($xy, x^2 - y^2$) for atoms at the Co and NM surfaces to account for the weaker average potential experienced by the orbitals with lobes pointing towards the vacuum; such a crystal splitting is also considered to be an important factor for the MCA at transition metal/oxide interfaces [11]. In the present case, the value of this splitting is approximated as $0.05W_d$ [26] with the d bandwidth W_d, equal to $W_d(\mathrm{Co}) = 4.32$ eV, $W_d(\mathrm{Pd}) = 5.50$ eV, $W_d(\mathrm{Pt}) = 7.10$ eV,
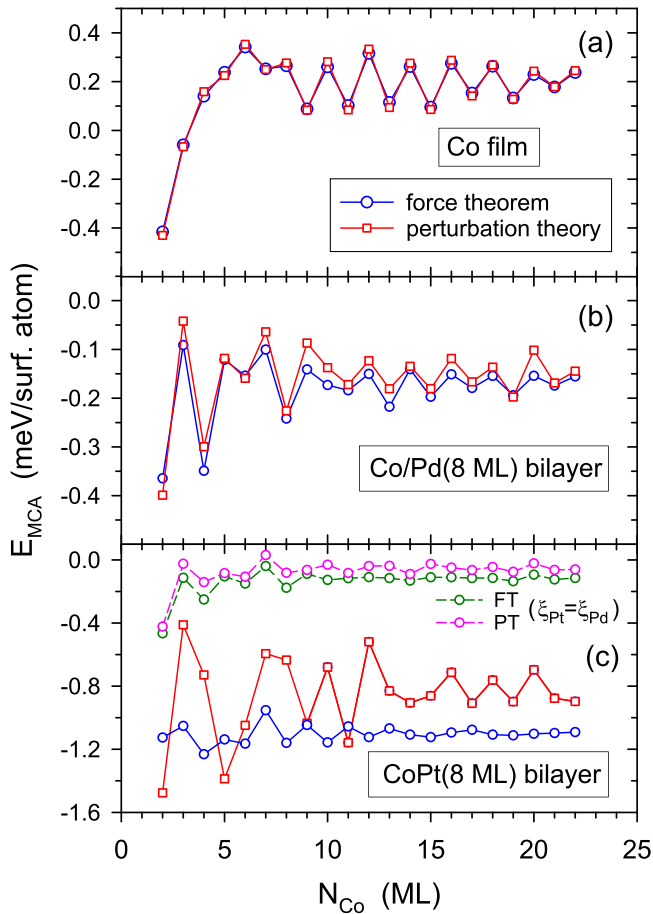
FIG. 1. MCA energy E_{MCA} calculated with the FT [Eq. (5)] and the PT [Eq. (10)] for the (001) fcc slabs: (a) Co(N_{Co} ML) film, (b) Co(N_{Co} ML)/Pd(8 ML) bilayer, and (c) Co(N_{Co} ML)/Pt(8 ML) bilayer. The dashed lines in (c) show the MCA energies obtained with the FT and PT for the Co/Pt bilayer with the decreased SOC constant of Pt, $\xi_{Pt} = \xi_{Pd}$.

as found from the TB energy bands reported for various elements in Ref. [57]. A similar splitting is set at the Co/NM interface, as the difference between the crystal splittings at the Co and NM surfaces (Co/vaccum and NM/vaccum). Accordingly, this splitting is set to $0.05[W_d(Co) − W_d(NM)]$ in the Co interface atomic layer and $0.05[W_d(NM) − W_d(Co)]$ in the NM interface atomic layer [2]. Further details of the applied TB model can be found in Refs. [33,58]. The SOC constants assumed for the d bands of Co, Pd, and Pt metals are $\xi_{Co} = 0.085$ eV, $\xi_{Pd} = 0.23$ eV, and $\xi_{Pt} = 0.65$ eV, respectively [2,32,58].

III. RESULTS

The calculations of the MCA energy and the orbital moments are performed for the (001) fcc Co film and the (001) fcc Co/NM bilayers with the nommagnetic layers of the Pd and Pt metals which both have d states at the Fermi level. The investigated systems have the Co layer with the thickness N_{Co} from 2 to 22 ML and the Pd and Pt overlayers which are 8 ML thick. The converged results are obtained by summing, in Eqs. (7), (8), (11), (19), and (21) over the 60 × 60 (100 × 100
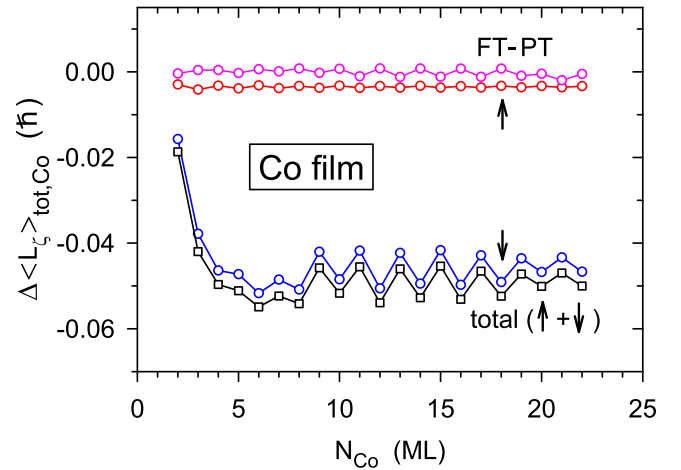
FIG. 2. AOM (per surface atom) and its terms coming from the spin-down and spin-up energy bands obtained for the (001) fcc Co(N_{Co} ML) film with the PT and the difference of the AOM obtained with the FT and the PT.

for the Co/Pt bilayers) **k** points in the full two-dimensional BZ for the finite temperature of $T = 300$ K. The BZ is of the square shape and corresponds to the unit cell of the square lattice formed by first nearest neighbours in the (001) atomic planes. Its lattice constant is $a_{2d} = a/\sqrt{2}$, expressed with the fcc lattice constant a, and the primitive vectors that define the unit cell are $(a/2, −a/2, 0)$ and $(a/2, a/2, 0)$. The MCA energies obtained for these systems with the FT [Eq. (5)] and the PT [Eq. (10)] are shown in Fig. 1.

The spin magnetic moment is also determined in the calculations and it is found to be enhanced to $1.80 \mu_B$ at the Co surface layer and nearly equal to the bulk moment ($1.57 \mu_B$) in the interior Co layers. This result is in very good agreement with the *ab initio* calculations which also predict the enhanced Co moments at the (001) surface of the fcc Co, e.g., the moment of $1.84 \mu_B$ is reported in Ref. [60]. In addition, small moments of $0.22 \mu_B$ and $0.06 \mu_B$, induced by the proximity effect, are presently obtained in the first and second Pd layers closest to the Co/Pd interface, and slightly smaller moments of $0.20 \mu_B$ and $0.03 \mu_B$ are in the first two Pt layers at the Co/Pt interface. Similar spin moments in the first interface Pd layer, $0.25 \mu_B$ and $0.3 \mu_B$, are found for (111) fcc Co/Pd multilayers in the XMCD experiment and with the DFT calculations, respectively [21]. Also, the Pt moment of $0.3 \mu_B$ at the Fe/Pt(001) interface has been obtained in the *ab initio* calculations reported in Ref. [42].

A. Oscillations of MCA energy and orbital moment in Co film

The MCA energy and the AOM obtained with the FT [Eqs. (5) and (19)] for the Co films follow very closely the respective quantities found with the PT approach [Eqs. (10) and (21)]; see Figs. 1 and 2. Thus the PT formulation is valid for these films and it will be used in the following discussion. The mean value of the MCA energy obtained for the Co film, around 0.2 meV (per surface atom) or 0.1 meV for each Co surface, well agrees with the mean contribution of around 0.17 meV from the Co surface (the Co/vaccum interface) which can be derived from the results of the *ab*
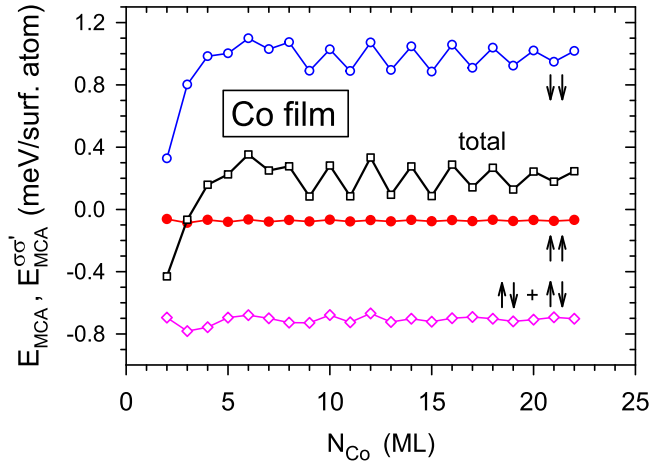
FIG. 3. MCA energy E_{MCA} and its spin-pair contributions $E_{\text{MCA}}^{\downarrow\downarrow}$, $E_{\text{MCA}}^{\uparrow\uparrow}$, $E_{\text{MCA}}^{\downarrow\uparrow}$, $E_{\text{MCA}}^{\uparrow\downarrow} + E_{\text{MCA}}^{\downarrow\uparrow} = 2E_{\text{MCA}}^{\downarrow\uparrow}$ obtained for the (001) fcc Co(N_{Co} ML) film with the PT.

initio calculations for the MCA energies of the Co/Cu(001) and Cu/Co/Cu(001) fcc systems [30]. A very similar *ab initio* result, with the mean MCA energy of 0.35 meV for the (001) fcc Co slab, was obtained in another DFT calculation [61], while a slightly higher mean value of 0.5 meV is reported in

Ref. [13] (note the opposite sign convention for the MCA energy used in Refs. [30,61]). The results found for the Co(N_{Co} ML) film (Figs. 2 and 3) show that the MCA energy and the AOM oscillate with increasing the Co thickness N_{Co} in similar way, with the dominant oscillation period close to 2 ML. The magnetic anisotropy oscillations with the 2 ML period have been predicted theoretically in the previous TB [33] and *ab initio* calculations [13,30,61], and later confirmed experimentally for Co films on vicinal Cu substrate [28].

The oscillations of the MCA energy of the (001) fcc Co film have been analyzed in detail in Ref. [33] and have been shown to come mainly from the pairs of QW states which have wave vectors in the vicinity of the $\overline{\Gamma}$ point [$\mathbf{k} = (0, 0)$] in the two-dimensional BZ and are degenerate at this point. Their energies move with increasing the Co thickness and, according to Eq. (11), a pair of such states gives a large contribution to E_{MCA} when one of them is above and the other below the Fermi energy ϵ_F for $\mathbf{k}$ close to $\overline{\Gamma}$. These states originate from the minority-spin bulk d band of the Δ_5 symmetry and are composed of the yz and xz orbitals mainly. The periods of MCA energy oscillations are determined by the extremal dimensions k_{z0} of the three-dimensional Fermi surface [31–33], in particular, at the high-symmetry $\mathbf{k} = (k_x, k_y)$ points, in a similar way as the oscillation periods of interlayer exchange coupling in FM/NM/FM structures [34].
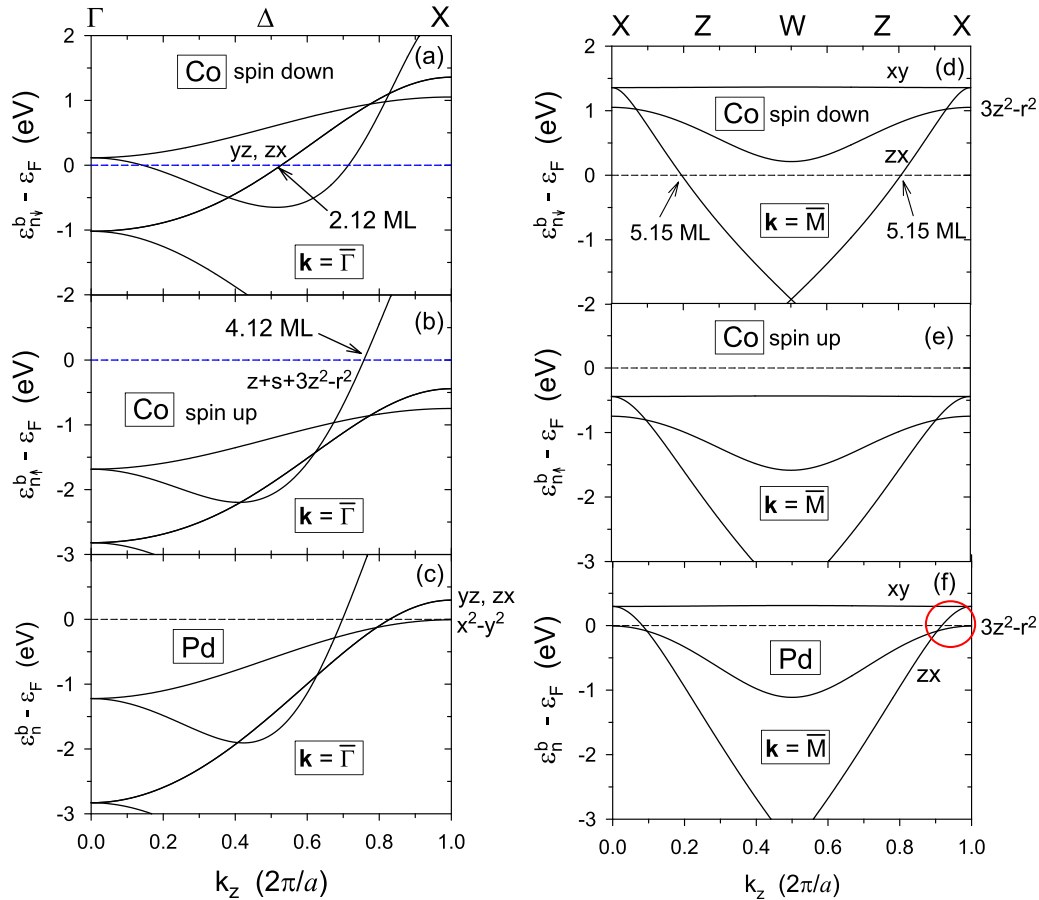

FIG. 4. Energy bands $\epsilon_{n\downarrow}^{b}(\mathbf{k}, k_z)$ along the [(a)–(c)] ΓX and [(d)–(f)] XW lines in the three-dimensional BZ for bulk fcc [(a), (b), (d), and (e)] Co and [(c) and (f)] Pd. The extremal dimensions $k_z = k_{z0}$ of the Co Fermi surface that correspond to the 2.12 ML, 4.12 ML, and 5.15 ML periods are marked.
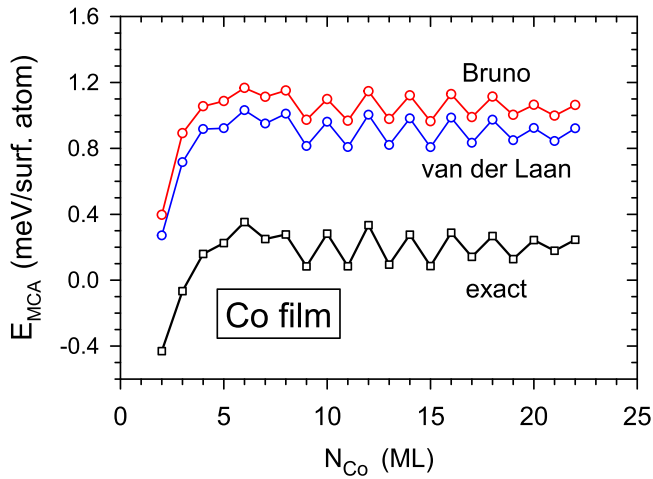
FIG. 5. MCA energy (squares) for the (001) fcc Co(N_{Co} ML) film, calculated with the PT, and its approximations (circles) obtained with the original Bruno and van der Laan relations, Eqs. (40) and (39), respectively.

These specific values of $k_z = k_{z0}$ correspond to the locations where the energy bands $\epsilon_{n\sigma}^{b}(\mathbf{k}, k_z)$ of bulk Co cross the Fermi energy as marked in Fig. 4. Since the applied TB model reproduces the bulk band structure very accurately the same applies to the oscillation periods determined with the extremal dimensions of the respective Fermi surface. In the present case, the extremal dimension for the relevant sheet of the three-dimensional Fermi surface at $\mathbf{k} = \overline{\Gamma}$ is $k_{z0} = 0.528\frac{2\pi}{a}$ which gives the exact oscillation period of 2.12 ML [33]. The variation of the MCA energy also includes the second minor oscillatory term with the oscillation period of 5.15 ML which comes the minority-spin QW states that originate from the Co bulk band with the zx symmetry on the XW line in the three-dimensional BZ [Fig. 4(d)]. These QW states are close to the $\overline{M}$ point at $\mathbf{k} = (k_x', k_y') = (1, 1)(\pi/a_{2d})$ as well as three other equivalent points at the corners of the square two-dimensional BZ. Here, the wave vectors are expressed in the rotated frame of reference with the x' and y' axes along the $(1\overline{1}0)$ and (110) directions, respectively, while the original x and y axes are oriented along the (001) and (010) directions.

The MCA oscillations come almost entirely from the minority-spin diagonal contribution $E_{MCA}^{\downarrow\downarrow}$ (Fig. 3) which also determines the minority-spin term of the anisotropy $\Delta\langle L_\zeta\rangle_{tot,Co}^{\downarrow} = -(4/\xi_{Co})E_{MCA}^{\downarrow\downarrow}$ of the total Co orbital moment while its majority-spin term $\Delta\langle L_\zeta\rangle_{tot,Co}^{\uparrow} = (4/\xi_{Co})E_{MCA}^{\uparrow\uparrow}$ [see Eqs. (35), (36) for the pure Co film] is virtually independent of the Co thickness; Fig. 2. As a result, the oscillatory part of the MCA energy is accurately reproduced by both the sum of the two terms $\Delta\langle L_\zeta\rangle_{tot,Co}^{\downarrow} + \Delta\langle L_\zeta\rangle_{tot,Co}^{\uparrow} = \Delta\langle L_\zeta\rangle_{tot,Co}$, i.e., the AOM of Co, and their difference $\Delta\langle L_\zeta\rangle_{tot,Co}^{\downarrow} - \Delta\langle L_\zeta\rangle_{tot,Co}^{\uparrow}$, with the scaling factor of $4/\xi_{Co}$. Thus the Bruno relation (40) and the van der Laan relation (39) are very well satisfied up to a constant shift for the pure Co film if the variations of the MCA energy, the AOM and its spin terms with increasing the Co thickness are concerned; see Fig. 5. The small difference between the predictions of the two relations reflects the almost negligible contribution of the majority-spin band to the orbital moment.
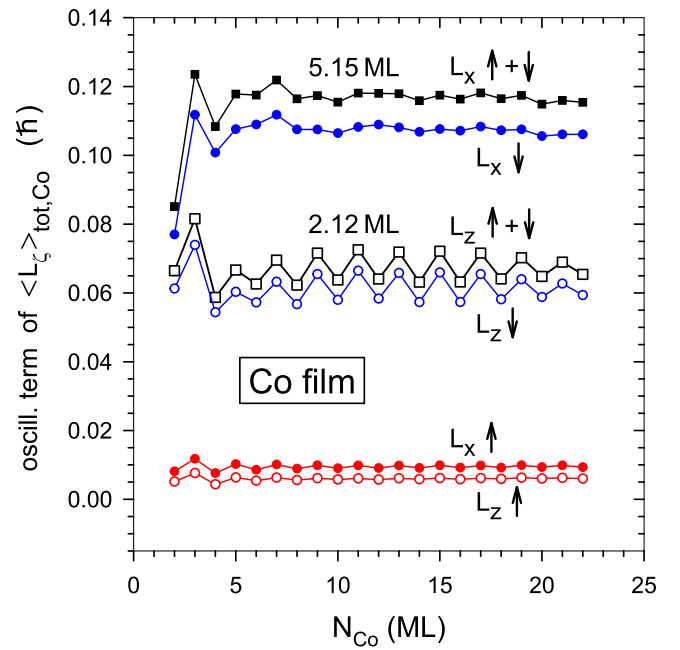

FIG. 6. Oscillatory term (including the constant part) of the total orbital moment (per surface atom) along the magnetization $\mathbf{M}$, calculated with the PT, and the respective terms of the spin-up and spin-down band contributions to this moment for the (001) fcc Co(N_{Co}ML) film with $\mathbf{M}||\mathbf{z}$ (open symbols) and $\mathbf{M}||\mathbf{x}$ (closed symbols). The plots are obtained by subtracting the linear term bN_{Co} with $b = 0.1030\,\hbar$ from the moment $\langle L_\zeta\rangle_{tot,Co}$ and the terms $b^\sigma N_{Co}$ with $b^\downarrow = 0.1122\,\hbar$ and $b^\uparrow = -0.0092\,\hbar$ from its spin components $\langle L_\zeta\rangle_{tot,Co}^{\sigma}$.

The finite orbital moments due to the SOC are present in all Co atomic layers and differ significantly from their bulk value only very close to the Co film surfaces (cf. Sec. III D). Thus the spatial distribution of the AOM is strongly localized at the surfaces, in a similar way, as reported for Fe films [16]. Since the total orbital moment $\langle L_\zeta\rangle_{tot,Co}$ of the Co film grows almost linearly with increasing the film thickness, a linear term bN_{Co}, with parameter b representing the atomic orbital moment in bulk fcc Co (independent of the magnetization direction ζ in the leading order of the SOC), can be subtracted from $\langle L_\zeta\rangle_{tot,Co}$ to investigate the oscillations of this moment separately for specific orientations ζ of magnetization. The remaining part $c_\zeta + \langle L_\zeta\rangle_{tot,Co}^{osc}$ of the total orbital moment (Fig. 6) has two terms. The constant term c_ζ is larger for the in-plane direction of the magnetization than for its out-of-plane direction, thus leading to the negative AOM, as seen in Fig. 2. The other term $\langle L_\zeta\rangle_{tot,Co}^{osc}$ oscillates with the 2 ML period for the out-plane orientation of magnetization (the z direction) and has smaller oscillations with period of around 5 ML for its in-plane direction (along the x axis) while the difference between the oscillatory terms $\langle L_\zeta\rangle_{tot,Co}^{osc}$ for the two magnetization directions gives the oscillatory part of the full AOM $\Delta\langle L\rangle_{tot,Co}$.

This interesting finding is the result of the symmetry of the QW states which lead to the oscillations of the MCA energy and the AOM. In particular, the pairs of the minority-spin states close to the $\overline{\Gamma}$ point that are responsible for the dominating 2 ML oscillatory term are built of the yz and zx orbitals.

As a result, they contribute to the MCA energy and the orbital moment only for the out-of-plane magnetization direction ($\zeta = z$) since the respective matrix elements $\langle \mu \downarrow | \mathbf{L} \cdot \mathbf{S} | \nu \downarrow \rangle = \langle \mu \downarrow | L_\zeta S_\zeta | \nu \downarrow \rangle = -\frac{1}{2} \langle \mu | L_\zeta | \nu \rangle$ and $\langle \mu | L_\zeta | \nu \rangle$ vanish for the in-plane direction ($\zeta = x$, and also for $\zeta = y$). Indeed, the two orbitals can be represented as $|yz\rangle = \frac{i}{\sqrt{2}} (|2, -1\rangle + |2, 1\rangle)$ and $|zx\rangle = \frac{1}{\sqrt{2}} (|2, -1\rangle - |2, 1\rangle)$ by the eigenstates $|L, m_L\rangle$ of $\mathbf{L}^2$ and L_z with the orbital number L and the magnetic number m_L. Accordingly, the matrix elements $\langle \mu | L_\zeta | \nu \rangle$ are finite for $L_\zeta = L_z$ with $\mu = yz$, $\nu = zx$ and $\mu = zx$, $\nu = yz$, and vanish for $L_\zeta = L_x = (L_+ + L_-)/2$ (or $L_\zeta = L_y$) since the states $L_+ |L, m_L\rangle \sim |L, m_L + 1\rangle$ and $L_- |L, m_L\rangle \sim |L, m_L - 1\rangle$ with $m_L = \pm 1$ have even magnetic numbers (-2, 0, or 2) so that $L_+ |\nu\rangle$ is orthogonal to $|\mu\rangle$ for any combination of $\mu, \nu = yz, zx$.

On the other hand, the minority-spin QW states $|n\mathbf{k} \downarrow\rangle$ with $\mathbf{k}$ close to the $\overline{M}$ point that cross the Fermi energy at regularly spaced Co thicknesses with the period of 5.15 ML [33] are built mainly of the zx orbital, for the $\overline{M}$ points at $k_x = \pm 2\pi/a$, $k_y = 0$, or the yz orbital for the equivalent points at $k_x = 0$, $k_y = \pm 2\pi/a$ (i.e., the corners of the two-dimensional BZ at $k'_x = \pm \pi/a_{2d}$, $k'_y = \pm \pi/a_{2d}$). According to the band structure of bulk Co shown in Fig. 4(d), a QW state $|n\mathbf{k} \downarrow\rangle$ derived from the minority-spin bulk band with the zx symmetry ($m_L = \pm 1$) close to the Fermi level can couple to other QW minority-spin states $|n'\mathbf{k} \downarrow\rangle$ built of either the $3z^2 - r^2$ orbital (with small addition of s and z components) with $m_L = 0$ or the xy orbital with $m_L = \pm 2$. However, such a coupling is finite only for the operator $L_x = (L_+ + L_-)/2$ which changes the magnetic number m_L by ± 1 while the matrix elements of L_z vanish for both pairs of the QW states. Thus the matrix elements of the operators $\mathbf{L} \cdot \mathbf{S}$ (reducing to $-\frac{1}{2} L_\zeta$ for states with the minority spin) and L_ζ between such QW states $|n\mathbf{k} \downarrow\rangle$ and $|n'\mathbf{k} \downarrow\rangle$ with $\mathbf{k}$ close to $\overline{M}$ are finite for the in-plane direction of magnetization ($\zeta = x$) but vanish for its out-of-plane direction ($\zeta = z$) which explains why the 5.15 ML period oscillations of the orbital moment, calculated with Eq. (21), are present only for the in-plane magnetization direction.

In this way, the AOM oscillations due to the QW states which come from the vicinities of the $\overline{\Gamma}$ and $\overline{M}$ points, can be separated in the orbital moment of the Co film since only one type of the QW states manifests itself for specific orientation ζ of magnetization, as an oscillatory variation of the orbital moment $\langle L_\zeta \rangle_{\text{tot,Co}}$ with the respective oscillation period, 2 ML for $\zeta = z$ and 5 ML $\zeta = x$; see Fig. 6.

Let us also note that the oscillation amplitudes of the MCA energy and the total orbital moment in the Co film, both calculated per surface atom, decay slowly with increasing the film thickness. If the average atomic moment $\langle L_\zeta \rangle_{\text{Co}} = \langle L \rangle_{\text{tot,Co}}/N_{\text{Co}}$ (per atom in the film volume) is considered, its oscillations are additionally damped by $1/N_{\text{Co}}$ factor.

B. Co/Pd bilayers

1. Magnetic anisotropy: surface, interface, and volume terms. Comparison with experiment

The MCA energy of the Co(N_{Co} ML)/Pd(8 ML) bilayer is negative (Fig. 1) and thus promotes the out-of-plane orientation of magnetization. It counteracts the shape anisotropy which favours the in-plane magnetization direction and prevails for thicker Co layers as the magnetic dipole-dipole energy (per surface atom) grows linearly with increasing N_{Co}.

Apart from the shape anisotropy, the total anisotropy energy in Co/Pd layered systems can include another positive volume term which is the part of the MCA energy due to the tetragonal distortion of the Co fcc lattice resulting from the lattice mismatch between Co and Pd [62]. Such a volume MCA term, linear in the Co thickness, is found, e.g., in the *ab initio* calculations for a (111) fcc Co/Pd superlattice [21] (note the MCA energy is defined with the opposite sign in Refs. [21,39,41,42]). For the Co/Pd bilayer, the strain due to the lattice distortion can gradually relax with increasing the Co thickness [62] which would make the description of the MCA even more complex. Thus, for the sake of simplicity, the effect of the lattice mismatch is not taken into account in the present calculations so that this investigation is focused, in fact, on the parts of the MCA energy, the orbital moments and the AOM that come from the Co surface and the Co/Pd interface (the same applies to the Co/Pt bilayer discussed in Sec. III C).

The MCA contribution from the Co/Pd interface can be estimated by subtracting, from the MCA energy of the Co/Pd bilayer, the Co surface contribution, calculated as half the MCA energy of the Co film. Thus we obtain the mean value of the Co/Pd interface contribution equal to around -0.25 meV (per surface atom) which can also be expressed as -0.64 erg/cm^2 (using the experimental value of $a = 3.55$ Å for fcc Co [63]). In experiment, it has been observed [64] that while the volume term of Co/Pd multilayers strongly depends in their surface orientation, the Co/Pd interface term is very similar for different orientations and equal to -0.65 erg/cm^2, very close to the theoretical value presently obtained.

2. Intraband contribution to MCA energy

The MCA energies obtained with the FT and PT formulations [Eqs. (5) and (10), respectively] are very close to each other also for the Co/Pd(8 ML) bilayers (Fig. 1) so the results of the PT approach can be used to analyze the MCA energy of this system. The intraband part of this energy, given the sum of the diagonal terms, with $(n\sigma) = (n'\sigma')$, in the PT expression (11), is finite for the Co/Pd bilayers due to the absence of the inversion symmetry, as argued in Sec. II A. The inclusion of the diagonal terms is, in fact, vital to obtain the correct value of the MCA energy. Indeed, the intraband part of this energy, coming from the contribution from the first-order corrections $\epsilon_{n\sigma}^{(1)}$ of the state energies to the second-order correction $\Omega^{(2)}$, largely cancels the interband (off-diagonal) term of the MCA energy, coming directly from the second-order corrections $\epsilon_{n\sigma}^{(2)}$, so that the resultant MCA energy has much smaller magnitude than each of the two contributions; see Fig. 7. However, it is the interband term that it is mainly responsible for the oscillations of the MCA energy, which confirms the role of the pairs of states in leading to the MCA oscillations, as previously identified in Refs. [31–33] for the Co films and the symmetric Co/Pd/Co trilayers, i.e., the systems with the inversion symmetry where the intraband term of the MCA energy is absent. A more detailed analysis also shows that
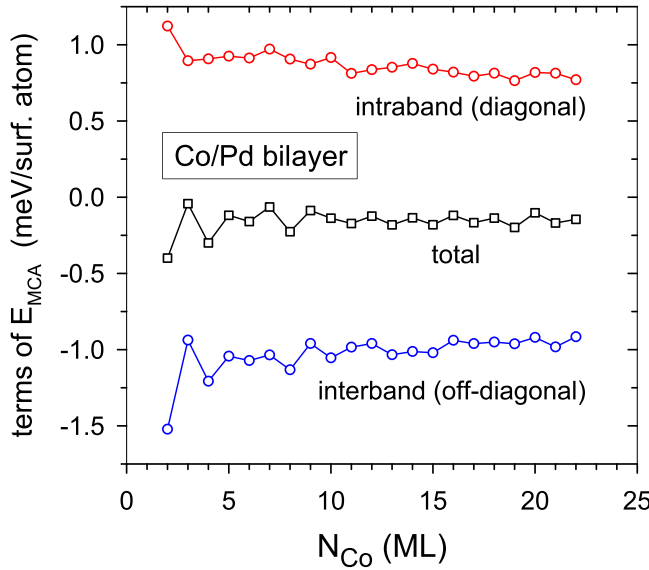
FIG. 7. Intraband and interband parts of the MCA energy which come, respectively, from the diagonal and off-diagonal terms in Eq. (11) for the (001) fcc Co(N_{Co} ML)/Pd(8 ML) bilayer within the PT.

the contribution from degenerate states [which formally contribute to both the diagonal and off-diagonal terms of $\Omega^{(2)}$ in Eq. (11)] is negligible for the applied number N_{2D} of **k** points and is expected to vanish in the limit $N_{2D} \to \infty$ since the degenerate states present on the high-symmetry lines of the BZ cross the Fermi level at discrete number of **k** points. Thus the intraband part of the MCA energy for the Co/Pd bilayers comes from nondegenerate states with energies very close to ϵ_F and wave vectors at or very close to the Fermi surface (forming lines in the two-dimensional BZ) due to the presence of the factor $f'_0(\epsilon_{n\sigma}(\mathbf{k}))$ in the diagonal terms of $\Omega^{(2)}$. It is also seen in Fig. 7 that while the MCA energy tends to a constant value with increasing the Co thickness, its intraband and interband terms are not exactly constant since both parts have contributions which are roughly linear in the investigated range of the Co thickness but fully cancel out.

3. Spin-pair and element-pair terms of MCA energy

It is found within the PT that unlike for the Co film the MCA energy of the Co/Pd bilayer has large contributions $E_{MCA}^{\sigma\sigma'}$ from pairs of states $|n\mathbf{k}\sigma\rangle$ and $|n'\mathbf{k}\sigma'\rangle$ with all four combinations of spins σ and σ' (Fig. 8). Also, all the spin-pair contributions to the MCA energy oscillate strongly with increasing the thickness of the Co layer but the oscillations cancel out largely once these contributions are summed up so that the resulting total MCA energy oscillates with a much smaller amplitude. The variations of $E_{MCA}^{\sigma\sigma'}(N_{Co})$ include oscillations with different periods which correspond to the extremal dimensions k_{z0} of the three-dimensional Fermi surface at the $\mathbf{k} = \overline{\Gamma}$ and $\overline{M}$ points of the two-dimensional BZ; the identified exact periods are 2.12 ML (at $\overline{\Gamma}$) and 5.15 ML (at $\overline{M}$) for minority spin [33] as well as 4.12 ML (at $\overline{\Gamma}$) for majority spin [65]; see Fig. 4. The oscillations with the respective periods not only are present in the diagonal ($\downarrow\downarrow$ and $\uparrow\uparrow$) spin-pair contributions to the MCA energy, but also occur
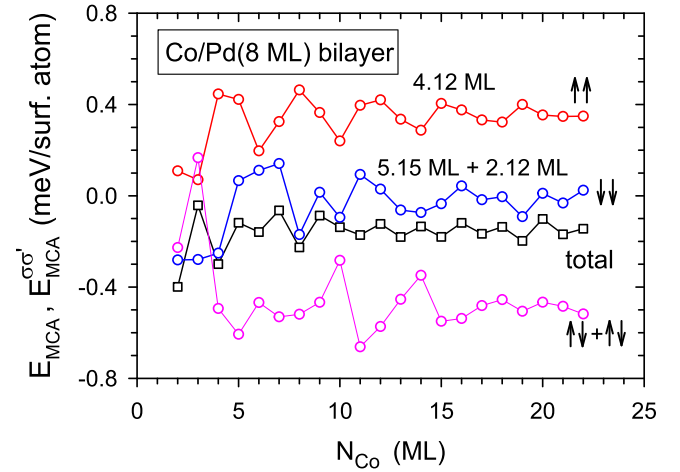

FIG. 8. MCA energy E_{MCA} and the spin-pair contributions $E_{MCA}^{\sigma\sigma'}$ for the (001) fcc Co(N_{Co} ML)/Pd(8 ML) bilayer, obtained with the PT. The periods of the QW states contributing to the oscillations are marked.

in the spin-flip ($\downarrow\uparrow$ and $\uparrow\downarrow$) contributions (Fig. 8) since the relevant states spanning over the whole bilayer are built of the QW states in Co hybridized with d states in Pd and, as a result, they can strongly couple, via the SOC of Pd, to other states of both spins, with large d component in Pd and energies close to the Fermi level (a similar mechanism was previously found [29] for Co/Cu bilayers where d states in Co, hybridized with sp QW states in Cu, mediate in the emergence of MCA oscillations versus the Cu thickness). However, the oscillatory MCA terms with periods other than the shortest one cancel out largely in the sum of the spin-pair contributions so that the resulting energy $E_{MCA}(N_{Co})$ has oscillations with a clear period close to 2 ML similar to the MCA energy of the pure Co film.

To understand why such a cancellation takes place we first decompose the MCA energy into the XY parts E_{MCA}^{XY} and examine their spin-pair terms $E_{MCA}^{XY,\sigma\sigma'}$; Figs. 9 and 10. It is found that while the 2 ML oscillations come from both the $XY =$ CoCo and CoPd (PdCo) parts of the MCA energy they are nearly absent in the $XY =$ PdPd part, and all its spin-pair terms $E_{MCA}^{PdPd,\sigma\sigma'}$, which means that the contribution from the states in Pd that hybridize with the 2 ML period QW states in Co is small. The oscillations of the spin-pair terms $E_{MCA}^{\sigma\sigma'}$ with the two longer periods, 4.12 and 5.15 ML, come mainly from the Pd part of the Co/Pd bilayer, since they are present only in the variations of $E_{MCA}^{XY,\sigma\sigma'}(N_{Co})$ for $XY =$ PdPd. Since d states of both spins are present in Pd near the Fermi level, a minority-spin state $|n\mathbf{k}\downarrow\rangle$ composed of the 5.15 ML period QW state in Co hybridized with a state in Pd can lead to similar contributions when it couples to other minority- and majority-spin states $|n'\mathbf{k}\sigma'\rangle$ with large amplitude in Pd. However, these contributions to the MCA energy are of the opposite signs for $\sigma' = \downarrow$ and $\sigma' = \uparrow$ so they oscillate in antiphase. Indeed, the minority-spin state of the 5.15 ML period is built of zx orbitals, with $m_L = \pm 1$, so when the SOC couples this state to another state with the same $m_L = \pm 1$ the SOC operator $\mathbf{L} \cdot \mathbf{S}$ is effectively reduced to $L_z S_z$ as the matrix elements of L_+ and L_- vanish. Thus,
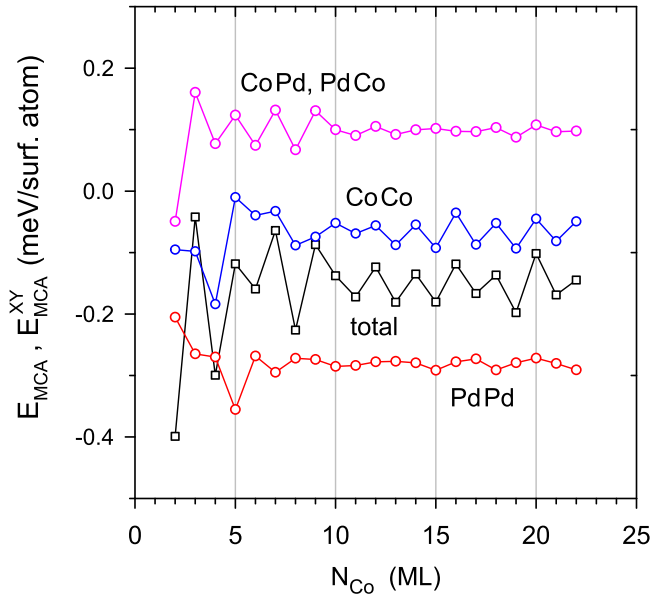
FIG. 9. The XY contributions to the MCA energy from the SOC in the X and Y parts of the (001) fcc Co(N_{Co} ML)/Pd(8 ML) bilayer, obtained with the PT.
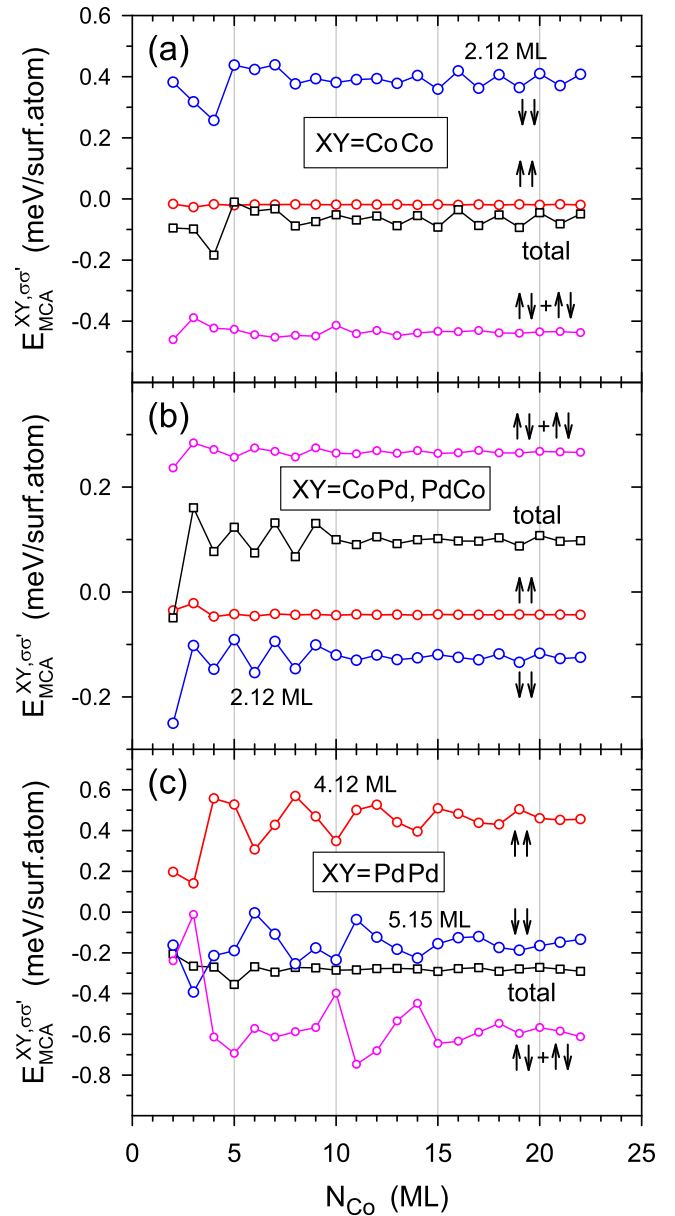

FIG. 10. Spin-pair terms (circles) of the XY contributions (squares) to the MCA energy from the SOC in the X and Y parts of the (001) fcc Co(N_{Co} ML)/Pd(8 ML) bilayer; (a) XY=CoCo, (b) XY = CoPd, PdCo, and (c) XY = PdPd. The results are obtained with the PT.

if the two states have the same, minority, spin, the coupling (matrix element of H_{so}) is finite only for $\zeta = z$ magnetization direction (in this case $L_z S_z = L_z S_\zeta$), while if their spins are different the coupling is finite for only $\zeta = x$ since then we have $L_z S_z \sim L_z(S'_+ - S'_-)$. As a result, such two pairs of states, one with $\sigma = \sigma' = \downarrow$ and the other with $\sigma = \downarrow, \sigma' = \uparrow$, lead to the contributions of opposite signs in the MCA energy defined as the difference of $\Omega^{(2)}(\hat{\mathbf{M}})$ for the two magnetization directions, $\zeta = z$ and $\zeta = x$, in Eq. (10). The situation is reversed, if the minority-spin state $|n\mathbf{k} \downarrow\rangle$ of the zx symmetry is coupled to a state $|n'\mathbf{k}\sigma'\rangle$ built of the orbitals with $m_L = 0$ or $m_L = \pm 2$, since in this case the finite contribution to $\Omega^{(2)}$ comes from the pair of states with the same spins for $\zeta = x$ only and the pair with the opposite spins only for $\zeta = z$. However, this again leads to respective contributions with opposite signs for $\sigma' = \downarrow$ and $\sigma' = \uparrow$ in the MCA energy. Similar conclusions can also be drawn for the contributions from the 4.12 ML period QW state in Co with majority-spin which can couple to states of minority and majority spins with large amplitude in Pd. As a result, the oscillations of the different spin-pair contributions in E_{MCA}^{PdPd} largely cancel out so that this term varies only slightly with increasing the Co thickness (Fig. 10).

Thus it is the contribution E_{MCA}^{CoCo} to the MCA from SOC in Co and, for $N_{Co} < 10$ ML, also the mixed contribution $E_{MCA}^{CoPd} + E_{MCA}^{PdCo} = 2E_{MCA}^{CoPd}$, due to the SOC in Co and Pd, that are almost entirely responsible for the 2 ML period oscillations of the total MCA energy with increasing N_{Co}. The analysis done in Fig. 10 reveals that it is mainly the $\downarrow\downarrow$ contributions to the terms E_{MCA}^{CoCo} and $E_{MCA}^{CoPd} + E_{MCA}^{PdCo}$ from the pairs of minority-spin states, and, to a lesser extent, the $\downarrow\uparrow$ and $\uparrow\downarrow$ contributions to these terms from pairs of states with opposite spins, that give rise to the obtained variation of $E_{MCA}(N_{Co})$ while the $\uparrow\uparrow$ contributions from the pairs of majority-spin states are small and almost independent of N_{Co}.

Although the oscillations of E_{MCA}^{PdPd} are almost canceled out, the XY = PdPd part of the MCA energy, which originates from the large SOC of the Pd layer, is still the largest, and clearly negative, contribution to this energy. This term is finite, since the electrons with majority and minority spins have different wave functions in the Pd part of the bilayer. The reason for this difference is that they are subject to different boundary conditions at the Co/Pd interface due to the different effective potentials in the ferromagnetic Co part [32] (in the absence of the adjacent Co layer, the MCA energy of a paramagnetic Pd slab, with identical spin-down and spin-up energy bands, vanishes since its spin-pair terms contributions, though finite, cancel completely).
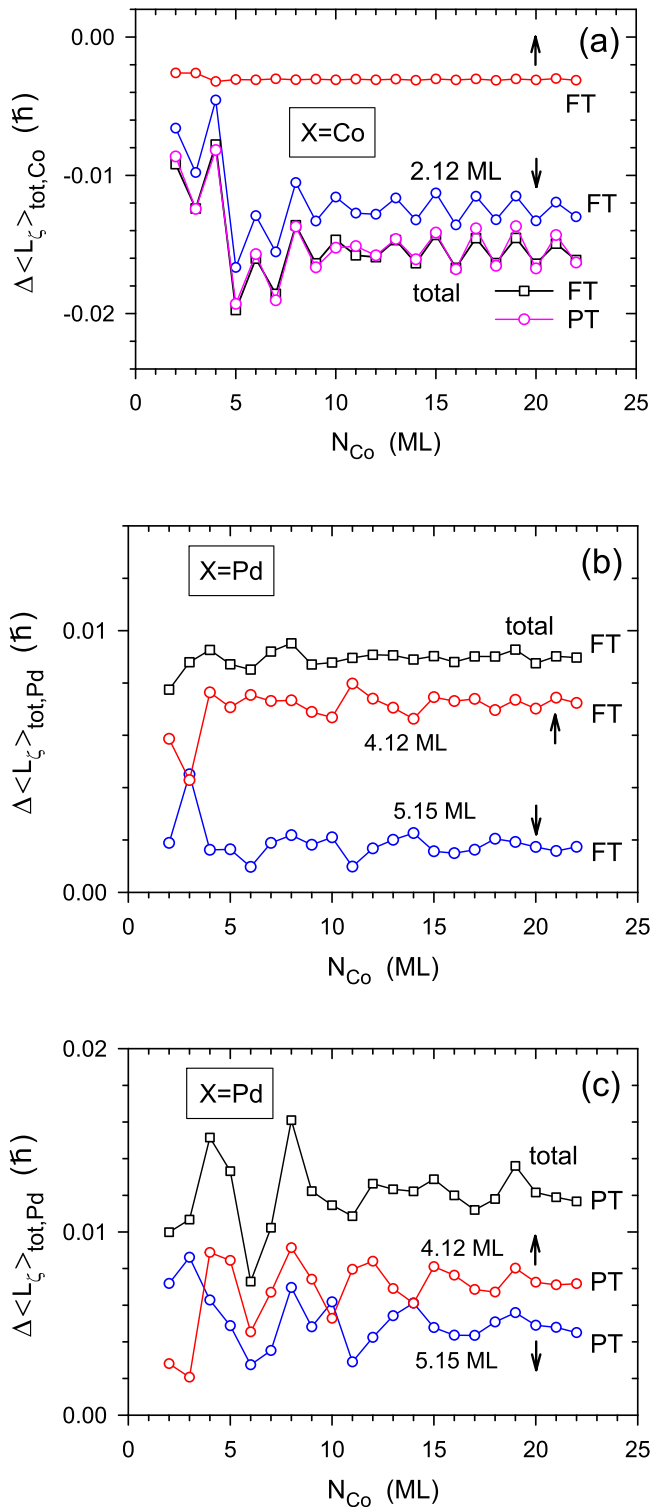
FIG. 11. AOM (per surface atom) in (a) Co and [(b) and (c)] Pd parts of the (001) fcc Co(N_{Co} ML)/Pd(8 ML) bilayer obtained with [(a) and (b)] the FT approach and [(a) and (c)] the PT and the contributions to this AOM from the minority-spin and majority-spin energy bands.

For the same reason, the total orbital moment in Pd and, consequently, the AOM in Pd are finite (Fig. 11) since the moment $\langle L_\zeta \rangle_{tot,Pd} = \langle L_\zeta \rangle^\downarrow_{tot,Pd} + \langle L_\zeta \rangle^\uparrow_{tot,Pd}$ calculated with the

PT is proportional to the difference of the ↑↑ and ↓↓ contributions to the sum of the PdPd and PdCo components of $\Omega^{(2)}$ [Eqs. (35) and (36)]; for a freestanding Pd slab its orbital moment is proportional to $\Omega^{(2)}_{\uparrow\uparrow} - \Omega^{(2)}_{\downarrow\downarrow}$ and vanishes. Another consequence of the spin-dependent boundary conditions due to the presence of the ferromagnetic Co layer is the small spin magnetic moments induced in the Pd atomic layers closest to the Co/Pd interface, 0.22 μ_B in the first Pd layer and 0.06 μ_B in the second layer, as presently found.

4. Validity of Bruno and van der Laan relations, and their extensions. Anisotropy of orbital moments

Equation (31) is the relation, derived with the PT, between the sum of diagonal spin-pair (↑↑ and ↓↓) parts of the MCA energy and the spin components of the AOM in Co and Pd. The two terms in this relation, $-\frac{1}{4}\xi_{Co}[\Delta\langle L_\zeta\rangle^\downarrow_{tot,Co} - \Delta\langle L_\zeta\rangle^\uparrow_{tot,Co}]$ and $-\frac{1}{4}\xi_{Pd}[\Delta\langle L_\zeta\rangle^\downarrow_{tot,Pd} - \Delta\langle L_\zeta\rangle^\uparrow_{tot,Pd}]$, represent the sums of the ↓↓ and ↑↑ contributions to the $E^{CoCo}_{MCA} + E^{CoPd}_{MCA}$ and $E^{PdPd}_{MCA} + E^{PdCo}_{MCA}$ components of the MCA energy, respectively. In the first term, the difference of the two spin components of the AOM in Co can be replaced, to a good approximation, by the full AOM in Co (i.e., the sum of these AOM components) since the majority-spin term of the AOM in Co is much smaller than the minority-spin one and almost independent of the Co thickness (Fig. 11).

In an attempt to establish an approximate relation between the full MCA energy and the AOM we first need to add the spin-flip (↓↑ and ↑↓) parts of this energy to both sides of Eq. (31) so that its left-hand side becomes E_{MCA}. The CoCo and CoPd components of these spin-flip MCA terms, or in other words, the spin-flip contributions to the CoCo and CoPd components of E_{MCA}, vary much weaker with increasing the Co thickness than the corresponding ↓↓ contributions while the ↑↑ contributions are nearly thickness-independent (Fig. 10). Thus adding the ↓↑ and ↑↓ terms of $E^{CoCo}_{MCA} + E^{CoPd}_{MCA}$ to the first term on the right-hand side of Eq. (31) does not change significantly its oscillatory pattern and results mainly in a constant shift of this term. The spin-pair contributions to the $E^{PdPd}_{MCA} + E^{PdCo}_{MCA}$ part of the MCA energy, both diagonal (↓↓, ↑↑) and spin-flip (↓↑, ↑↓) terms, have oscillations of a large amplitude. However, when all these spin-pair terms are summed up, the resulting component $E^{PdPd}_{MCA} + E^{PdCo}_{MCA}$ of the MCA energy has much weaker dependence on the Co thickness, with small oscillations coming from its PdCo part and even weaker variation of the PdPd part since the oscillations of its spin-pair contributions almost cancel out as explained above. Thus the sum $E^{PdPd}_{MCA} + E^{PdCo}_{MCA}$ is effectively replaced by a constant in the constructed relation between the full MCA and the AOM. In this way, we finally conclude that the oscillations of the MCA energy versus the Co thickness are well approximated by the AOM in the Co part of the Co/Pd bilayer:

$$E_{MCA}(N_{Co}) \approx -w\frac{1}{4}\xi_{Co}\Delta\langle L_\zeta\rangle_{tot,Co} + c \qquad (45)$$

where c is a constant shift. The phenomenological factor w, presumably larger than 1, is introduced here to account for the neglected terms of the MCA energy oscillations coming fom E^{PdCo}_{MCA} as well as the spin-flip terms of E^{CoCo}_{MCA} and E^{CoPd}_{MCA}.
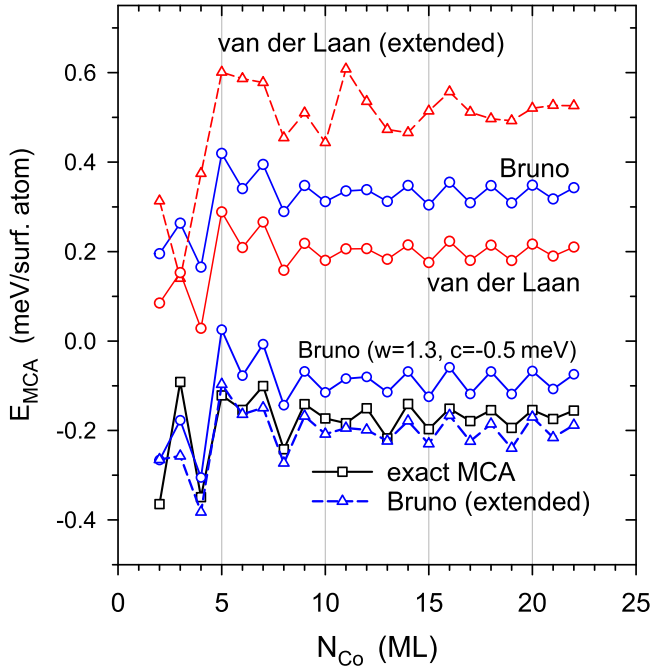
FIG. 12. Exact MCA energy (squares) for the (001) fcc Co(N_{Co} ML)/Pd(8 ML) bilayer and its approximations (circles, triangles) obtained with the original, modified and extended Bruno relations, Eqs. (40) and (45) (with $w = 1.3$, $c = -0.5$ meV) and (41), as well as the original and extended van der Laan relations, Eqs. (39) and (38). Based on the results obtained with the FT.

This Bruno-like relation, which involves the AOM in Co only, yields a very similar oscillation pattern to the full MCA energy with dominating oscillations of 2 ML period and the oscillation amplitude is well reproduced with the scaling factor $w = 1.3$; see Fig. 12. However, a large constant shift of around $c = -0.6$ meV is also needed to get good agreement with E_{MCA} which means that the AOM in Co, though well represents the oscillatory variation of E_{MCA} with the Co thickness, does not well reproduce the mean value of the MCA energy. In particular, the original Bruno relation (40), with no shift ($c = 0$), gives the incorrect prediction of a positive MCA energy, and, consequently, predicts in-plane magnetization for any Co thickness. The same holds for the original van der Laan relation [Eq. (39)] which gives a similar prediction as the Bruno relation (40), in particular for the MCA oscillations, since the majority-spin term of the AOM in Co is a few times smaller than the minority one [Fig. 11(a)] and is almost constant.

The approximate relation Eq. (45) does not include the Pd orbital moment though the spin components of this moment are present in the starting exact relation (31). According to the above discussion, the AOM in Co well represents the oscillatory term of $E_{MCA}^{CoCo} + E_{MCA}^{CoPd}$, while the remaining part of the MCA energy, i.e., the sum $E_{MCA}^{PdPd} + E_{MCA}^{PdCo}$, has smaller oscillations, especially for $N_{Co} \geqslant 10$ ML. These oscillations cannot be expressed with the AOM in Pd found with the PT as it strongly varies with increasing the Co thickness and follows a different oscillation pattern; see Fig. 11. However, while the AOM in Pd obtained with the PT has large oscillations, the exact AOM calculated with the FT oscillates weakly. Thus the

oscillation pattern of the approximated MCA energy remains almost unaffected if the term with the AOM in Pd is added, rather arbitrarily, in Eq. (45), with the parameters w and c skipped, which leads to the extended Bruno formula given by Eq. (41) with NM = Pd. This formula correctly predicts the negative sign of the exact MCA energy for the Co/Pd bilayers, unlike the original Bruno relation. Surprisingly, it reproduces not only the oscillations of the MCA energy but also its mean value with very good accuracy. However, such an excellent agreement is specific to the Co/Pd bilayer in the present calculation as the results the Co/Pt bilayer discussed below show.

The extended van der Laan formula, Eq. (38), which includes, instead of the AOMs in Co and Pd, the differences of the minority- and majority-spin terms of these AOMs, gives prediction that differ most from the exact MCA energy, with the incorrect positive sign, like the original Bruno and van der Laan relations. The oscillations of the MCA energy for the Co/Pd(8 ML) bilayer are also poorly represented by the extended van der Laan relation, with the dominating oscillatory term of around 5 ML period; see Fig. 12. The reason for this particular failure is that the spin-down and spin-up components of the AOM in Pd, found with the FT, oscillate, with the dominant periods of 5 and 4 ML, respectively, and mostly in antiphase (due to opposite spins). Thus these oscillations are amplified in the difference $\Delta \langle L_\zeta \rangle_{tot,Pd}^{\downarrow} - \Delta \langle L_\zeta \rangle_{tot,Pd}^{\uparrow}$ of these components while they largely cancel out in their sum which defines the full AOM in Pd, used in the extended Bruno relation. Note that the spin terms $\Delta \langle L_\zeta \rangle_{tot,X}^{\sigma}$ of the AOM $\Delta \langle L_\zeta \rangle_{tot,X}$ calculated with the FT [Eq. (32)] are found by decomposing the exact layer orbital moments, defined with Eq. (19), into the spin parts. This is done by representing each state $|m\mathbf{k}\rangle$ (the eigenstate of $H + H_{SO}$) as the sum of its projections on the two spin subspaces and taking into account that the operator of the orbital momentum L_ζ is diagonal in spin.

5. Oscillations of orbital moments

The oscillation periods of the AOM and their association with electron states of a particular spin and specific wave vectors can be identified clearly if one considers the Co and Pd orbital moments, found with the FT, for each magnetization direction ζ (x and z) and plots the contributions from the regions around the three high-symmetry points, $\overline{\Gamma}$, $\overline{M}$, and $\overline{X}$ [$\mathbf{k} = (k_x', k_y') = (1, 0)(\pi/a_{2d})$], in the two-dimensional BZ; see Figs. 13 and 14. It is found that, once the bulk-like term, linear in the Co thickness, is subtracted from the total orbital moment in the Co part of the bilayer, the remaining oscillatory term varies with increasing N_{Co} in a similar manner as for the unsupported Co film (Fig. 6). Indeed, the orbital moment $\langle L_\zeta \rangle_{tot,Co}$ along the out-of-plane magnetization direction ($\zeta = z$) oscillates with the period of around 2 ML while the oscillations with a smaller amplitude and the period of around 5 ML are found for the in-plane direction ($\zeta = x$). The 2 ML period is present in the contribution from the region around the $\overline{\Gamma}$ point while contribution from the vicinity of the $\overline{M}$ point oscillates with the period of 5 ML. Further decomposition of these contributions into the spin terms (not shown) confirms that both periods come from the QW states of the minority
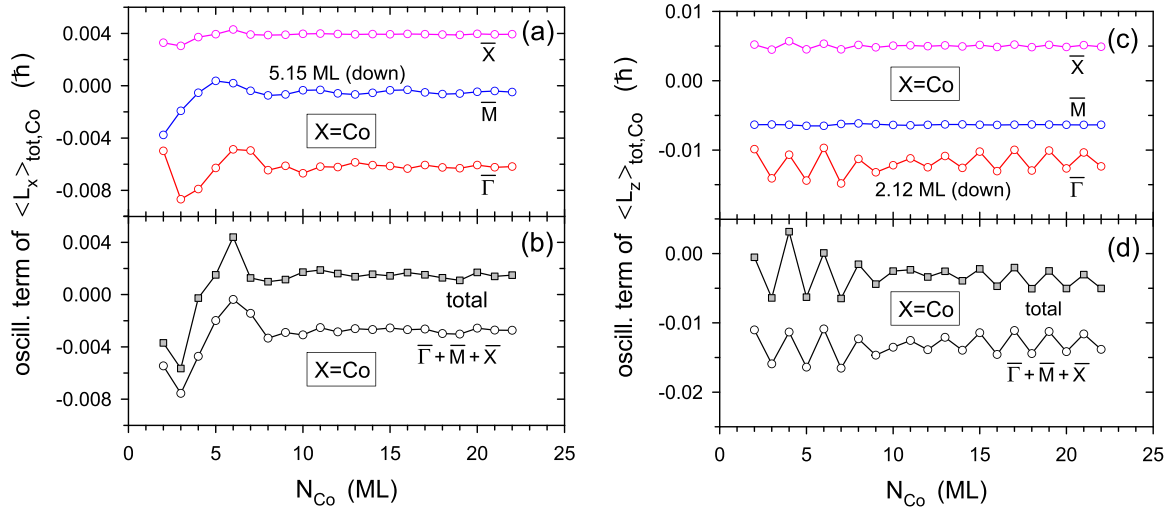
FIG. 13. Oscillatory part of the total orbital moment (per surface atom) along the [(a) and (b)] $\zeta = x$ and [(c) and (d)] $\zeta = z$ directions in the Co part of the (001) fcc Co(N_{Co} ML)/Pd(8 ML) bilayer and [(a) and (c)] the contributions to this moment from the square regions $|\mathbf{k} - \mathbf{k}_s| \leqslant \frac{1}{4}\pi/a_{2d}$ around the high-symmetry points $\mathbf{k}_s = \overline{\Gamma}, \overline{M}$, and $\overline{X}$ in the two-dimensional BZ, and [(b) and (d)] the sum of these three contributions (the plots are labeled respectively), all results obtained with Eq. (19) (the FT approach) The oscillation periods and the spin of the relevant QW states are marked.

spin, as marked in Figs. 13(a) and 13(c). The minority-spin QW states around the $\overline{M}$ point which lead to 5 ML period oscillations of $\langle L_\zeta \rangle_{tot,Co}$ for $\zeta = x$ do not contribute to the Co orbital moment for the out-of-plane magnetization ($\zeta = z$) for a similar reason why they do not contribute to the orbital moment in the Co film, as explained in Sec. III A.

The 2 ML and 5 ML periods due to minority-spin electrons are also present in the variations of the Pd orbital moment shown in Fig. 14. However, the variation of the orbital moment in Pd along the $\zeta = z$ magnetization direction is not dominated by the 2 ML period oscillations as for the Co moment though they are clearly present for the Co thickness less than 10 ML. The oscillation patterns of the orbital

moment in Pd found within the FT approach [Eq. (19)] are similar for the $\zeta = x$ and $\zeta = z$ directions, with the 5 ML period oscillations that prevail for $N_{Co} > 10$ ML (Fig. 15) and come from electron states around the $\overline{M}$ point. It is accompanied by the terms, with the period of around 2 ML that comes from the respective minority-spin QW states with $\mathbf{k}$ close to $\overline{\Gamma}$. There is also a very small contribution from the majority-spin QW states with the 4.12 ML period close to the $\overline{\Gamma}$ point. However, this contribution is clearly revealed only in the spin-up term of the AOM in Pd, especially after it is compared with the respective term obtained with the PT, oscillating very strongly with the period of 4 ML (Fig. 11).
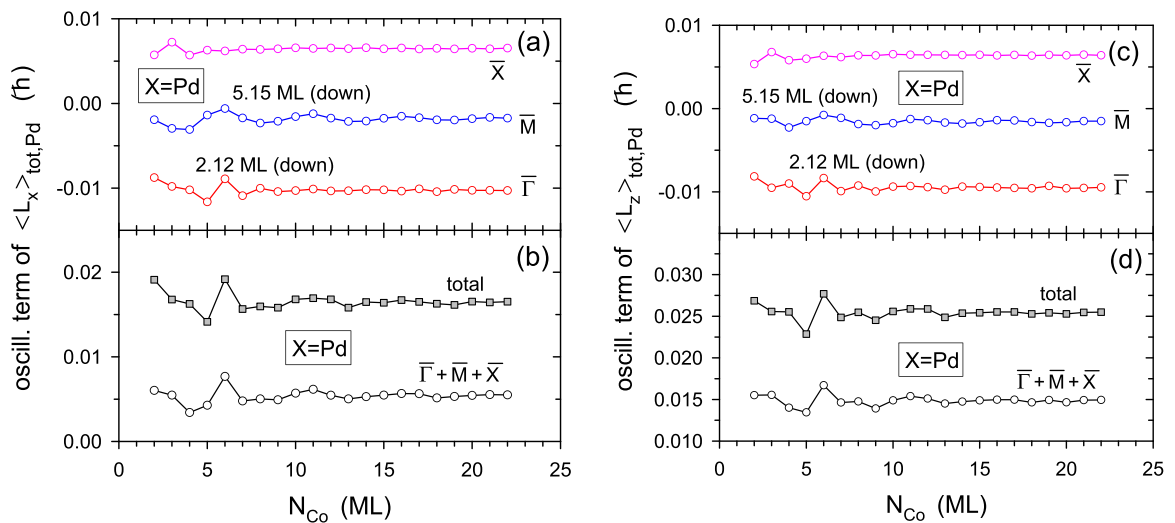

FIG. 14. Total orbital moment (per surface atom) along t[(a) and (b)] $\zeta = x$ and [(c) and (d)] $\zeta = z$ direction in the Pd part of the (001) fcc Co(N_{Co} ML)/Pd(8 ML) bilayer and [(a) and (c)] the oscillatory contributions to this moment from the square regions $|\mathbf{k} - \mathbf{k}_s| \leqslant \frac{1}{4}\pi/a_{2d}$ around the high-symmetry points $\mathbf{k}_s = \overline{\Gamma}, \overline{M}$, and $\overline{X}$ in the two-dimensional BZ, and (b,d) the sum of these three contributions (shifted by constant), all results obtained with Eq. (19) (the FT approach). The oscillation periods and the spin of the relevant QW states are marked.
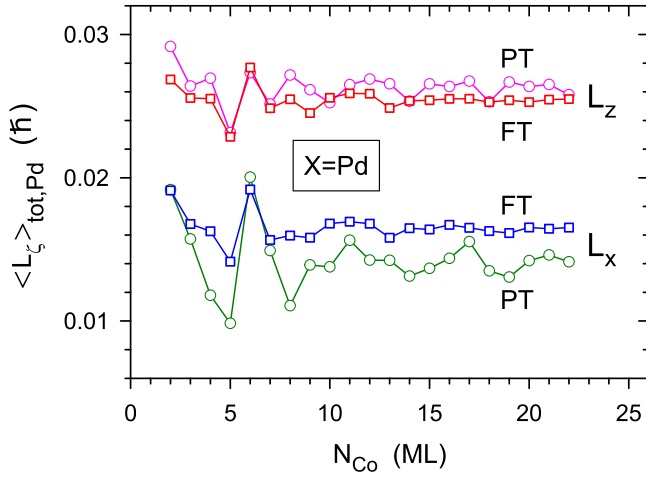
FIG. 15. Total Pd orbital moment obtained with the PT [Eq. (21)] and from Eq. (19) (the FT approach) for the (001) fcc Co(N_{Co} ML)/Pd(8 ML) bilayer.

Only tiny oscillatory contributions to the Co and Pd orbital moments along the x and z directions of magnetization come from the vicinity of the $\overline{X}$ point while virtually no oscillations arise in the Co moment along the $\zeta = z$ direction due to the states with **k** close to the $\overline{M}$ point (Figs. 13 and 14).

Although the exact orbital moment $\langle L_z \rangle_{\text{tot,Pd}}$ in Pd obtained with Eq. (19) has oscillations of much smaller amplitude than the Pd moment found with the PT [Eq. (21)] their oscillations patterns are roughly similar for the both directions, $\zeta = x$ and $\zeta = z$ (Fig. 15). Thus the origin of these oscillations can still be investigated within the PT formulation. In particular, the presence of the 5 ML period oscillations in the Pd moment along $\zeta = x$ and $\zeta = z$ directions can be explained if one notes that the operator $\mathbf{L} \cdot \mathbf{S}$ reduces to $L_\zeta S_\zeta$ in the matrix elements between states of the same spin which are used to express the orbital moment in Eq. (21) within the PT. Thus the minority-spin QW states with zx symmetry ($m_L = \pm 1$), corresponding to the 5.15 ML period, can be coupled by the SOC to other minority-spin states with the same symmetry for the $\zeta = z$ direction and to minority-spin states with $m_L = 0, \pm 2$ for the $\zeta = x$ direction. In fact, d states with $m_L = 0, \pm 1, \pm 2$ are present in the Pd layer, close to the Fermi energy in the region around the $\overline{M}$ point where the QW states of the 5.15 ML period occur since there are states of such symmetries close to ϵ_F along the XW line in bulk Pd as marked with a red oval in Fig. 4.

The present finding that the oscillations of the Pd moment calculated with the exact perturbed states $|m\mathbf{k}\rangle$ (i.e., as in the FT approach) are smaller than the ones found with the PT, can be attributed to the fact that the pairs of unperturbed states $|n\mathbf{k}\sigma\rangle$, $|n'\mathbf{k}\sigma'\rangle$, with closely lying energies are split by the SOC, with minimum splitting given by the matrix element (its absolute value) of H_{so} between these states. This stems from the simple model of two-state system [66] and implies that the exact energies of the two perturbed states are not well described in the 2nd order of the PT if the matrix element of H_{so} is larger than the difference $\epsilon_{n\sigma} - \epsilon_{n'\sigma'}$ between the unperturbed energies. Thus the contribution to the MCA and orbital moments from such pairs of states is expected to be not

well approximated by the PT, especially if both states have large amplitude in Pd so that the strong SOC in Pd leads to large values of $\langle n\mathbf{k}\sigma | H_{\text{so}} | n'\mathbf{k}\sigma' \rangle$. In particular, this applies to the 5.15 ML period minority-spin QW states in Co around the $\overline{M}$ point, which are hybridized with d states in Pd and thus couple, within the PT, to other d states with energies also close to ϵ_F and large amplitude in Pd. Again, this scenario is possible as there are nearly degenerate (due to accidental degeneracy) states, of zx and $3z^2 - r^2$ symmetries, near the Fermi level in bulk Pd, for the three-dimensional wave vectors $(\mathbf{k}, k_z)$ with $\mathbf{k} \approx \overline{M}$; see Fig. 4.

Although, for the Co/Pd bilayer, the described deficiency of the PT description for some contributing pairs of states has a significant effect on the oscillations of the orbital moment in Pd both the mean MCA energy and its oscillations found with the FT are reproduced with good accuracy by the PT. The reason for this is that the dominating 2 ML period oscillations of the MCA energy calculated with the PT come from its $XY = $ CoCo and $XY = $ CoPd, PdCo parts while the $XY = $ PdPd part of this energy oscillates much weaker (Fig. 9) and thus does not significantly affect the oscillatory pattern of $E_{\text{MCA}}(N_{Co})$.

C. Co/Pt bilayers

The mean values of the MCA energies obtained with the FT and PT are also quite close for the (001) fcc Co/Pt(8 ML) bilayer, being shifted by around 0.2 meV with respect to each other; see Fig. 1. However, while the PT predicts large oscillations of the MCA energy with increasing the Co thickness the oscillations of $E_{\text{MCA}}(N_{Co})$ found with the FT are much smaller and have a similar pattern, with the 2 ML period, and a similar amplitude as for the Co film and the Co/Pd bilayer. The fact that the MCA energy of the Co/Pt bilayer obtained with the FT formula does not oscillate in the way predicted by the PT, with the oscillation amplitude strongly quenched, can be attributed to the large SOC of Pt. Indeed, if the original SOC constant of Pt, $\xi_{\text{Pt}} = 0.65$ eV, is decreased threefold by taking $\xi_{\text{Pd}} = 0.23$ eV instead, the MCA energies obtained with the FT and PT are found to have very similar oscillation patterns and amplitudes, being only slightly shifted with respect to each other (Fig. 1). The MCA energy for such modified Co/Pt bilayers, with $\xi_{\text{Pt}} = \xi_{\text{Pd}}$, is close to the MCA energy of the Co/Pd bilayers due to the similar electronic structure Pd and Pt metals [57].

As for the Co/Pd system, the MCA energy found for the Co/Pt bilayer with the PT has large contributions $E_{\text{MCA}}^{\sigma\sigma'}$ from all four spin pairs (Fig. 16) due to the presence of d states of both spins in the Pt part of the bilayer. The strong SOC in Pt, compared to Co, with $\xi_{\text{Pt}}/\xi_{\text{Co}} \approx 7.65$, makes the $XY = $ PtPt part of the MCA energy its most significant term while the $XY = $ CoPt, PtCo parts are several times smaller and the $XY = $ CoCo part is negligible (Fig. 17). As a result, the $XY = $ PtPt part of the MCA energy not only determines its mean value but also provides the main oscillatory term of $E_{\text{MCA}}(N_{Co})$ found with the PT, unlike for the Co/Pd bilayer where the respective $XY = $ PdPd part of the MCA energy has the oscillation amplitude smaller by around $(\xi_{\text{Pd}}/\xi_{\text{Pt}})^2 \approx 0.125$ times and thus does not dominate the oscillatory terms coming from the $XY = $ CoCo and $XY = $ CoPd, PdCo parts
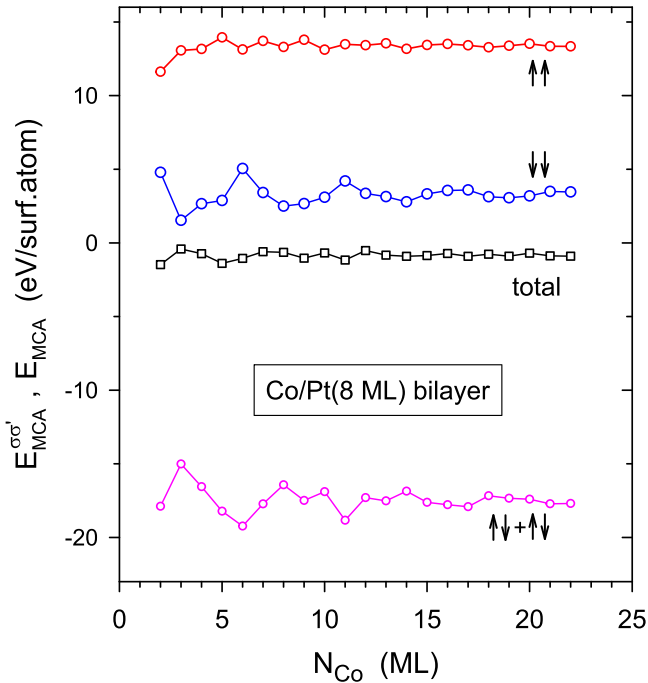
FIG. 16. MCA energy E_{MCA} and the spin-pair contributions $E_{MCA}^{\sigma\sigma'}$ obtained in the PT approach for the (001) fcc Co(N_{Co} ML)/Pt(8 ML) bilayer.

of the MCA energy; cf. Fig. 9. Thus, if the MCA oscillations coming from the $XY = $ PdPd and $XY = $ PtPt parts within the PT approach are both largely quenched once the exact form of the MCA energy is calculated with the FT, the result of this is much more evident in the oscillatory pattern of the MCA energy for the Co/Pt bilayer than the Co/Pd one, just as it is found in Fig. 1. The proposed explanation of such quenching for the Co/Pt bilayer is that the PT description becomes inaccurate, due to the large SOC of Pt, for the MCA contributions from pairs of closely lying states, for similar reasons as discussed for the oscillations of the Pd orbital moment in the Co/Pd bilayer in Sec. III B 5.
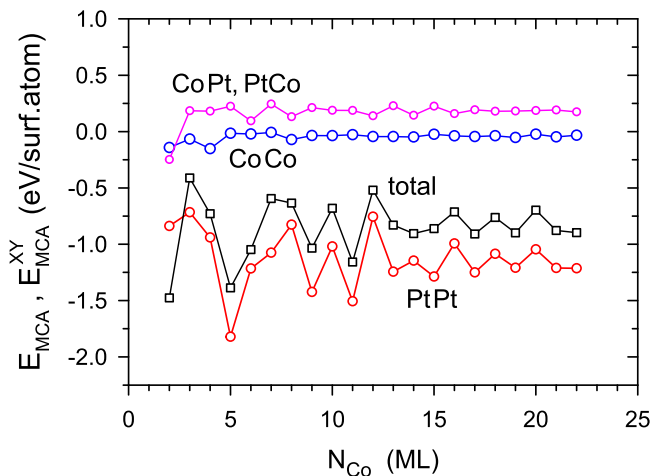

FIG. 17. The XY contributions to the MCA energy E_{MCA} obtained with the PT approach from the SOC in the X and Y parts of the (001) fcc Co(N_{Co} ML)/Pt(8 ML) bilayer.
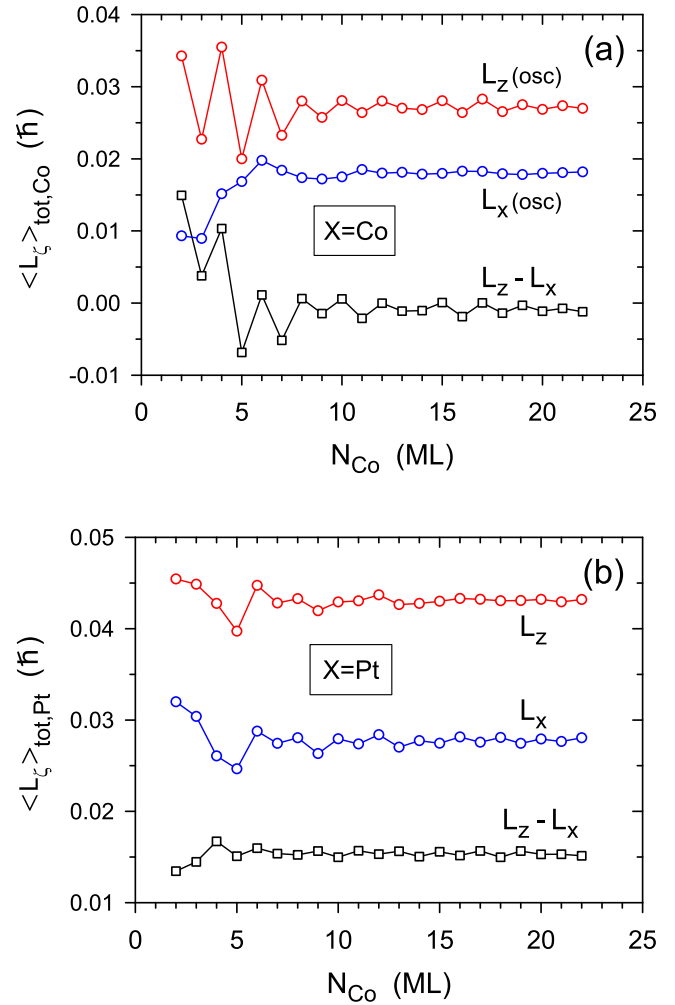
FIG. 18. Total orbital moments (per surface atom) in Co and Pt parts for the (001) fcc Co(N_{Co} ML)/Pt(8 ML) bilayer, calculated with Eq. (19) (the FT approach). The oscillatory term of the Co orbital moment is shown.

These conclusions are in agreement with the results obtained with the FT for the orbital moments in Co and Pt and the respective AOM; see Figs. 18 and 19. It is found the AOM in Co oscillates with increasing the Co thickness with the dominating 2 ML period, in a similar way as for the Co film and the Co/Pd bilayer; cf. Fig. 11. The 2 ML oscillations are found for the Co orbital moment along the $\zeta = z$ direction, i.e., for the out-of-plane magnetization, while, only faint oscillations of the moment $\langle L_\zeta \rangle_{tot,Co}$, with the around 5 ML period, are found for the in-plane magnetization ($\zeta = x$). The variation of the orbital moments of Pt is quite similar for the two magnetization directions which results in the AOM in Pt which varies only slightly with the Co thickness, like the AOM in Pd for the Co/Pd bilayers (Figs. 11(b) and 14), The similar variations of $\langle L_\zeta \rangle_{tot,Pt}$ for the $\zeta = x$ and $\zeta = z$ can be explained in the same way as for the Pd orbital moment in Sec. III B 5.

Finally, a possible relation between the MCA energy and the AOM is investigated for the Co/Pt bilayer. It is found (Fig. 20) that, like for the Co/Pd bilayer, the original Bruno and van der Laan relations quite well reproduce the dominant,
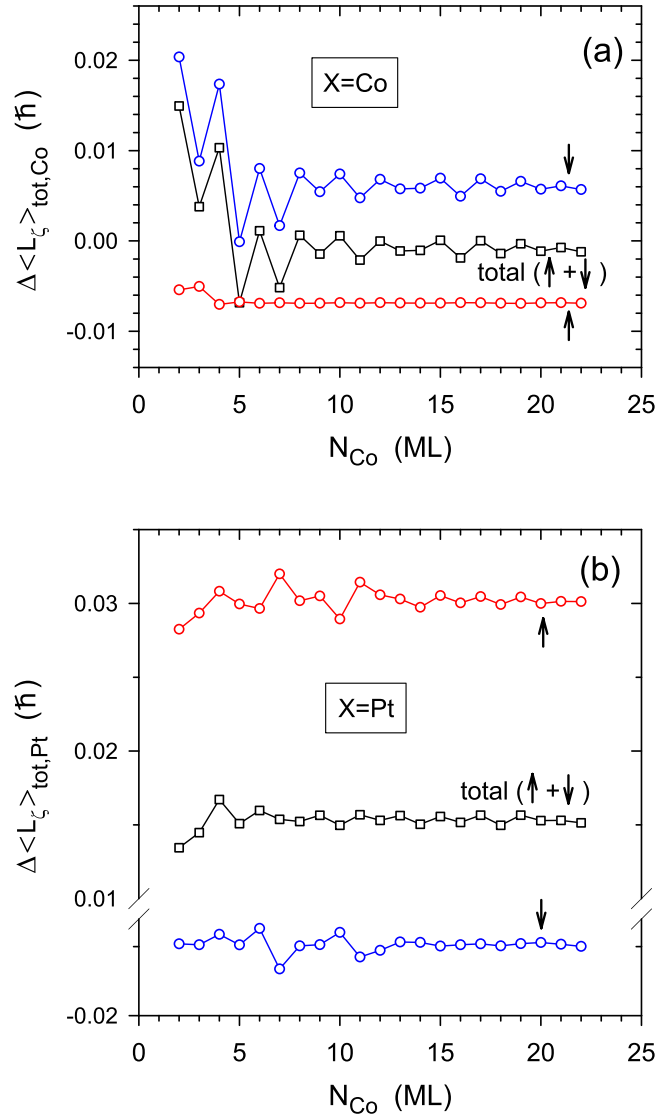
FIG. 19. AOM $\Delta\langle L_\zeta\rangle_{\text{tot},X}$ (per surface atom) and its spin terms in (a) Co and (b) Pt parts for the (001) fcc Co(N_{Co} ML)/Pt(8 ML) bilayer, calculated with the FT [Eqs. (32) and (19)].

FIG. 20. Exact MCA energy (squares) for the (001) fcc Co(N_{Co} ML)/Pt(8 ML) bilayer and its approximations (circles, triangles) obtained with the original, modified and extended Bruno relations, Eqs. (40) and (45) (with $w = 2$, $c = -1$ meV) and (41), as well as the original and extended van der Laan relations, Eqs. (39) and (38). Based on the results obtained with the FT.

2 ML period, term in the oscillation pattern of the MCA energy, provided the scaling factor of around 2 is applied. However, the mean value of $E_{\text{MCA}}(N_{\text{Co}})$ is not well predicted by neither of these relations unless sizable shifts are introduced, in particular, the shift of -1.2 meV is needed in the modified Bruno relation, Eq. (45). The values of E_{MCA} approximated by the original Bruno and van der Laan relations are too small since these relations, given by Eqs. (40) and (39), result from considering the $XY = \text{CoCo}$ and CoPt parts of the MCA energy only [see Eqs. (35) and (36)], and do not take into account the dominating $XY = \text{PtPt}$ part of the MCA energy.

The extension of the Bruno relation, where the AOM in Pt is included alongside the AOM in Co, leads to the correct sign of the approximated MCA energy which is clearly negative however its magnitude is too large, by roughly a factor of 2, compared to the exact MCA energy found with the FT. The oscillation pattern of the MCA energy is not well reproduced
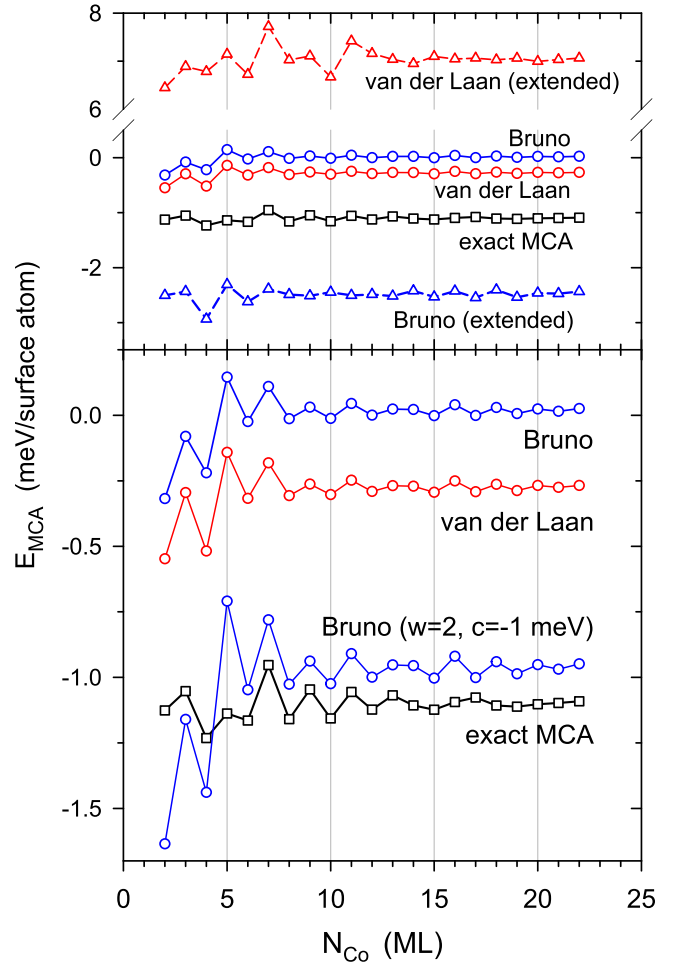
the extended Bruno relation (41) though oscillation amplitude is of a similar order.

The reason why the inclusion of the AOM in Pt has a moderate effect on the oscillation amplitude of the approximated MCA energy, despite the large SOC of Pt, is that the spin-up and spin-down terms of this AOM oscillate roughly in the same way but in antiphase (Fig. 19) so that their oscillations largely cancel out when the two terms are added. At the same time, the mean value of the AOM in Pt is big enough to produce large shift, of more than -2 meV, in the approximated MCA energy if the term $-\frac{1}{4}\xi_{\text{Pt}}\Delta\langle L_\zeta\rangle_{\text{tot},\text{Pt}}$ is included in the extended Bruno relation.

The extended van der Laan relation (38), including the differences of the spin-down and spin-up terms in AOMs of both Co and Pt, incorrectly predicts the mean value of E_{MCA}, with the positive sign and magnitude several times larger than the exact MCA energy. The reason for this failure is that this relation, though reproduces the spin-diagonal ($\downarrow\downarrow$ and $\uparrow\uparrow$) terms of the MCA energy, lacks the spin-flip MCA terms which are vital to obtain the negative value of the mean

MCA energy; see Fig. 16. Nevertheless, the oscillations of $E_{\text{MCA}}(N_{\text{Co}})$ with the 2 ML period are roughly reproduced by this relation but far less accurately than by the original Bruno and van der Laan relations, and only for $N_{\text{Co}} < 15$ ML while the predicted oscillation amplitude is too large by a factor of 2.

D. Layer contributions to MCA energy and layer orbital moments

While the PT expression for the MCA energy determines the contributions that come from the SOC in pairs of layers [Eq. (13)], the MCA contributions from individual layers cannot be uniquely defined. One possible method is summing the layer pair contributions $E_{\text{MCA}}^{(ll')}$ (which are symmetric in l, l') over one of layer indices, e.g., l',

$$E_{\text{MCA}}^{(l)} = \sum_{l'} E_{\text{MCA}}^{(ll')}. \tag{46}$$

These layer MCA contributions, defined within the PT, are real since the same is true for each term $E_{\text{MCA}}^{(ll')}$ (this can be proved by taking a complex conjugate of Eq. (14) and exchanging the index pairs $n\sigma$ and $n'\sigma'$). An equivalent definition of the MCA layer contributions has been proposed and applied in Refs. [21,39,41,42].

Alternatively, the MCA energy can decomposed using the layer-projected density of states (DOS) and this method has been used, e.g., in Refs. [2,12,13,32] as well as presumably also in Refs. [1,30] where layer-resolved band-energy contributions to the MCA energy are reported. The layer-projected density of states (DOS)

$$n_l(\epsilon) = \sum_{m\mathbf{k}} p_{ml}(\mathbf{k})\delta(\epsilon - \epsilon_m(\mathbf{k})) \tag{47}$$

includes, for each perturbed state $|m\mathbf{k}\rangle = |n\sigma\mathbf{k}\rangle^{\text{per}}$, the sum $p_{ml}(\mathbf{k}) = \sum_{\mu\sigma'} |\langle \mathbf{k}l\mu\sigma'|m\mathbf{k}\rangle|^2$ of its projections onto Bloch basis states $|\mathbf{k}l\mu\sigma'\rangle$ in layer l, which is the probability that the electron occupying this state is in layer l. Integrating $n_l(\epsilon)$ with the function $g_0(\epsilon) = g(\epsilon; \epsilon_F = \epsilon_{F0})$ gives the layer contribution to the perturbed grand potential

$$\Omega_l = \sum_{m\mathbf{k}} p_{ml}(\mathbf{k})g_0(\epsilon_m(\mathbf{k})), \tag{48}$$

which can be further used to define the layer contribution to the MCA energy within the FT approach as follows

$$\widetilde{E}_{\text{MCA}}^{(l)} = \Omega_l(\hat{\mathbf{M}}_\perp) - \Omega_l(\hat{\mathbf{M}}_{||}). \tag{49}$$

The sum of $\widetilde{E}_{\text{MCA}}^{(l)}$ over l yields the full MCA energy E_{MCA} since the sum of p_{ml} is equal to 1. This specific decomposition refers to the FT definition (9) of the MCA energy with the grand potential at $\epsilon_F = \epsilon_{F0}$, which leads the PT formula (10) for the MCA energy. The latter formula is also used to define the MCA layer contributions $E_{\text{MCA}}^{(l)}$ in the first method so that the direct comparison of the results found with the two methods that lead the same total MCA energy can be done once $\widetilde{E}_{\text{MCA}}^{(l)}$ are represented within the PT.

The PT expression for the layer contribution Ω_l can be conveniently found [2] using the Dyson expansion of the perturbed Green function $G = G_0 + G_0 H_{\text{so}} G_0 + G_0 H_{\text{so}} G_0 H_{\text{so}} G_0$ which includes the unperturbed Green function G_0 and leads

to the corresponding expansion for $\Omega_l = \Omega_l^{(0)} + \Omega_l^{(1)} + \Omega_l^{(2)}$. As shown in Ref. [2], the first-order layer-projected term $\Omega_l^{(1)}$ vanishes, like the total first-order term $\Omega^{(1)}$, while the second-order layer-projected term has the following form:

$$\Omega_l^{(2)} = \frac{1}{N_{\text{2D}}} \sum_{\mathbf{k}\in\text{BZ}} \sum_{\sigma,\sigma'} \sum_{n_1,n_2,n_3} \sum_{\mu} (a_{n_1 l\mu}^\sigma)^* a_{n_3 l\mu}^\sigma$$
$$\times J(\epsilon_{n_1\sigma}, \epsilon_{n_2\sigma'}, \epsilon_{n_3\sigma})$$
$$\times \langle n_1\mathbf{k}\sigma|H_{\text{so}}|n_2\mathbf{k}\sigma'\rangle \langle n_2\mathbf{k}\sigma'|H_{\text{so}}|n_3\mathbf{k}\sigma\rangle, \tag{50}$$

where the dependence on $\mathbf{k}$ is partly skipped for sake of clarity. The function

$$J(\epsilon_1, \epsilon_2, \epsilon_3) = \frac{1}{\epsilon_2 - \epsilon_1}\left[\frac{g_0(\epsilon_2) - g_0(\epsilon_3)}{\epsilon_2 - \epsilon_3} - \frac{g_0(\epsilon_1) - g_0(\epsilon_3)}{\epsilon_1 - \epsilon_3}\right]. \tag{51}$$

is fully symmetric under any permutation of its three arguments which can be clearly seen after rewriting the above definition as the sum of three terms, with the prefactors $g_0(\epsilon_i)$, $i = 1, 2, 3$. The form of $J(\epsilon_1, \epsilon_2, \epsilon_3)$ given in Eq. (51) is, however, more suitable in computations as it readily allows for deriving the power expansions if two or three arguments of this function are close to each other. The formula for $\Omega_l^{(2)}$ is presently written in a simpler form which is more compact than the original expression given in Ref. [2]. This form also allows for its straightforward application in *ab initio* calculations using a localized orbital basis, with $a_{nl\mu}^\sigma(\mathbf{k})$ being the projections of the electron states $|n\mathbf{k}\sigma\rangle$ onto the basis states μ in layer l. With the second-order terms $\Omega_l^{(2)}$ found, the MCA contribution from the lth layer can determined within the PT approach as follows:

$$\widetilde{E}_{\text{MCA}}^{(l)} = \Omega_l^{(2)}(\hat{\mathbf{M}}_\perp) - \Omega_l^{(2)}(\hat{\mathbf{M}}_{||}). \tag{52}$$

While both methods of decomposing the MCA energy within the PT theory provide the layer contributions [Eqs. (46) and (52)] that, when summed up, give the same total value of E_{MCA} their predictions can be significantly different. In particular, the results obtained for the (001) fcc Co(8 ML)/Pd(8 ML) bilayer (Fig. 21) show that although each method predicts that most significant MCA contributions to the MCA energy come from the immediate vicinities of the Co surface and Co/Pd interface, the specific patterns of these contributions are different. Among the MCA layer contributions $E_{\text{MCA}}^{(l)}$, found with Eq. (46), the largest one comes from the Pd interface layer. It is negative and its magnitude is at least three times larger than contributions from any other layer, both in Pd and Co parts of the bilayer. A similar pattern with the largest and dominant MCA contribution from the Pd interface layer, though of the opposite sign, has been found for (001) fcc Fe/Pd multilayers in the *ab initio* calculations [42], while for the (111) fcc Co/Pd multilayers [21], a large and negative layer MCA contribution comes from the Co interface layer while the contribution from Pd interface layer is much smaller.

The spatial distribution of the MCA energy is different from $E_{\text{MCA}}^{(l)}$ if its decomposition is based on resolving the DOS into the layer-projected terms. In particular, the resulting contributions $\widetilde{E}_{\text{MCA}}^{(l)}$ from the neighboring Co and Pd layers at the Co/Pd interface are also negative, but their values are
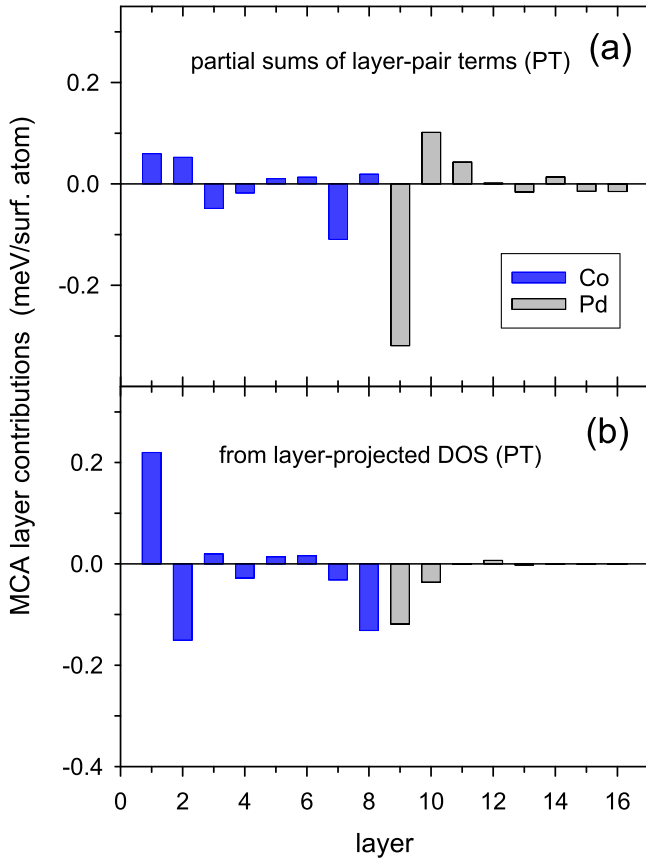
FIG. 21. Layer contributions to the MCA energy for the (001) fcc Co(8 ML)/Pd(8 ML) bilayer obtained in the PT as (a) $E_{\mathrm{MCA}}^{(l)}$ with Eq. (46) and (b) $\widetilde{E}_{\mathrm{MCA}}^{(l)}$ with Eq. (52).

almost equal to each other and around 2.5 times smaller than the Pd interface contribution $E_{\mathrm{MCA}}^{(l)}$ obtained with the first method. The two methods also give different predictions close to the Co surface. The significant contributions $E_{\mathrm{MCA}}^{(l)}$ come from the first three Co layers, with similar positive values for $l = 1, 2$ and a negative value for $l = 3$. The layer contributions $\widetilde{E}_{\mathrm{MCA}}^{(l)}$ obtained with the second method are much larger and form a characteristic pattern close to the Co surface, with a positive contribution from the very surface layer ($l = 1$) and a negative one from the second Co layer ($l = 2$) while the rapidly decaying oscillations of $\widetilde{E}_{\mathrm{MCA}}^{(l)}$ with 2 ML period are also present inside the Co part of the bilayer. A similar pattern of the layer-projected MCA contributions close to the Co surface, oscillating with the same period, has also been found for the Co films in the DFT calculations in Refs. [13,30]. In particular, the presently obtained contribution of 0.22 meV from the surface Co layer in the Co(8 ML)/Pd(8 ML) bilayer is very close to the Co surface layer term of 0.18 meV reported for a Co film on the (001) fcc Cu substrate in Ref. [30] (Fig. 4 therein).

It is also found that, for atomic layers l in Co and the Pd interface layer, the main contributions to $E_{\mathrm{MCA}}^{(l)}$ defined with Eq. (46) come from the on-site term $E_{\mathrm{MCA}}^{(ll')}$ from the same layer, $l' = l$, and the two layer-pair terms $E_{\mathrm{MCA}}^{(ll')}$, of the sign opposite to the on-site term, from the nearest-neighboring

layers $l' = l - 1$ and $l' = l + 1$; see Fig. 22(a). An exception is the surface Co layer $l = 1$ for which largest layer-pair terms come from layers $l' = 2$ and 3, while the on-site term ($l' = l = 1$) is negligible. A similar pattern of the $E_{\mathrm{MCA}}^{(ll')}$ terms at the Co surface layer l has been recently found for a Co(5 ML) film with hcp-like stacking in *ab initio* calculations [50]. The layer-pair contributions $E_{\mathrm{MCA}}^{(ll')}$ do not vanish for interior Co layers l, though they almost fully cancel out for such layers once they are summed up over l' to obtain $E_{\mathrm{MCA}}^{(l)}$ with Eq. (46). An important conclusion is that the main contribution to the $XY = \mathrm{CoPd}, \mathrm{PdCo}$ parts of the MCA energy come from the pair of the Co and Pd atomic layers at the very interface [$l = 8, l' = 9$ or $l = 9, l' = 8$ in Fig. 22(a)] though this contribution does not account for the whole term $E_{\mathrm{MCA}}^{\mathrm{CoPd}} = E_{\mathrm{MCA}}^{\mathrm{PdCo}}$ and minor contributions from other pairs of layers l, l', one in Co and the other in Pd, have to be included to accurately reproduce $E_{\mathrm{MCA}}^{\mathrm{CoPd}}$ shown in Fig. 9.

The decompositions of the MCA energy into layer contributions can be compared with the distribution of orbital moments $\langle L_\zeta \rangle_l$ at different layers l for $\zeta = x$ and $\zeta = z$ directions of magnetization. These layer moments as well as their difference $\Delta \langle L_\zeta \rangle_l = \langle L_z \rangle_l - \langle L_x \rangle_l$ defining the layer terms of the AOM are shown for the Co(8 ML)/Pd(8 ML) bilayer in Fig. 23. The moments are found be significantly different from the bulk values ($0.10\hbar$ for Co and 0 for Pd) only at the very surface Co layer where the orbital moment is largely enhanced for both magnetization orientations (to $0.17\hbar$ and $0.14\hbar$ for the x and z directions, respectively) as well as at the Pd layer at the Co/Pd interface where the orbital moment of $0.025\hbar$ is induced. The AOM in the Co part of the bilayer has significant layer terms $\Delta \langle L_\zeta \rangle_l$ only in two atomic layers, one at the Co surface and the other at the Co/Pd interface, while the distribution of the AOM in the Pd part is less localized, with the largest term coming, a bit surprisingly, from not the first but from the second Pd layer near the Co/Pd interface.

The obtained spatial distribution of the AOM, with largest and positive layer contribution $\Delta \langle L_\zeta \rangle_l$ at the Co interface layer, is similar as for the (111) fcc Co/Pd multilayer [21] though for the latter system no sizable contributions are found from the Pd layers, unlike in the present case. Obviously, such differences, also present for the MCA, can be expected due to different geometry of the two Co/Pd systems and the absence of strain in the presently investigated bilayers.

Another interesting finding is that the layer orbital moment in each layer, be it in Co or Pd, arises almost entirely due to the SOC in the same layer, as the decomposition of $\langle L_\zeta \rangle_l$ into terms $\langle L_\zeta \rangle_l^{l'}$ [Eqs. (24) and (25], coming from the SOC in different layers l' shows; see Fig. 22(b). As a result, the part $\langle L_\zeta \rangle_{\mathrm{tot,Co}}^{\mathrm{Pd}}$ of the total orbital moment $\langle L_\zeta \rangle_{\mathrm{tot,Co}} = \sum_{l \in \mathrm{Co}} \langle L_\zeta \rangle_l$ in Co is almost negligible and the same is true for the $\langle L_\zeta \rangle_{\mathrm{tot,Pd}}^{\mathrm{Co}}$ part of the total orbital moment $\langle L_\zeta \rangle_{\mathrm{tot,Pd}} = \sum_{l \in \mathrm{Pd}} \langle L_\zeta \rangle_l$ in Pd see Eqs. (26) and (27). The contributions from various layers l' to the layer term $\Delta \langle L_\zeta \rangle_l$ of the AOM are also localized around $l' = l$, though significant contributions also come from the nearest-neighboring layers, $l' = l \pm 1$, for the Co and Pd layers l at the Co/Pd interface. In particular, around half of the AOM layer term at the Co interface layer comes from the SOC of Pd so that also the total AOM in Co, $\Delta \langle L_\zeta \rangle_{\mathrm{tot,Co}} = \sum_{l \in \mathrm{Co}} \Delta \langle L_\zeta \rangle_l$, includes a substantial component due to the
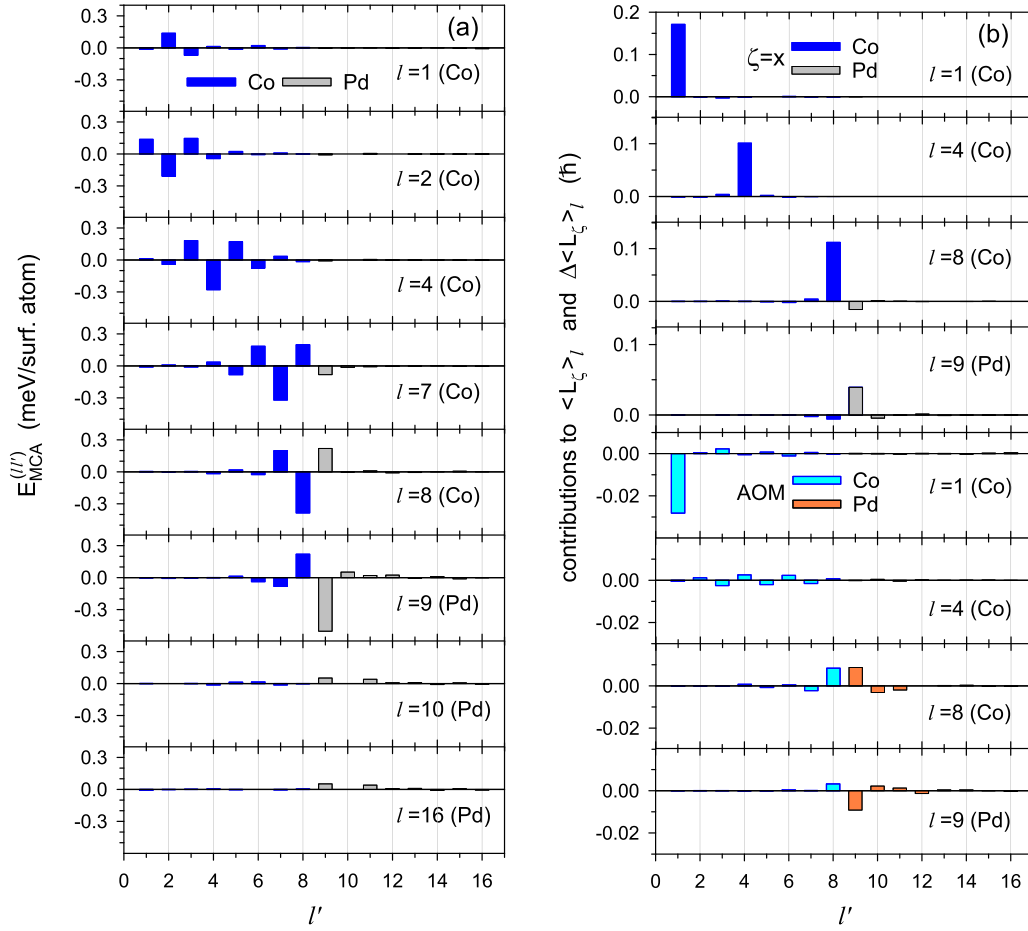
FIG. 22. (a) Layer-pair contributions $E_{MCA}^{(ll')}$ to the MCA energy, (b) the contributions $\langle L_\zeta \rangle_l^{l'}$ from different layers l' to the layer orbital moment $\langle L_\zeta \rangle_l$ along the $\zeta = x$ magnetization direction and the contributions $\Delta\langle L_\zeta \rangle_l^{l'} = \langle L_z \rangle_l^{l'} - \langle L_x \rangle_l^{l'}$ to the layer terms $\Delta\langle L_\zeta \rangle_l$ of the AOM for the (001) fcc Co(8 ML)/Pd(8 ML) bilayer, obtained with the PT.

SOC in Pd. The largest AOM contribution comes from the on-site term $\Delta\langle L_\zeta \rangle_l^{l'}$ at the Co surface ($l = l' = 1$) while the contributions $\Delta\langle L_\zeta \rangle_l^{l'}$ are negligible for the interior Co layers l, unlike for the MCA layer-pair terms $E_{MCA}^{(ll')}$; Fig. 22(a).

The analysis of the results plotted in Figs. 21 and 23 shows that the layer contributions to the MCA, $E_{MCA}^{(l)}$ or $\widetilde{E}_{MCA}^{(l)}$, obtained for the Co/Pd bilayer with either of the two discussed methods [Eqs. (46) and (52)] are not closely correlated with the respective distribution of the layer terms $\Delta\langle L_\zeta \rangle_l$ of the AOM. Nevertheless, some general relations are still found. Both the MCA and AOM layer terms are localized around the Co surface and the Co/Pd interface, with small contributions from the interior of the Co film and the rest of Pd part. Also, the overall contribution from the Co surface (obtained by partial summation of a few layer terms) is positive for the MCA energy and negative for the AOM, while the reverse is true for the summed contribution from layers around the Co/NM interface which is negative for the MCA and positive for the AOM. However, the detailed profiles of $\Delta\langle L_\zeta \rangle_l$ and $E_{MCA}^{(l)}$ or $\Delta\langle L_\zeta \rangle_l$ and $\widetilde{E}_{MCA}^{(l)}$ do not follow this general rule of opposite signs which would be valid if the Bruno relation held locally between the MCA and AOM terms in individual atomic layers. This relation is also not satisfied by the layer-pair contributions to the MCA and AOM shown in Fig. 22.

IV. CONCLUSIONS

The presented calculations of the MCA energy and the orbital moments for the Co film and the Co/NM bilayers, confirm that the investigated Bruno [8] and van der Laan [9] relations between the MCA energy and the orbital moments are largely inaccurate. Their incorrect predictions concern the sign of the predicted energy (and thus the easy direction of the magnetization), as for the Co/Pd bilayer, as well as its magnitude which is several times larger than the exact MCA energy for the Co film and a several times smaller for the Co/Pt bilayer. However, it is found, similarly as for the Fe film [16], that the Bruno and van der Laan relations very accurately reproduce the oscillatory pattern of the MCA energy variation with increasing the Co thickness for the Co film. They also give a very good prediction of this pattern for the Co/Pd bilayer and less accurate one for the Co/Pt bilayer. However, the oscillation amplitude predicted by these relations for the Co/NM bilayers is too small and the scaling factor is needed, different for each type of the bilayers, to get the agreement with the oscillations of the exact MCA energy. These theoretical predictions agree with the experimental results for the Fe/Ag epitaxial films where correlation between the MCA energy and the AOM of Fe is found [17].
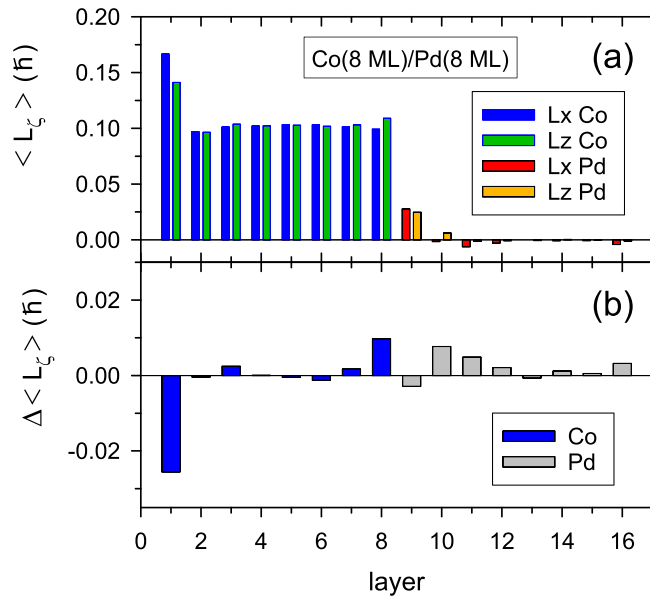
FIG. 23. (a) Layer orbital moments $\langle L_\zeta \rangle_l$ along the magnetization directions $\zeta = x$ and $\zeta = z$, (b) their difference $\Delta \langle L_\zeta \rangle_l = \langle L_z \rangle_l - \langle L_x \rangle_l$ in the (001) fcc Co(8 ML)/Pd(8 ML) bilayer.

The failure to reproduce the mean value of the MCA energy by the Bruno and van der Laan relations results from the fact that neither the AOM of Co nor the difference its spin terms, used in these relations, represent, even roughly, the whole MCA energy. For the Co film, the important neglected part of this energy is the spin-flip terms while for the Co/NM bilayers it is mainly the neglected XY element-pair contribution from the SOC of NM alone ($X = Y = $ NM), In particular, with the SOC of Pt several times larger than the SOC of Co, the MCA energy of the Co/Pt bilayer includes the large $XY = $ PtPt contribution which is, in fact, dominant, while the AOM of Co is related to much smaller MCA contributions from the $XY = $ CoCo and $XY = $ CoPt SOC pairs, only. Thus it can be expected that the original Bruno and van der Laan relations also fail to reproduce the mean value of the MCA energy for other FM/NM systems where the NM is a heavy metal with a strong SOC and a large density of states (DOS) at the Fermi level, while they are likely to give correct predictions for FM films on NM substrates with a weaker SOC or a low DOS at $\epsilon_{\rm F}$.

The original Bruno and van der Laan relations have been presently extended by including the orbital moments of nonmagnetic (Pd, Pt) layers, in addition to the moment of the ferromagnetic (Co) layer. Similar extended relations can also be formulated for more complex magnetic multilayers with layer-dependent SOC constants, and, in fact, for any multicomponent magnetic system with collinear magnetization. The extension of the Bruno relation with the AOM of NM leads to the correct sign of the MCA energy and provides a better approximation of its mean value, especially for the Co/Pd bilayer, and, in this case, the MCA oscillations are also reproduced with good accuracy. Including the AOM of Pd or Pt as a difference of its spin terms in the extended van der Laan relation has the opposite effect as it leads to the approximate MCA energy very different from the exact one, with the wrong sign, the mean value distant from the

exact MCA energy much more than for the original relation, and a different oscillation pattern. The extended van der Laan relation exactly reproduces the diagonal spin-pair terms of the MCA energy (unlike the Bruno relation), however, the absence of the neglected spin-flip terms prevents this relation from providing an even qualitatively correct approximation of the MCA energy. Thus, though constructed in a more arbitrary way, the extended Bruno relation presents a substantial improvement over its original version while the extension of the van der Laan relation leads to worse predictions. The large negative spin-flip terms of the MCA energy, missing in the latter relation and having the crucial role in emerging the negative sign of this energy for the (001) fcc Co/Pd bilayer, arise due to hybridization of the minority-spin d states at the Co/Pd interface and the presence d states of the majority-spin in Pd; similar origin of the perpendicular magnetocrystalline anisotropy was previously established for the (111) fcc Co/Pd superlattices [21].

The calculations of the orbital moments also resulted in interesting findings about their variation with the thickness of the Co layer. In particular, for the Co film as well as the Co/Pd and Co/Pt bilayers, the orbital moment of Co is found to have different oscillatory patterns for out-of-plane and in-plane magnetization directions, with the clear oscillation periods of 2 and 5 ML, respectively, which is related to different symmetries of the involved QW states from the vicinity of the high-symmetry **k** points in the two-dimensional BZ. However, the AOM in Co reflects mainly the 2 ML period oscillations of the orbital moment in Co $\langle L_\zeta \rangle_{\rm tot,Co}$ for the out-of-plane direction ($\zeta = z$) since its oscillations of the 5 ML period for the in-plane direction ($\zeta = x$) have much a smaller amplitude. The orbital moment in Pd (or Pt) oscillates in a similar way for both magnetization directions, and includes oscillatory terms with both the short and long periods. These findings can be of practical importance for other magnetic layered systems as they not only predict possible occurrence of different oscillatory patterns in the orbital moments measured for different directions of magnetization but also provide a sound explanation for such a result and, thus, show the possibility of drawing conclusions about the symmetry of the QW states that lead to the observed oscillations of the orbital moments and the MCA energy.

It is also shown that layer contributions to the MCA energy are not uniquely determined and the two methods used for their calculation lead to significantly different breakdowns of this energy. It is found for the Co/Pd bilayer that neither of these decompositions gives the spatial MCA profile well correlated with the profile of the AOM whose layer terms are defined with layer orbital moments. Thus the extended Bruno relation, though quite accurate for this specific bilayer, is not well satisfied locally, in individual atomic layers. In addition, it is found that the orbital moment in each Co layer as well as the moment in the Pd interface layer originate almost entirely from the SOC in the same atomic layer, while each layer term of the MCA energy has also contributions from the SOC of a few neighboring layers.

Other important findings of the present investigation concern the theoretical methods used for calculating the MCA energies, orbital moments and the AOM. It is shown that the PT expression for the MCA energy also includes intraband

terms which are usually neglected but they are finite for the systems without the inversion symmetry and, in fact, are necessary to obtain the correct results for the Co/Pd bilayer. Note that similar intraband terms, alongside interband ones, are also present in the Kamberský formula [58,67,68] for the Gilbert damping which describes the effect of the SOC on the magnetization dynamics. It is found that while, for the Co film and the Co/Pd bilayer, the MCA energy calculated with the PT is very close to the exact MCA energy determined with the FT, the two energies differ considerably from each other for the Co/Pt bilayer. As the mean values of these energies are quite close to each other also for this bilayer, the main difference between them concerns their oscillations versus the Co thickness, with large amplitude predicted by the PT compared to much smaller amplitude found with the FT. This discrepancy is shown to be related to the large strength of the SOC in Pt so that the contributions from the QW states responsible for the MCA oscillations are not accurately described by the PT. Thus, while the PT formalism gives good predictions for the mean value of the MCA energy, the present results show that the oscillations of this energy as well as the oscillations of the orbital moments, especially in NM, should be investigated with the FT approach for the magnetic systems including elements with large SOC.

ACKNOWLEDGMENT

APPENDIX: SECOND-ORDER PERTURBATION EXPANSION OF FREE ENERGY AND GRAND POTENTIAL. INTRABAND TERMS AND DEGENERATE STATES IN THE EXPRESSION FOR MCA ENERGY AT FINITE TEMPERATURE

The free energy $F = \Omega + \epsilon_F N$ of the perturbed system with N electrons at finite temperature T,

$$F = F_0 + \delta\Omega + N\delta\epsilon_F \tag{A1}$$

can be represented with the free energy $F_0 = \Omega_0 + \epsilon_{F0} N$ of the unperturbed system, the change $\delta\Omega$ of the grand potential due to the SOC and the respective the shift $\delta\epsilon_F = \epsilon_F - \epsilon_{F0}$ of the Fermi energy (chemical potential). Upon the PT expansion of the state energies $\epsilon_m = \epsilon_{n\sigma}^{per} = \epsilon_{n\sigma} + \epsilon_{n\sigma}^{(1)} + \epsilon_{n\sigma}^{(2)}$ up to the second-order in H_{so}, the following expression

$$\delta\Omega = \Omega(\epsilon_F) - \Omega_0(\epsilon_{F0}) = \Omega^{(1)} + \Omega^{(2)} - N\delta\epsilon_F \tag{A2}$$

can be obtained with the Taylor series expansion of the function used to define the grand potential in Eq. (7),

$$g(\epsilon_m) = g_0(\epsilon_{n\sigma} + \delta\epsilon_{n\sigma} - \delta\epsilon_F) = g_0(\epsilon_{n\sigma})$$
$$+ f_0(\epsilon_{n\sigma})(\delta\epsilon_{n\sigma} - \delta\epsilon_F) + \tfrac{1}{2} f_0'(\epsilon_{n\sigma})(\delta\epsilon_{n\sigma} - \delta\epsilon_F)^2, \tag{A3}$$

where $\delta\epsilon_{n\sigma} = \epsilon_{n\sigma}^{(1)} + \epsilon_{n\sigma}^{(2)}$, while the functions $g_0(\epsilon) = g(\epsilon; \epsilon_F = \epsilon_{F0})$ and the occupation factors $f_0(\epsilon) = dg_0/d\epsilon = f(\epsilon; \epsilon_F = \epsilon_{F0})$ are calculated for the electron energies $\epsilon = \epsilon_{n\sigma}(\mathbf{k})$ in the unperturbed system with the respective Fermi

energy ϵ_{F0}. Accordingly, the unperturbed grand potential and its corrections are expressed as follows:

$$\Omega_0 = \frac{1}{N_{2D}} \sum_{n\sigma\mathbf{k}} g_0(\epsilon_{n\sigma}), \tag{A4}$$

$$\Omega^{(1)} = \frac{1}{N_{2D}} \sum_{n\sigma\mathbf{k}} f_0(\epsilon_{n\sigma}) \epsilon_{n\sigma}^{(1)}, \tag{A5}$$

$$\Omega^{(2)} = \frac{1}{N_{2D}} \left[\sum_{n\sigma\mathbf{k}} f_0(\epsilon_{n\sigma}) \epsilon_{n\sigma}^{(2)} + \frac{1}{2} \sum_{n\sigma\mathbf{k}} f_0'(\epsilon_{n\sigma}) (\epsilon_{n\sigma}^{(1)})^2 \right]. \tag{A6}$$

Since the first-order energy correction $\epsilon_{n\sigma}^{(1)} = \langle n\mathbf{k}\sigma | H_{so} | n\mathbf{k}\sigma \rangle$ either vanishes for systems with the inversion symmetry or has opposite values at $\mathbf{k}$ and $-\mathbf{k}$ for systems without this symmetry, like the Co/NM bilayers, the first-order term $\Omega^{(1)}$ vanishes, as it is proved in detail in the Appendix A of Ref. [2]. Thus the difference between the free energies of the perturbed and unperturbed systems is given by the second-order correction to the free energy

$$F - F_0 = F^{(2)} = \Omega^{(2)} \tag{A7}$$

equal to the second-order correction to the grand potential calculated at $\epsilon_F = \epsilon_{F0}$ (this result, in a similar form, has been derived for the interacting homogeneous electron gas in Ref. [69]). In consequence, the PT approximation to the MCA energy, defined with the FT in Eq. (5), is given by Eq. (10). This expression can also be obtained by starting with the FT formula (9) where the MCA energy is expressed as the difference of the grand potentials for the two magnetization directions calculated with the Fermi energy of the unperturbed system ϵ_{F0}.

To amend the argument that leads to Eq. (A7) it remains to show that the shift $\delta\epsilon_F$ of the Fermi energy due to the SOC is also of the second-order in the SOC so that it enters only in the linear term in the expansion of $g(\epsilon_m)$ in Eq. (A3) and, thus, leads to the term $-N\delta\epsilon_F$ in Eq. (A2). With the number of electrons N fixed in the canonical ensemble, the Taylor series expansion of $f(\epsilon_m) = f_0(\epsilon_{n\sigma} + \delta\epsilon_{n\sigma} - \delta\epsilon_F)$ applied in Eq. (8) leads to

$$\frac{1}{N_{2D}} \left[\sum_{n\sigma\mathbf{k}} f_0(\epsilon_{n\sigma}) + \sum_{n\sigma\mathbf{k}} f_0'(\epsilon_{n\sigma})(\delta\epsilon_{n\sigma} - \delta\epsilon_F) \right.$$
$$\left. + \frac{1}{2} \sum_{n\sigma\mathbf{k}} f_0''(\epsilon_{n\sigma})(\delta\epsilon_{n\sigma} - \delta\epsilon_F)^2 \right] = N. \tag{A8}$$

The first sum gives number of electrons in the unperturbed system, also equal to N, while the sums $\sum_{n\sigma\mathbf{k}} f_0'(\epsilon_{n\sigma})\epsilon_{n\sigma}^{(1)}$ and $\sum_{n\sigma\mathbf{k}} f_0''(\epsilon_{n\sigma})\delta\epsilon_{n\sigma}\delta\epsilon_F = \sum_{n\sigma\mathbf{k}} f_0''(\epsilon_{n\sigma})\epsilon_{n\sigma}^{(1)}\delta\epsilon_F$ vanish as their $\mathbf{k}$ and $-\mathbf{k}$ terms cancel out. Thus we conclude that the Fermi energy shift is equal to

$$\delta\epsilon_F = \left[\sum_{n\sigma\mathbf{k}} f_0'(\epsilon_{n\sigma}) \epsilon_{n\sigma}^{(2)} + \frac{1}{2} \sum_{n\sigma\mathbf{k}} f_0''(\epsilon_{n\sigma}) (\epsilon_{n\sigma}^{(1)})^2 \right] \bigg/ \sum_{n\sigma\mathbf{k}} f_0'(\epsilon_{n\sigma}) \tag{A9}$$

and, indeed, it is of the second order in the SOC.

The first sum in the Eq. (A6) includes the second-order corrections

$$\epsilon_{n\sigma}^{(2)} = \sum_{\mathbf{k}} \sum_{n'\sigma' \neq n\sigma} \frac{|\langle n'\mathbf{k}\sigma'|H_{\text{so}}|n\mathbf{k}\sigma\rangle|^2}{\epsilon_{n\sigma}(\mathbf{k}) - \epsilon_{n'\sigma'}(\mathbf{k})} \qquad \text{(A10)}$$

and gives the formula (11) with the $(n'\sigma') = (n\sigma)$ terms excluded (such a form of the considered sum is achieved by dividing it into two halves and exchanging the indices $(n'\sigma')$, $(n\sigma)$ in one of them). However, the first-order correction $\epsilon_{n\sigma}^{(1)}$, which can be finite for bilayers, also contributes to the second-order term $\Omega^{(2)}$ via the second sum in Eq. (A6). This contribution is equal to the sum of the omitted $(n'\sigma') = (n\sigma)$ terms in the formula (11) if each such term is defined by applying the limit $\epsilon_{n\sigma} \to \epsilon_{n'\sigma'}$ to the ratio $[f_0(\epsilon_{n\sigma}) - f_0(\epsilon_{n'\sigma'})]/(\epsilon_{n\sigma} - \epsilon_{n'\sigma'})$, which yields the derivative $f_0'(\epsilon_{n\sigma})$. Thus the second-order term $\Omega^{(2)} = \Omega^{(2)}(\hat{\mathbf{M}})$ of the grand potential is given by Eq. (11) with all $(n'\sigma')$ $(n\sigma)$ terms included and defines the MCA energy at finite temperature within the PT approach.

In case there are degenerate states, the usual recipe given by the PT is to first diagonalize the matrix $A_{ij} = \langle n_i\mathbf{k}\sigma|H_{\text{so}}|n_j\mathbf{k}\sigma\rangle$ of the perturbation in each subspace of M states $|n_i\mathbf{k}\sigma\rangle$ which have same energies $\epsilon_{n_i\sigma}(\mathbf{k}) = \epsilon_{n_j\sigma}(\mathbf{k})$ $(i, j = 1, \ldots, M)$. The calculations of the energy corrections are then done using the equivalent set of the degenerate states $|n_i\mathbf{k}\sigma\rangle_{\text{d}}$ which are eigenstates of the matrix A so that the diagonal matrix elements ${}_{\text{d}}\langle n_i\mathbf{k}\sigma'|H_{\text{so}}|n_i\mathbf{k}\sigma\rangle_{\text{d}}$ are equal to the eigenvalues λ_i of the matrix A while the off-diagonal elements of H_{so} vanish. Thus the values λ_i define the first-order corrections to the energies of these transformed degenerate states while the second-order corrections for each $n = n_i$ are given by Eq. (A10) with all $n' = n_j$ excluded for $\sigma' = \sigma$. Accordingly, the overall contribution of the second-order corrections $\epsilon_{n\sigma}^{(2)}$ to $\Omega^{(2)}$ defined with Eq. (A6) is given by the formula (11) excluding (nn) terms from nondegenerate states as well as all M^2 terms $(nn') = (n_in_j)$ for each degenerate subspace. The contribution from the first-order corrections $\epsilon_{n\sigma}^{(1)}$ to $\Omega^{(2)}$ is given by the sum $\sum_{i=1}^{M} \lambda_i^2$ [i.e., the second sum in Eq. (A6)] for every nondegenerate state ($M = 1$) and each degenerate subspace with the common factor $f'(\epsilon_{n\sigma})$ (where $n = n_i$).

However, one readily avoids the need for diagonalization of degenerate states since the sum of the contributions to $\Omega^{(2)}$ from the first- and second-order corrections to state energies leads to the same results as the formula (11) calculated with the original states and all terms included. Indeed, the part of sum in Eq. (11) that comes from the original set of degenerate states is given by the sum $\sum_{i,j=1}^{M} A_{ij}A_{ji} = \text{Tr}(AA)$ multiplied by the common prefactor $f'(\epsilon_{n\sigma})$ ($n = n_i$). Since the trace $\text{Tr}(AA)$ is invariant upon the transformation $PAP^{-1} = D$ of matrix A to the diagonal form $D = (\lambda_i\delta_{ij})$ with the transformation matrix P, this trace is equal to $\sum_{i=1}^{M} \lambda_i^2$ which is the contribution from the first-order corrections $\epsilon_{n\sigma}^{(1)}$ obtained after diagonalization.

It remains to show that the subsum of terms coming from a subspace of orthonormal degenerate states $|n\sigma\mathbf{k}\rangle$ ($n = n_j$, $j = 1, \ldots, M$) coupled to another state $|n'\sigma'\mathbf{k}\rangle$ with energy $\epsilon_{n'\sigma'} \neq \epsilon_{n\sigma}$ does also not depend on the particular choice of the degenerate states. Indeed, if the degenerate states are represented as $|n_i\sigma\mathbf{k}\rangle = \sum_{j=1}^{M} P_{ij}|n_j\sigma\mathbf{k}\rangle_{\text{d}}$, the considered subsum is given by the sum

$$\sum_{i=1}^{M} |\langle n'\mathbf{k}\sigma'|H_{\text{so}}|n_i\mathbf{k}\sigma\rangle|^2$$

$$= \sum_{i=1}^{M} \sum_{j=1}^{M} \sum_{j'=1}^{M} P_{ij}P_{ij'}^* {}_{\text{d}}\langle n_j\mathbf{k}\sigma|H_{\text{so}}|n'\mathbf{k}\sigma'\rangle$$

$$\times \langle n'\mathbf{k}\sigma'|H_{\text{so}}|n_j\mathbf{k}\sigma\rangle_{\text{d}} \qquad \text{(A11)}$$

multiplied by the common prefactor $[f(\epsilon_{n\sigma}) - f(\epsilon_{n'\sigma'})]/(\epsilon_{n\sigma} - \epsilon_{n'\sigma'})$. However, since transformation matrix P is unitary ($P^+ = P^{-1}$) the sum $\sum_{i=1}^{M} P_{ij}P_{ij'}^*$ is equal to $\delta_{jj'}$ and the contribution given by Eq. (A11) reduces to the same form

$$\sum_{j=1}^{M} |\langle n'\mathbf{k}\sigma'|H_{\text{so}}|n_j\mathbf{k}\sigma\rangle_{\text{d}}|^2 \qquad \text{(A12)}$$

as for the initial set of the degenerate states. This property, alongside the argument presented in the previous paragraph, finally proves that $\Omega^{(2)}$ is expressed with Eq. (11) including all terms and does not depend on the particular choice of degenerate states at the $\mathbf{k}$ points where some of the eigenstates of the unperturbed Hamiltonian are degenerate.

[1] L. Szunyogh, B. Újfalussy, and P. Weinberger, Phys. Rev. B **51**, 9552 (1995).

[2] M. Cinal and D. M. Edwards, Phys. Rev. B **55**, 3636 (1997).

[3] B. T. Thole, P. Carra, F. Sette, and G. van der Laan, Phys. Rev. Lett. **68**, 1943 (1992).

[4] P. Carra, B. T. Thole, M. Altarelli, and X. Wang, Phys. Rev. Lett. **70**, 694 (1993).

[5] C. T. Chen, Y. U. Idzerda, H.-J. Lin, N. V. Smith, G. Meigs, E. Chaban, G. H. Ho, E. Pellegrin, and F. Sette, Phys. Rev. Lett. **75**, 152 (1995).

[6] J. Stöhr and H. Konig, Phys. Rev. Lett. **75**, 3748 (1995).

[7] J. Stöhr, J. Magn. Magn. Mater. **200**, 470 (1999).

[8] P. Bruno, Phys. Rev. B **39**, 865 (1989).

[9] G. van der Laan, J. Phys.: Condens. Matter **10**, 3239 (1998).

[10] C. Andersson, B. Sanyal, O. Eriksson, L. Nordström, O. Karis, D. Arvanitis, T. Konishi, E. Holub-Krappe, and J. H. Dunn, Phys. Rev. Lett. **99**, 177207 (2007).

[11] B. Dieny and M. Chshiev, Rev. Mod. Phys. **89**, 025008 (2017).

[12] D. Li, A. Smogunov, C. Barreteau, F. Ducastelle, and D. Spanjaard, Phys. Rev. B **88**, 214413 (2013).

[13] D. Li, C. Barreteau, M. R. Castell, F. Silly, and A. Smogunov, Phys. Rev. B **90**, 205409 (2014).

[14] S. Bornemann, J. Minár, J. B. Staunton, J. Honolka, A. Enders, K. Kern, and H. Ebert, Eur. Phys. J. D **45**, 529 (2007).

[15] M. Košuth, V. Popescu, H. Ebert, and G. Bayreuther, Europhys. Lett. **72**, 816 (2005).

[16] L. M. Sandratskii, Phys. Rev. B **92**, 134414 (2015).

[17] M. Dąbrowski, T. R. F. Peixoto, M. Pazgan, A. Winkelmann, M. Cinal, T. Nakagawa, Y. Takagi, T. Yokoyama, F. Bisio, U. Bauer, F. Yildiz, M. Przybylski, and J. Kirschner, Phys. Rev. Lett. **113**, 067203 (2014).

[18] A. Manchon, C. Ducruet, L. Lombard S. Auffret, B. Rodmacq, B. Dieny, S. Pizzini, J. Vogel, V. Uhlîr, M. Hochstrasser, and G. Panaccione, J. Appl. Phys. **104**, 043914 (2008).

[19] M. Kotsugi, M. Mizuguchi, S. Sekiya, M. Mizumaki, T. Kojima, T. Nakamura, H. Osawa, K. Kodama, T. Ohtsuki, T. Ohkochi, K. Takanashi, and Y. Watanabe, J. Magn. Magn. Mater. **326**, 235 (2013).

[20] K. Ikeda, T. Seki, G. Shibata, T. Kadono, K. Ishigami, Y. Takahashi, M. Horio, S. Sakamoto, Y. Nonaka, M. Sakamaki, K. Amemiya, N. Kawamura, M. Suzuki, K. Takanashi, and A. Fujimori, Appl. Phys. Lett. **111**, 142402 (2017).

[21] J. Okabayashi, Y. Miura, and H. Munekata, Sci. Rep. **8**, 8303 (2018).

[22] R. Miyakaze, S. Sakamoto, T. Kawabe, T. Tsukahara, Y. Kotani, K. Toyoki, T. Nakamura, M. Goto, Y. Suzuki, and S. Miwa, Phys. Rev. B **102**, 014419 (2020).

[23] F. Gimbert and L. Calmels, Phys. Rev. B **86**, 184407 (2012).

[24] M. Weinert, R. E. Watson, and J. W. Davenport, Phys. Rev. B **32**, 2115 (1985).

[25] D.-S. Wang, R. Wu, and A. J. Freeman, Phys. Rev. B **47**, 14932 (1993).

[26] M. Cinal, D. M. Edwards, and J. Mathon, Phys. Rev. B **50**, 3754 (1994).

[27] J. Li, M. Przybylski, F. Yildiz, X. D. Ma, and Y. Z. Wu, Phys. Rev. Lett. **102**, 207206 (2009).

[28] M. Przybylski, M. Dąbrowski, U. Bauer, M. Cinal, and J. Kirschner, J. Appl. Phys. **111**, 07C102 (2012).

[29] S. Manna, P. L. Gastelois, M. Dąbrowski, P. Kuświk, M. Cinal, M. Przybylski, and J. Kirschner, Phys. Rev. B **87**, 134401 (2013).

[30] L. Szunyogh, B. Újfalussy, C. Blaas, U. Pustogowa, C. Sommers, and P. Weinberger, Phys. Rev. B **56**, 14036 (1997).

[31] M. Cinal and D. M. Edwards, Phys. Rev. B **57**, 100 (1998).

[32] M. Cinal, J. Phys.: Condens. Matter **13**, 901 (2001).

[33] M. Cinal, J. Phys.: Condens. Matter **15**, 29 (2003).

[34] D. M. Edwards, J. Mathon, R. B. Muniz, and M. S. Phan, Phys. Rev. Lett. **67**, 493 (1991); Erratum **67**, 1476(E) (1991).

[35] P. V. Ong, N. Kioussis, P. K. Amiri, and K. L. Wang, Phys. Rev. B **94**, 174404 (2016).

[36] J. Qiao, S. Peng, Y. Zhang, H. Yang, and W. Zhao, Phys. Rev. B **97**, 054420 (2018).

[37] M. Ślęzak, P. Dróżdż, K. Matlak, A. Kozioł-Rachwał, J. Korecki, and T. Ślęzak, J. Magn. Magn. Mater. **497**, 165963 (2019).

[38] L. I. Schiff, *Quantum Mechanics*, 3rd ed. (McGraw-Hill, New York, 1968).

[39] K. Masuda and Y. Miura, Phys. Rev. B **98**, 224421 (2018).

[40] Note that the function $g(\epsilon)$ is denoted with the symbol $L(\epsilon)$ in Ref. [2] and the prefactor $-k_B T$ in now included in its definition.

[41] Y. Miura, S. Ozaki, Y. Kuwahara, M. Tsujikawa, K. Abe, and M. Shirai, J. Phys.: Condens. Matter **25**, 106005 (2013).

[42] Y. Miura, M. Tsujikawa, and M. Shirai, J. Appl. Phys. **113**, 233908 (2013).

[43] G. Kresse and J. Hafner, Phys. Rev. B **47**, 558 (1993); **49**, 14251 (1994).

[44] G. Kresse and J. Furthmüller, Comput. Mater. Sci. **6**, 15 (1996).

[45] G. Kresse and J. Furthmüller, Phys. Rev. B **54**, 11169 (1996).

[46] Note that although the diagonal terms are excluded in the expression for the MCA energy given by Eq. (19) in Ref. [2] it is explained in the discussion following this equation that such terms must be included for cubic films without mirror symmetry, thus also lacking the inversion symmetry.

[47] D.-S. Wang, R. Wu, and A. J. Freeman, Phys. Rev. Lett. **70**, 869 (1993).

[48] C. Li, A. J. Freeman, H. J. F. Jansen, and C. L. Fu, Phys. Rev. B **42**, 5433 (1990).

[49] E. Abate and M. Asdente, Phys. Rev. **140**, A1303 (1965).

[50] T. P. T. Nguyen, K. Yamauchi, K. Nakamura, and T. Oguchi, J. Phys. Soc. Jpn. **89**, 114710 (2020).

[51] D. Amoroso, P. Barone, and S. Picozzi, Nat. Commun. **11**, 5784 (2020).

[52] R. Cuadrado, R. F. L. Evans, T. Shoji, M. Yano, A. Kato, M. Ito, G. Hrkac, T. Schrefl, and R. W. Chantrell, J. Appl. Phys. **130**, 023901 (2021).

[53] D. Go, F. Freimuth, J.-P. Hanke, F. Xue, O. Gomonay, K.-J. Lee, S. Blügel, P. M. Haney, H.-W. Lee, and Y. Mokrousov, Phys. Rev. Research **2**, 033401 (2020).

[54] R. Resta, J. Phys.: Condens. Matter **22**, 123201 (2010).

[55] T. Thonhauser, Int. J. Mod. Phys. B **25**, 1429 (2011).

[56] F. Aryasetiawan and K. Karlsson, J. Phys. Chem. Solids **128**, 87 (2019).

[57] D. A. Papaconstantopoulos, *Handbook of the Band Structure of Elemental Solids* (Plenum, New York, 1986).

[58] E. Barati, M. Cinal, D. M. Edwards, and A. Umerski, Phys. Rev. B **90**, 014420 (2014).

[59] C. Li and A. J. Freeman, J. Magn. Magn. Mater. **75**, 53 (1988).

[60] M. Aldén, S. Mirbt, H. L. Skriver, N. M. Rosengaard, and B. Johansson, Phys. Rev B **46**, 6303 (1992).

[61] H. Zhang, *Relativistic Density Functional Treatment of Magnetic Anisotropy*, thesis, Dr. rer. nat., Technische Universität Dresden (2009).

[62] A. V. Davydenko, A. G. Kozlov, A. V. Ognev, M. E. Stebliy, A. S. Samardak, K. S. Ermakov, A. G. Kolesnikov, and L. A. Chebotkevich, Phys. Rev. B **95**, 064430 (2017).

[63] E. A. Owen and D. Madoc Jones, Proc. Phys. Soc. B **67**, 456 (1954).

[64] B. N. Engel, C. D. England, R. A. Van Leeuwen, M. H. Wiedmann, and C. M. Falco, Phys. Rev. Lett. **67**, 1910 (1991).

[65] J. L. Perez-Diaz and M. C. Munoz, Phys. Rev. B **52**, 2471 (1995).

[66] P. Atkins and R. Friedman, *Molecular Quantum Mechanics*, 4th ed. (Oxford University Press, Oxford, 2005).

[67] V. Kamberský, Czech. J. Phys. B **26**, 1366 (1976).

[68] V. Kamberský, Phys. Rev. B **76**, 134416 (2007).

[69] A. L. Fetter and J. D. Walecka, *Quantum Theory of Many-Particle Systems* (McGraw-Hill, San Francisco, 1971).